Search for single production of vector-like quarks decaying into W(ℓν)b in pp collisions at √s=13 $ TeV with the ATLAS detector

Collaborators: Algren, Malte; Alves Cardoso, Mario; Antel, Claire; Axiotis, Konstantinos; Bezio, Lucas; Bozianu, Léon; Cepaitis, Vilius; Clark, Allan Geoffrey; Della Volpe, Domenico; Drozdova, Mariia; Ferrere, Didier; Franchellucci, Stefano Froch, Alexander [**and 22 more**]

How to cite

ATLAS Collaboration. Search for single production of vector-like quarks decaying into W(ℓν)b in pp collisions at √s=13 $ TeV with the ATLAS detector. In: The journal of high energy physics, 2025, vol. 2025, p. 12. doi: 10.1007/jhep12(2025)012

This publication URL: https://archive-ouverte.unige.ch/unige:191253

Publication DOI: 10.1007/jhep12(2025)012

Published for SISSA by Springer

Received: *June 19, 2025*
Revised: *October 19, 2025*
Accepted: *October 28, 2025*
Published: *December 1, 2025*

Search for single production of vector-like quarks decaying into $W(\ell\nu)b$ in pp collisions at $\sqrt{s} = 13$ TeV with the ATLAS detector

The ATLAS collaboration

E-mail: atlas.publications@cern.ch

Abstract: A search for single production of a vector-like quark Q, which could be either a singlet T, with charge $\frac{2}{3}$, or a Y from a (T, B, Y) triplet, with charge $-\frac{4}{3}$, is performed using data from proton-proton collisions at a centre-of-mass energy of 13 TeV. The data correspond to the full integrated luminosity of 140 fb^{-1} recorded with the ATLAS detector during Run 2 of the Large Hadron Collider. The analysis targets $Q \to Wb$ decays where the W boson decays leptonically. The data are found to be consistent with the expected Standard Model background, so upper limits are set on the cross-section times branching ratio, and on the coupling of the Q to the Standard Model sector for these two benchmark models. Effects of interference with the Standard Model background are taken into account. For the singlet T, the 95% confidence level limit on the coupling strength κ ranges between 0.22 and 0.52 for masses from 1150 to 2300 GeV. For the (T, B, Y) triplet, the limits on κ vary from 0.14 to 0.46 for masses from 1150 to 2600 GeV.

Keywords: Beyond Standard Model, Exotics, Hadron-Hadron Scattering, Vector-Like Quarks

ArXiv ePrint: 2506.15515

https://doi.org/10.1007/JHEP12(2025)012

JHEP12(2025)012

Contents

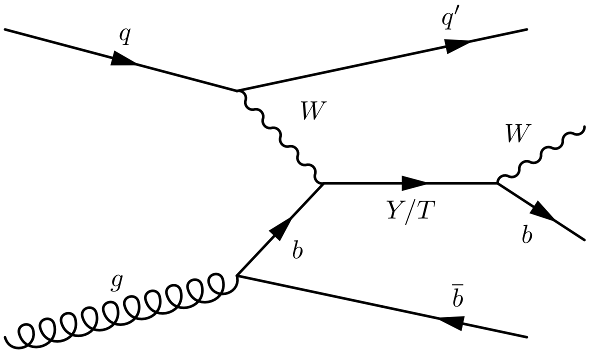

Figure 1. Leading-order Feynman diagram for single Y/T production in Wb fusion and subsequent decay into Wb.

1 Introduction

Vector-like quarks (VLQs) are hypothetical spin-$\frac{1}{2}$ coloured particles with left-handed and right-handed components that transform in the same way under the Standard Model (SM) gauge group. Their masses, m_Q, are therefore not generated by a Yukawa coupling to the Higgs field [1].

Although the Higgs-boson production and decay rates observed at the Large Hadron Collider (LHC) [2, 3] exclude a fourth generation of perturbatively coupled chiral quarks [4], the effects of VLQs via quantum-loop processes [1] are much smaller than the uncertainty in the current measurements, so this family of models remains compatible with the latest indirect experimental constraints.

VLQs appear in several extensions of the SM addressing the hierarchy problem, such as extra dimensions [5], composite Higgs [6, 7] and Little Higgs [8] models, where they are added to the SM in multiplets. They can also appear in supersymmetric models [9] and are able to stabilise the electroweak vacuum [10]. In many such models, VLQs mix mainly with the SM quarks of the third generation because of the large masses of the bottom and top quarks [11, 12]. In addition, the radiative neutrino mass generation mechanism usually requires vector-like quarks to generate the tiny masses of neutrinos via loops involving VLQs [13–15].

The set of possible VLQs are the B and T quarks, named in analogy with the SM b- and t-quarks and with their electromagnetic (EM) charges $-\frac{1}{3}$ and $+\frac{2}{3}$, and X and Y quarks with more exotic charges $+\frac{5}{3}$ and $-\frac{4}{3}$. This paper presents a direct search for a heavy vector-like T quark or Y quark, or their antiparticles.[1] The different charges in the final states, $Y^{+4/3} \to W^+\bar{b}^{+1/3}$ and $T^{+2/3} \to W^+b^{-1/3}$, are not exploited here. The analysis focuses on the production of a single VLQ ($Q = T$ or Y) produced via Wb fusion ($qg \to q'Qb$), which then decays back into Wb ($Q \to Wb$). The subsequent leptonic W decays are considered, complementing a similar search in the fully hadronic final state [16]. While it is possible for the VLQ to couple also to light quarks, as e.g. investigated in another recent search in ref. [17], only coupling to b-quarks is considered here. An example of a leading-order Feynman diagram for this production process is shown in figure 1.

---

[1] Antiparticles are implicitly included in all discussions.

1.1 VLQ phenomenology

Several Lagrangian formulations exist for VLQ interactions, including a renormalisable extension of the SM parameterised by chiral left- and right-handed mixing angles θ_{L} and θ_{R} related through multiplet symmetries [1], and a non-renormalisable effective theory parameterised by chiral c_{L}^{Wb} and c_{R}^{Wb} couplings [18, 19]. The principal difference between these approaches is that the non-renormalisable model's Lagrangian allows for additional terms that could result in larger production cross-sections. These formalisms were used in previous ATLAS and CMS papers [20–26], but here the simplified Lagrangian from ref. [27] is adopted:

$$\mathcal{L} = \sum_{Q,q,\zeta} \left[\frac{g_w}{\sqrt{2}} \kappa_\zeta^{Qq} \bar{Q} \not{W} P_\zeta q + \frac{g_w}{2c_W} \tilde{\kappa}_\zeta^{Qq} \bar{Q} \not{Z} P_\zeta q + \hat{\kappa}_\zeta^{Qq} H \bar{Q} P_\zeta q \right] + \mathrm{h.c.} \tag{1.1}$$

Here, Q represents the VLQ flavour(s), ζ is the chirality and P_ζ is its projection operator, q represents the interacting SM quark, c_W and g_W are electroweak parameters, and κ_ζ^{Qq}, $\tilde{\kappa}_\zeta^{Qq}$, and $\hat{\kappa}_\zeta^{Qq}$ are the electroweak couplings between Q and q when mediated by the W, Z, and H bosons respectively.

This paper focuses on the $Q = \{T, Y\}$ VLQs and their W interaction mode with $q = b$, i.e. the first term in eq. (1.1) and a reduction of the sum to chiral projections only. Since the relations between chiral states are determined by the multiplet structure, the results of this analysis are interpreted in terms of the cross-section times branching ratio and a single coupling-strength parameter $\kappa \equiv \kappa_\zeta^{Qb}$ with an assumed branching ratio, as a function of the VLQ mass.

Vector-like T quarks can belong to any weak-isospin SU(2) multiplet, while vector-like Y quarks cannot exist as singlets. This analysis focuses on Y quarks from a (T, B, Y) triplet, or a singlet T quark. T quarks in a (T, B, Y) triplet do not couple to Wb [1]. For singlet T quarks, the branching ratios ($\mathcal{B}$) are model- and mass-dependent, but in the high-mass limit considered in this analysis, they converge towards $(Wb : Zt : Ht) = (2 : 1 : 1)$ [1]. Due to its $-\frac{4}{3}$ charge, Y quarks can be produced singly in pp collisions only via Wb fusion, and they can decay only into Wb. Consequently, $\mathcal{B}(Y \to Wb) = 100\%$.

In this paper it is assumed that T quarks are produced in Wb fusion only. For single production of a T quark, Zt fusion could in principle contribute as well, but is neglected in this T-singlet search primarily because the cross-section for Zt fusion is much smaller than for Wb fusion. For equal values of the TZt and TWb couplings, it is about one order of magnitude smaller [19]. However, for the T-singlet case, the TZt coupling is about a factor of $\sqrt{2}$ smaller than the TWb coupling. Since the single-VLQ production cross-section scales with the coupling squared, the cross-section for Zt fusion is about an extra factor of two lower than that for Wb fusion. Similarly, $\mathcal{B}(T \to Zt)$ is about a factor of two smaller than $\mathcal{B}(T \to Wb)$. In addition, the selection efficiency for $tZ \to T \to Wb$ events in this search is about a factor of two smaller than for $bW \to T \to Wb$, because in $tZ \to T \to Wb$ the accompanying top quark from the gluon splitting leads to additional jets in the final state (see section 5).

Single production of vector-like quarks is enabled by their mixing with the SM quarks, whereas pair production is dominated by the model-independent QCD coupling. As a result, searches for VLQ pair production can set absolute bounds on the VLQ masses, while searches for single production provide a complementary mapping of their couplings to the SM quarks as a function of those masses. In addition, single production can become the dominant VLQ production mechanism at the LHC for high VLQ masses (about 1000 GeV for a coupling of 0.5), where the energy threshold for pair production suppresses that cross-section enough to offset the difference between the coupling strengths of QCD and weak interactions.

1.2 Previous studies

The ATLAS and CMS Collaborations have published searches for single and pair production of vector-like T quarks in all three decay channels [20, 21, 21–26, 28–40], and have set 95% confidence level (CL) lower limits on the T- and Y-quark masses. Assuming $\mathcal{B} = 100\%$ for the corresponding decay channel, the strongest observed T-quark mass limits are $m_T > 1430$ GeV for $T \to Ht$ [34], 1340 GeV for $T \to Zt$ [22] and 1350 GeV for $T \to Wb$ [32], independent of the size of the c^{Wb} couplings. Reinterpretation studies combining LHC measurements [41] observe a κ-dependent sensitivity to single-production at higher masses, setting $m_{T/Y}$ limits between 1500 to 2000 GeV for high values of κ (typically $\kappa > 0.6$) depending on the assumed multiplet structure. In ref. [40], seven individual ATLAS analyses searching for $B\bar{B}$ or $T\bar{T}$ pair production were combined, significantly improving on the model-independent cross-section limits from individual analyses and, in particular, excluding T-quark masses lower than 1310 GeV for any combination of decays into SM particles. The observed lower limit on the pair-produced Y-quark's mass is 1350 GeV [37].

These searches also reported limits as a function of the assumed branching ratios. The strongest observed limits are $m_T > 1310$ GeV and $m_T > 1280$ GeV for a weak-isospin doublet [34] and singlet [38] respectively. In the $T \to Zt$ decay channel, assuming a mixing parameter $\sin\theta_\mathrm{L}$ as low as 0.7, T quarks with masses between 450 GeV and 650 GeV are excluded [20], while for QWb couplings satisfying $\left(c_\mathrm{L}^{Wb}\right)^2 + \left(c_\mathrm{R}^{Wb}\right)^2 = 1$ and assuming $\mathcal{B}(T \to Wb) = 50\%$, the observed lower limit on the T-quark mass is 950 GeV [21, 23]. The CMS Collaboration studied single T- and Y-quark production using various subsets of Run 2 data at $\sqrt{s} = 13$ TeV collected in 2015 [24–26, 36, 39], and set upper limits on the single-T-quark production cross-section times $\mathcal{B}(T \to Ht)$ that are between 0.31 pb and 0.93 pb for T-quark masses in the range 1000–1800 GeV [25]. Single-T-quark production cross-section times $\mathcal{B}(T \to Zt)$ upper limits between 0.98 pb and 0.15 pb (0.6 pb and 0.13 pb) were set for T-quark masses in the range 700–1700 GeV in the left-handed $T(b)$ (right-handed $T(t)$) production channel [36]. For a mass of 1000 GeV, a T-quark production cross-section times branching ratio above 0.8 pb (0.7 pb) is excluded for the $T \to Ht$ decay channel assuming left-handed (right-handed) coupling of the T quark to SM particles [24]. For Y quarks with a coupling of 0.5 and $\mathcal{B}(Y \to Wb) = 100\%$, the observed and expected lower limits on the VLQ mass are $m_Y > 1400$ and 1000 GeV respectively [39].

1.3 Analysis overview

This paper describes a search for $Q \to Wb$ ($Q = T$ or Y) production, with the W boson decaying via $W \to \ell\nu$, with $\ell = e$ or μ. It uses the full Run 2 dataset from $\sqrt{s} = 13\,\mathrm{TeV}$ pp collisions recorded by the ATLAS detector at the LHC between 2015 and 2018, corresponding to an integrated luminosity of $140\,\mathrm{fb}^{-1}$ [42, 43]. A set of single-electron [44] and single-muon triggers [45] were used, with requirements depending on the lepton flavour and data-taking period. All detector subsystems were required to be operational during data taking and data-quality requirements [46] were applied.

The analysis in this paper supersedes the previous ATLAS analysis [23] using Run 2 data with an integrated luminosity of 36.1 fb^{-1} recorded in 2015–2016. A singly produced Q, followed by a leptonically decaying W boson results in a lepton-plus-jets signature characterised by the presence of exactly one electron or muon,[2] three or more jets and missing transverse momentum from the escaping neutrino. The analysis is optimised to search for decays of massive VLQs with a high-momentum b-jet (i.e. coming from the hadronisation of a b-quark) in the final state. The b-jet and the charged lepton originating from the Q decay are approximately back-to-back in the transverse plane since both originate from the decay of a heavy object.

The outgoing light quark in the process depicted in figure 1 often produces a jet in the forward region of the detector. The second b-jet from the gluon splitting may be observed in either the forward or central region of the detector. Since this b-jet typically has low energy, it often falls outside the detector acceptance.

The main background process with a prompt lepton arises from W-boson production in association with jets (W+jets), followed by top-quark pair ($t\bar{t}$) production and single top-quark production, with smaller background contributions from Z-boson production in association with jets (Z+jets), and diboson production (WW, WZ, and ZZ). Multijet events also contribute to the selected sample via the misidentification of a jet or a photon as an electron or the presence of a non-prompt electron or muon. To estimate the backgrounds from $t\bar{t}$ and W+jets events in a consistent and robust fashion, several control regions and validation regions are used. These are defined to be orthogonal to the signal region in order to provide independent data samples enriched in particular background sources. The reconstructed mass of the heavy VLQ candidate is used as the discriminating variable in a binned likelihood fit to test for the presence of a signal, taking into account interference with SM background processes.

2 ATLAS detector

The ATLAS detector [47] at the LHC [48] covers nearly the entire solid angle around the collision point.[3] It consists of an inner tracking detector (ID) surrounded by a thin superconducting solenoid, electromagnetic and hadronic calorimeters, and a muon spectrometer incorporating three large superconducting air-core toroidal magnets.

The inner-detector system (ID) is immersed in a 2 T axial magnetic field and provides charged-particle tracking in the range $|\eta| < 2.5$. The high-granularity silicon pixel detector covers the vertex region and typically provides four measurements per track, the first hit generally being in the insertable B-layer (IBL) installed before Run 2 [49, 50]. It is followed

---

[2] Electrons and muons from decays of τ-leptons from $W \to \tau\nu$ might also pass this selection.

[3] ATLAS uses a right-handed coordinate system with its origin at the nominal interaction point (IP) in the centre of the detector and the z-axis along the beam pipe. The x-axis points from the IP to the centre of the LHC ring, and the y-axis points upwards. Polar coordinates (r, ϕ) are used in the transverse plane, ϕ being the azimuthal angle around the z-axis. The pseudorapidity is defined in terms of the polar angle θ as $\eta = -\ln\tan(\theta/2)$ and is equal to the rapidity $y = (1/2)\ln\left[(E + p_z)/(E - p_z)\right]$ in the relativistic limit. Angular distance is measured in units of $\Delta R \equiv \sqrt{(\Delta y)^2 + (\Delta\phi)^2}$.

by the SemiConductor Tracker (SCT), which usually provides eight measurements per track. These silicon detectors are complemented by the transition radiation tracker (TRT), which enables radially extended track reconstruction up to $|\eta| = 2.0$. The TRT also provides electron identification information based on the fraction of hits (typically 30 in total) above a higher energy-deposit threshold corresponding to transition radiation.

The calorimeter system covers the pseudorapidity range $|\eta| < 4.9$. Within the region $|\eta| < 3.2$, electromagnetic (EM) calorimetry is provided by barrel and endcap high-granularity lead/liquid-argon (LAr) calorimeters, with an additional thin LAr presampler covering $|\eta| < 1.8$ to correct for energy loss in material upstream of the calorimeters. Hadronic calorimetry is provided by the steel/scintillator-tile calorimeter, segmented into three barrel structures within $|\eta| < 1.7$, and two copper/LAr hadronic endcap calorimeters. The solid angle coverage is completed with forward copper/LAr and tungsten/LAr calorimeter modules optimised for electromagnetic and hadronic energy measurements, respectively.

The muon spectrometer (MS) comprises separate trigger and high-precision tracking chambers measuring the deflection of muons in a magnetic field generated by the superconducting air-core toroidal magnets. The field integral of the toroids ranges between 2.0 and 6.0 T m across most of the detector. Three layers of precision chambers, each consisting of layers of monitored drift tubes, cover the region $|\eta| < 2.7$, complemented by cathode-strip chambers in the forward region, where the background is highest. The muon trigger system covers the range $|\eta| < 2.4$ with resistive-plate chambers in the barrel, and thin-gap chambers in the endcap regions.

The luminosity is measured mainly by the LUCID-2 [43] detector that records Cherenkov light produced in the quartz windows of photomultipliers located close to the beampipe.

Events were selected by the first-level trigger system implemented in custom hardware, followed by selections made by algorithms implemented in software in the high-level trigger [51]. The first-level trigger accepted events from the 40 MHz bunch crossings at a rate close to 100 kHz, which the high-level trigger further reduced in order to record complete events to disk at about 1.25 kHz.

A software suite [52] is used in data simulation, in the reconstruction and analysis of real and simulated data, in detector operations, and in the trigger and data acquisition systems of the experiment.

3 Background and signal simulation

Except for the multijet background from non-prompt and fake leptons, the expected background and signal event contributions are estimated using Monte Carlo (MC) simulation samples, processed either through the full ATLAS detector simulation [53] based on GEANT4 [54] or through a faster simulation making use of parameterised showers in the calorimeters. Inelastic proton-proton interactions, modelled with PYTHIA 8.186 [55] and fully simulated, were overlayed in the fast or full detector simulation, according to the luminosity profile of the recorded data, to simulate activity from additional *pp* collisions in the same and nearby bunch crossings (in-time and out-of-time pile-up.)

All simulated events were processed using the same reconstruction algorithms and analysis selection requirements as for the data. Small corrections, obtained from comparisons of

Process	Generator + parton showering/hadronisation	Hard-process PDF set	Inclusive cross-section order in pQCD
Tqb **signal** (Yqb by reweighting)	MADGRAPH5_AMC@NLO 2.6.5 + PYTHIA 8.210	NNPDF2.3	NLO
$t\bar{t}$	POWHEG BOX v2 + PYTHIA 8.230	NNPDF3.0	NNLO
Single top	POWHEG BOX v2 + PYTHIA 8.230	NNPDF3.0	NNLO
Dibosons WW, WZ, ZZ	SHERPA 2.2.2	NNPDF3.0	NLO
Z+**jets**	SHERPA 2.2.1	NNPDF3.0	NNLO
W+**jets**	SHERPA 2.2.11	NNPDF3.0	NNLO
$t\bar{t}V$	MADGRAPH5_AMC@NLO 2.2.3 + PYTHIA 8.210	NNPDF2.3	NLO
$t\bar{t}H$	POWHEG BOX v2 + PYTHIA 8.230	NNPDF3.0	NLO

Table 1. MC generator configurations used to model the signal and background processes. All PYTHIA generation used the A14 tune for the parton shower, hadronisation and underlying event, together with the NNPDF2.3LO PDF set; all SHERPA generation used the default SHERPA tune for its generator version. The PDF set used for hard-process modelling, and the highest order of the perturbative QCD (pQCD) calculation used for cross-section normalisation are given for each sample. All background processes were generated at NLO in QCD. The signal processes were generated at LO, but normalised to cross-sections calculated at NLO in QCD. The LO cross-sections calculated for the Yqb signal processes in the simulation were normalised to the NLO theoretical cross-section taken from ref. [58].

simulated events with data in dedicated control regions, were applied to trigger and object-reconstruction efficiencies as well as detector resolutions, to better model the observed response.

The main configurations of the MC samples used in this search are summarised in table 1. All simulated event samples, other than for processes modelled using the SHERPA generator [56], use EVTGEN [57] to model the decays of heavy-flavour hadrons.

3.1 Simulated signal samples

Simulated events for T-quark signal processes were generated at leading order (LO) in QCD in the four-flavour scheme with the MADGRAPH5_AMC@NLO 2.6.5 generator [59] using the NNPDF2.3NLO PDF set [60], interfaced to PYTHIA 8 [61] for parton-showering and hadronisation using the A14 set of tuned parameters with the NNPDF2.3LO PDFset [62]. The VLQ model from ref. [27] was used in the computation of the matrix elements, and all tree-level processes were included. Signal events were processed with fast simulation.

Other possible decay modes of the T quark ($T \to Zt$ and $T \to Ht$) have negligible acceptance in this search, confirmed by testing samples generated for other analyses focused on those channels. The kinematics of the final-state particles are very similar for left-handed and right-handed couplings, and hence the acceptances for the two chiralities were also found to be equal. The LO cross-sections calculated for the signal processes in the simulation were normalised to the next-to-leading-order (NLO) benchmark calculation from ref. [58], which was performed in the narrow-width approximation, and a correction factor was applied to account for finite-width effects [63, 64]. The validity of these correction factors is limited to VLQ relative widths satisfying $\Gamma_Q/m_Q < 0.5$, following ref. [65].

Separate event samples were produced for T-quark masses from 1100 GeV to 2700 GeV in steps of 200 GeV, with the coupling between the T quark and the gauge boson set to $\kappa = 1.0$.[4] In order to determine the signal yields and acceptances for VLQ masses and couplings different from those at the 200 GeV mass steps and the nominal coupling strength of $\kappa = 1.0$, event-by-event reweighting factors were applied, following the same procedure as used in ref. [23]. Since the kinematic distributions of the decay products for the T quark and Y quark in the Wb decay channel are the same, these T-quark signal samples were also used to derive the results for the Yqb signals, via further event reweighting.

Interference effects between the amplitudes for VLQ signal production and the SM are possible, and depend on the VLQ multiplet model. In this analysis, two scenarios are considered:

1. T-quark production in a T-singlet model if the T quark has only a left-handed coupling [1], which could interfere with SM t-channel single-top-quark production if the top quark is far off-shell.

2. Y-quark production with only a left-handed coupling, which could interfere with SM electroweak W^-bq production.[5] This scenario is realised in a (T, B, Y) triplet model for which the right-handed coupling is heavily suppressed [1]. Since the T does not couple to Wb in the (T, B, Y) triplet model, T-quark production does not contribute to the final state under consideration.

To account for the effects of interference, further reweighting factors were calculated for each mass point and each κ [23], and for each interference scenario (T or Y as described above), using MadGraph5_aMC@NLO 2.6.5. The squared matrix element for the process $pp \to Wbq$ is given by

$$|M|^2 = |M_{\mathrm{SM}}|^2 + |M_{\mathrm{VLQ}}|^2 + 2\mathfrak{Re}(M^*_{\mathrm{SM}} M_{\mathrm{VLQ}}) ,$$

and hence the total cross-section for $pp \to Wbq$ at LO can be written as $\sigma^{\mathrm{LO}}_{\mathrm{tot}} = \sigma^{\mathrm{LO}}_{\mathrm{SM}} + \sigma^{\mathrm{LO}}_{\mathrm{VLQ}} + \sigma^{\mathrm{LO}}_{\mathrm{I}}$ where $\sigma^{\mathrm{LO}}_{\mathrm{SM}}$ is the LO SM cross-section, $\sigma^{\mathrm{LO}}_{\mathrm{VLQ}}$ is the LO VLQ cross-section, and $\sigma^{\mathrm{LO}}_{\mathrm{I}}$ is the contribution from interference effects. Therefore, in the final statistical analysis, the interference contribution $\sigma^{\mathrm{LO}}_{\mathrm{I}}$ is related to the total signal cross-section, scaling as $\sqrt{\sigma^{\mathrm{LO}}_{\mathrm{VLQ}}}$.

---

[4] This coupling κ corresponds to the parameter κ_T in ref. [27]. It is also related to the $c^{Wb}_{\mathrm{L,R}}$ coupling parameters in ref. [19] via $\kappa = f(m_Q)\, c^{Wb}_{\mathrm{L,R}}/\sqrt{2}$, where $f^2(m_Q) \approx 1 + \mathcal{O}(m_Q^{-4})$ and m_Q is the VLQ mass in GeV.

[5] The charge-conjugated state $W^+\bar{b}q$ interferes with the $\bar{Y}$ quark.

3.2 Simulated background samples

The main backgrounds originate from SM W-boson production in association with jets (W+jets) and from $t\bar{t}$ and single-top-quark production, with smaller contributions from Z-boson production in association with jets (Z+jets) and from diboson (WW, WZ, ZZ) production. Samples for all SM background processes were simulated with the full GEANT4 model of the ATLAS detector. This section summarises the different generators used for each process, and their nominal configurations; the details of systematic-uncertainty estimation for these theoretical predictions are discussed in section 8.

Standard Model $t\bar{t}$ events were produced with the NLO generator POWHEG BOX v2 [66–68] with the NNPDF3.0NLO [69] PDF set in the matrix-element calculations. Parton-showering, hadronisation and the underlying event were simulated using PYTHIA 8.230 with the NNPDF2.3LO PDF set and the A14 set of tuned parameters [62]. This sample was normalised to the integrated cross-section calculated by TOP++ 2.0 [70–76] at next-to-next-to-leading order (NNLO) in QCD, including resummation of next-to-next-to-leading logarithmic soft-gluon terms. Corrections for NLO electroweak effects in $t\bar{t}$ events [77] were applied to the generated top-quark kinematics as a function of both the flavour and centre-of-mass energy of the initial partons and the decay angle of the top quarks in the centre-of-mass frame of the initial partons. The h_{damp} parameter in POWHEG BOX, which controls the matching of the matrix element to the parton shower and effectively regulates the degree of high-p_{T} radiation, was set to $1.5m_t$ [78], where $m_t = 172.5\,\mathrm{GeV}$. Two alternative $t\bar{t}$ samples with matrix elements calculated by aMC@NLO and POWHEG BOX respectively, and using HERWIG 7.1.3 [79] instead of PYTHIA 8.230 for showering and hadronisation, were used to estimate the effects of using different matching prescriptions.

Single-top-quark background event samples corresponding to the Wt, t-channel and s-channel production mechanisms were generated with POWHEG BOX v2 with the NNPDF3.0NLO PDF set, and interfaced to PYTHIA 8.230, which used the A14 tune and NNPDF2.3LO PDF set. Overlaps between the $t\bar{t}$ and Wt final states were removed using the "diagram removal" scheme [80, 81]. Another set of single-top-quark samples were generated using MADGRAPH5_aMC@NLO interfaced to PYTHIA 8.230 to determine the systematic uncertainties associated with the generation of the hard process. Additional single-top-quark samples were generated using the same POWHEG BOX settings as the nominal sample, but with HERWIG 7.0.4 for parton-showering, hadronisation, and the underlying event.

Samples of W+jets and Z+jets events were generated using SHERPA 2.2.11 and SHERPA 2.2.1, respectively [56, 82]. The former includes improvements to the statistical population of phase-space regions where the W+jets production cross-section is low. The matrix-element calculation was performed with up to two partons at NLO and up to four partons at leading order using COMIX [83] and OPENLOOPS [84]. The matrix-element calculation, performed using the NNPDF3.0NNLO PDF set [69], was merged with the SHERPA parton shower [85] using the MEPS@NLO prescription [86]. Alternative W+jets and Z+jets event samples were produced with MADGRAPH5_aMC@NLO 2.2.1, using the NNPDF3.0NLO PDF set, and interfaced to PYTHIA 8.186, which used the A14 tune and NNPDF2.3LO PDF set [62].

Diboson events ($WW/WZ/ZZ$), with one of the bosons decaying hadronically and the other leptonically, were generated at NLO with SHERPA 2.2.2, using the NNPDF3.0NNLO PDF set. Processes containing up to four electroweak vertices were included. The matrix element included up to one (ZZ) or no (WW, WZ) additional partons at NLO and up to three partons at LO, using the same procedure as for W/Z+jets. All diboson samples were normalised to their NLO theoretical cross-sections provided by SHERPA.

Smaller backgrounds were also considered, including ones from SM $t\bar{t}$ production with an associated boson: $t\bar{t}V$ and $t\bar{t}H$ with $V = W, Z$. The $t\bar{t}V$ event samples were simulated with MADGRAPH5_aMC@NLO using the NNPDF3.0NLO PDF set and interfaced to PYTHIA 8 [61], which used the A14 tune and NNPDF2.3LO PDF set. The $t\bar{t}H$ events were modelled using NLO POWHEG BOX v2 and interfaced to PYTHIA 8.230.

4 Object definitions

This analysis seeks to identify events containing a single VLQ that decays to a final state with an electron or muon, missing transverse momentum from a neutrino, and a b-jet.

4.1 Lepton selection

Electron candidates are reconstructed from isolated energy deposits (clusters) in the EM calorimeter, each matched to a reconstructed ID track, within the fiducial region of $|\eta_{\text{cluster}}| < 2.47$, where η_{cluster} is the pseudorapidity of the centroid of the calorimeter energy deposit associated with the electron candidate. A veto is placed on electrons in the transition region between the barrel and endcap electromagnetic calorimeters, $1.37 < |\eta_{\text{cluster}}| < 1.52$. Electrons are required to satisfy the *tight-likelihood* identification criterion [87], based on shower-shape and track-cluster matching variables, and must have transverse energy $E_{\text{T}} = E_{\text{cluster}}/\cosh(\eta_{\text{track}}) > 27\,\text{GeV}$, where E_{cluster} is the electromagnetic cluster energy and η_{track} the track pseudorapidity.

Muons are reconstructed [88] by combining a track reconstructed in the ID with one in the MS, using the complete track information from both detectors and accounting for the effects of energy loss and multiple scattering in the material of the detector structure. The muon candidates must satisfy the *medium* selection criteria [88] and are required to have a transverse momentum of at least 27 GeV and to be in the region $|\eta| < 2.5$.

To reduce the contribution of leptons from hadronic decays (non-prompt leptons), electrons and muons must satisfy isolation criteria that apply to both track and calorimeter information, and are tuned to give an overall efficiency of 98%, independent of the lepton's p_{T}. Electron and muon candidates are required to have no additional tracks within a cone of angular radius $\Delta R \equiv \sqrt{(\Delta\eta)^2 + (\Delta\phi)^2}$ around their directions, with $\Delta R = \min\{0.2, 10\ \text{GeV}/p_{\text{T}}^{e}\}$ for electrons and $\Delta R = \min\{0.3, 10\ \text{GeV}/p_{\text{T}}^{\mu}\}$ for muons [88]. The significance of the transverse impact parameter d_0, calculated relative to the measured beam-line position, is required to satisfy $|d_0/\sigma(d_0)| < 3(5)$ for muons (electrons), where $\sigma(d_0)$ is the uncertainty in d_0. Finally, the lepton tracks are matched to the primary vertex of the event by requiring the longitudinal impact parameter z_0 to satisfy $|z_0 \sin\theta_{\text{track}}| < 0.5$ mm, where θ_{track} is the polar angle of the track.[6]

4.2 Jet selection

Hadronic jets are reconstructed from three-dimensional topological calorimeter energy clusters and information about the tracks of charged particles passing through the ID. Jets are reconstructed with the anti-k_t algorithm [89, 90] with a distance parameter of $R = 0.4$ [91] using particle flow [92]. Data-quality criteria are imposed to identify jets arising from non-collision sources or detector noise, and any event containing at least one such jet is removed [93]. Finally, jets considered in this analysis are required to have a $p_{\text{T}} > 25$ GeV. The pseudorapidity acceptance for jets differs between different selections: central jets are required to have $|\eta| < 2.5$, while forward jets are defined to have $2.5 < |\eta| < 4.5$. Furthermore, jets with a $p_{\text{T}} < 60$ GeV and $|\eta| < 2.4$ are required to satisfy criteria implemented in the jet vertex tagger (JVT) algorithm [94, 95] designed to select jets that originate from the hard scattering and reduce the effect of in-time pile-up. A high value of the JVT corresponds to a high probability that the jet originated from the primary vertex. Hence, a requirement on JVT removes contamination from pile-up vertices.

4.3 Jet flavour-tagging and selection

The identification of jets from b-hadron decays (b-tagging) is fundamental in this analysis. Jets containing b-hadrons are identified ("tagged") by a multivariate discriminant that combines information about the impact parameters of ID tracks associated with the jet, the presence of displaced secondary vertices, and the reconstructed flight paths of b- and c-hadrons inside the jet [96]. Jets are considered to be b-tagged if the value of the discriminant, based on the DL1r [97] deep neural-network algorithm, is larger than a certain threshold. The threshold criterion, with a fixed value of 0.46, is applied only to central jets ($|\eta| < 2.5$) with $p_{\text{T}} > 25$ GeV and has an efficiency of approximately 85% for b-jets in simulated $t\bar{t}$ events. The rejection factor for jets originating from light quarks and gluons (henceforth referred to as light-flavour jets) is about 100, and that for jets originating from charm quarks (c-jets) is about 5, determined in simulated $t\bar{t}$ events. Correction factors are defined to correct the tagging rates in the simulation to match the efficiencies measured in the data control samples [98–100].

4.4 Overlap removal

To avoid interpreting the same detector measurement as two or more objects, an overlap-removal procedure is used to resolve ambiguities. First, any muon that leaves an energy deposit in the calorimeter and shares an ID track with an electron is removed. Then, any electron sharing an ID track with a remaining muon is removed. Jets overlapping with identified electron candidates within a cone of $\Delta R = 0.2$ are removed, as the jet and the electron are very likely to be the same physics object. If the nearest jet surviving this requirement is within $\Delta R = 0.4$ of an electron, the electron is discarded; this ensures that

---

[6] The longitudinal impact parameter z_0 is the difference between the longitudinal position of the track along the beam line at the point where the transverse impact parameter (d_0) is measured and the longitudinal position of the primary vertex.

remaining electrons are sufficiently separated from nearby jet activity. Muons are removed if they are separated from the nearest jet by $\Delta R < \min\{0.4, 0.04 + 10\ \text{GeV}/p_{\text{T}}^{\mu}\}$, where p_{T}^{μ} is the muon transverse momentum, to reduce the background from muons from heavy-flavour hadron decays inside jets. Any jet with at least three associated tracks (within a $\Delta R = 0.2$ cone) around a muon is kept and the muon removed. If, instead, the jet has fewer than three such associated tracks, the muon is kept and the jet is removed; this avoids an inefficiency for high-energy muons that suffered significant energy loss in the calorimeter.

4.5 $E_{\text{T}}^{\text{miss}}$ definition and W-boson reconstruction

The missing transverse momentum $\vec{p}_{\text{T}}^{\text{miss}}$ (with magnitude $E_{\text{T}}^{\text{miss}}$) is a measure of the momentum of the particles that remain undetected. It is defined as the negative vector sum of the transverse momenta of all selected and calibrated objects in the event including a term to account for energy from soft particles which are not associated with any of the selected objects. This soft term is calculated from ID tracks matched to the selected primary vertex, reducing its dependence on pile-up interactions [101].

The $\vec{p}_{\text{T}}^{\text{miss}}$ is then used as the transverse momentum of the neutrino from the W-boson candidate. The W-boson candidate is reconstructed by summing the four-momenta of the charged lepton and the neutrino. To obtain the z-component of the neutrino momentum ($p_{z,\nu}$), the invariant mass of the lepton-neutrino system is set to the W-boson mass and the resulting quadratic equation is solved. If no real solution exists, the magnitude of $\vec{p}_{\text{T}}^{\text{miss}}$ is varied by the minimum amount required to produce exactly one real solution to the quadratic equation. If two real solutions are found, the one with the smaller $|p_{z,\nu}|$ is used.

4.6 Reconstruction of the VLQ candidate

A VLQ candidate for each event is reconstructed from the highest transverse momentum (leading p_{T}) b-tagged jet and the decay products of the leptonically decaying W-boson candidate, i.e. the neutrino (see section 4.5) and the lepton. The invariant mass of the reconstructed VLQ candidate, m_{VLQ}, is used in the final statistical analysis as the main variable that discriminates between signal and background events.

5 Preselection

To be considered for the analysis, an event must contain exactly one electron or muon with $p_{\text{T}} > 27$ GeV and it must be matched to the corresponding electron or muon trigger object. The muon trigger covers the region $|\eta| < 2.4$, and its efficiency decreases at larger $|\eta|$ values. Events must have at least two jets with $p_{\text{T}} > 25$ GeV. Furthermore, the highest-p_{T} jet ("leading jet") must be a b-tagged central jet ($|\eta| < 2.5$) with $p_{\text{T}} > 200$ GeV. The missing transverse momentum is required to satisfy $E_{\text{T}}^{\text{miss}} > 120$ GeV and to be separated from the leading jet by $|\Delta\phi(\text{leading jet}, \vec{p}_{\text{T}}^{\text{miss}})| \geq 2$. The requirements on the missing transverse momentum reduce the fraction of events that are diboson events or contain a non-prompt or misidentified lepton. These baseline requirements are referred to as the "preselection". A summary of the main preselection requirements is provided in table 2.

JHEP12(2025)012

Requirement	Preselection
Leptons	1
Jets	≥ 2
Leading-jet p_{T} [GeV]	> 200
Leading-jet is central ($\lvert\eta\rvert < 2.5$)	Yes
Leading-jet is b-tagged	Yes
$E_{\mathrm{T}}^{\mathrm{miss}}$ [GeV]	> 120
$\lvert\Delta\phi(\text{leading jet}, \vec{p}_{\mathrm{T}}^{\,\mathrm{miss}})\rvert$	≥ 2

Table 2. Summary of the preselection requirements for all signal, control, and validation regions.

Region Requirement	SR	$t\bar{t}$ CR	$t\bar{t}$ VR	W+jets CR	W+jets VR1	W+jets VR2
b-tagged jets	≥ 1	≥ 2	≥ 1	1	1	1
Leading-jet p_{T} [GeV]	> 350	> 200	> 200	> 250	> 250	> 250
$\lvert\Delta\phi(\text{lepton}, \text{leading jet})\rvert$	> 2.5	> 2.5	> 2.5	> 2.5	[1.5, 2.5]	[1.5, 2.5]
# additional hard central jets	0	0	≥ 1	—	—	—
# forward jets ($p_{\mathrm{T}} > 40$ GeV)	≥ 1	0	≥ 1	0	≥ 1	0

Table 3. Summary of the selection requirements for the SR compared with those for the $t\bar{t}$ and W+jets CRs and VRs. The SR, $t\bar{t}$ CR, and W+jets CR are split into low-, middle-, and high-p_{T}^{W} subregions depending on whether the p_{T} of the W boson is below 400 GeV, between 400 and 600 GeV or above 600 GeV, respectively.

6 Final selection

After the preselection requirements, events are separated into signal, control, and validation regions (SRs, CRs, and VRs) defined by sets of orthogonal event-variable requirements. These requirements are summarised in table 3, with the variable definitions and motivations given in the following.

6.1 Signal region

In each signal region event, the b-tagged highest-p_{T} jet must have $p_{\mathrm{T}} > 350$ GeV. To exploit the low multiplicity of high-p_{T} jets in the signal process relative to the $t\bar{t}$ background, events are rejected if they contain an additional central ($\lvert\eta\rvert < 2.5$) jet that has a $p_{\mathrm{T}} > 75$ GeV and is either close to ($\Delta R < 1.2$) or nearly back-to-back with ($\Delta R > 2.7$) the leading jet.

An azimuthal separation of $\lvert\Delta\phi(\text{lepton}, \text{leading jet})\rvert > 2.5$ is required between the leading jet and the lepton because the leptonically decaying W boson from a heavy-Q decay recoils against the b-quark.

Finally, like in t-channel single-top production, the single production of VLQs gives rise to a forward jet, so only events with at least one forward jet ($2.5 < \lvert\eta\rvert < 4.5$) with $p_{\mathrm{T}} > 40$ GeV are considered.

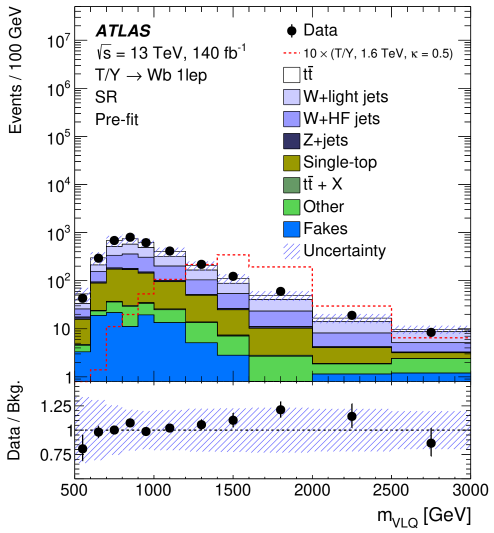

Figure 2. Pre-fit VLQ mass distribution in the signal region. The signal shown here is for a T/Y VLQ with $\kappa = 0.5$ and a mass of 1600 GeV, and is presented multiplying by ten its expected cross-section for clarity. "Other" includes diboson and other final states containing a top quark. The error band contains the statistical and systematic uncertainties added in quadrature. Weight corrections are applied to the $t\bar{t}$ and W+jets MC samples (see section 7).

Figure 2 shows the reconstructed VLQ invariant-mass distribution, m_{VLQ}, for data events, the expected SM events (pre-fit), and a VLQ signal in the SR. Events with "Fakes" are estimated as detailed in section 6.4. Weight corrections, obtained as described in section 7, are applied to the $t\bar{t}$ and W+jets MC samples. W+jets background is separated into light-flavour (W+light) and heavy-flavour (W+HF, with jets from c,b quarks) components. For the final fit, the SR is split into three subregions based on the reconstructed W-boson p_{T}: "low" with $p_{\mathrm{T}}^{W} < 400$ GeV, "middle" with 400 GeV $< p_{\mathrm{T}}^{W} <$ 600 GeV, and "high" with $p_{\mathrm{T}}^{W} > 600$ GeV. This improves the quality of the results, separating the better modelled, highly populated, low p_{T}^{W} region from the other two regions.

6.2 Control regions

The normalisation of W+jets and $t\bar{t}$ processes is partially constrained by fitting the predicted yields to data in CRs enriched in either W+jets or $t\bar{t}$ events. As with the SR, each of the two CRs in table 3 is split into three subregions based on W-boson p_{T}: "low", "middle" and "high" with p_{T}^{W} values below 400 GeV, between 400 and 600 GeV, and above 600 GeV respectively.

In addition to the preselection, the selection requirements common to the three W+jets CR subregions are that each event must have exactly one b-tagged jet with $p_{\mathrm{T}} > 250$ GeV, an azimuthal separation of $|\Delta\phi| > 2.5$ between the lepton and the leading jet, and no forward jets. These requirements ensure orthogonality with the SR and increase the fractional W+jets contribution. No veto is placed on additional central jets.

In addition to the preselection, the selection requirements common to the three $t\bar{t}$ CR subregions are that each event must contain at least two b-tagged jets, with the leading-jet p_{T} greater than 200 GeV. As in the SR, there must be no additional hard central jets satisfying the $\Delta R < 1.2$ or $\Delta R > 2.7$ distance criteria, and the lepton and leading jet must be azimuthally separated by $|\Delta\phi| > 2.5$. A forward jet veto is applied.

6.3 Validation regions

In addition to the CRs, W+jets and $t\bar{t}$ VRs are defined in order to verify that the main backgrounds are well modelled.

Two VRs are defined for W+jets events: VR1 and VR2. For each, events must pass the preselection and have exactly one b-tagged jet. Furthermore, the b-tagged jet must have a transverse momentum $p_{\mathrm{T}} > 250$ GeV, but rather than having a very large azimuthal separation from the lepton it must satisfy $1.5 < |\Delta\phi| < 2.5$. At least one forward jet must be present for VR1, whereas forward jets are vetoed for VR2. VR2 has a larger number of events, and it covers different kinematic regions.

The $t\bar{t}$ VR requires at least one b-tagged jet, the leading-jet p_{T} must be greater than 200 GeV, there must be at least one additional central high-p_{T} jet at a distance $\Delta R < 1.2$ or $\Delta R > 2.7$ from the leading jet, and a $|\Delta\phi| > 2.5$ separation is required between the lepton and the leading jet.

6.4 Estimation of multijet background

Multijet production results in hadrons, photons and non-prompt leptons that may satisfy the lepton selection criteria and give rise to so-called “non-prompt and fake” lepton backgrounds. The multijet background’s normalisation and shape in the m_{VLQ} distributions are estimated with a data-driven method, referred to as the matrix method. This approach uses the efficiencies for leptons selected using “loose” requirements (“loose” leptons) to pass the default “tight” lepton selection requirements. The efficiencies are obtained in dedicated control regions enriched in real leptons or in non-prompt and fake leptons, and applied to events selected with either the “loose” or “tight” lepton definition, to obtain the fraction of multijet events. The region enriched in real leptons is composed of events where the invariant mass $m_{\ell\ell}$ reconstructed from two lepton candidates in the final state, matches the Z-boson invariant mass with $|m_{\ell\ell} - m_Z| < 0.1 \times m_Z$. The default fake-enriched region for electrons is defined requiring $m_{\mathrm{T}}^{W} < 20\,\mathrm{GeV}$ and $E_{\mathrm{T}}^{\mathrm{miss}} + m_{\mathrm{T}}^{W} < 60\,\mathrm{GeV}$.[7] As a muon fake-enriched region, events with a single muon whose impact parameter significance satisfies $d_0/\sigma(d_0) > 5$ are used. Full details can be found in ref. [21].

7 Reweighting of the W+jets and top-quark backgrounds

The simulation of the main backgrounds, from $t\bar{t}$ and W+jets production, is susceptible to mismodelling in the highly energetic phase-space probed by this analysis, particularly in the modelling of QCD radiation. A set of theory and data-driven corrections was hence applied to the $t\bar{t}$ and W+jets MC samples to improve their accuracy.

Before deriving the data-driven reweightings, the MC samples were reweighted at generator level to the latest high-precision theory predictions [102]: the W+jets background

---

[7] The quantity m_{T}^{W} is built as the invariant mass of the $\ell\nu$ pair, neglecting the z-component.

to NLO precision in the electroweak couplings; the $t\bar{t}$ background to NNLO QCD precision in the two-dimensional (2D) space of top/anti-top p_{T} and $m_{t\bar{t}}$.

A data-driven reweighting was then used to correct the residual shape mismodelling in $t\bar{t}$ and W+jets distributions, as described in the steps listed below. For the W+jets background, the final fit provides the overall normalisation, separately for the light-flavour and heavy-flavour components (see section 9).

1. A W+jets enriched region was selected by applying the same selection cuts as in the preselection, but requiring the number of b-tagged jets to be zero (making it orthogonal to all other selection regions). This region is depleted of other backgrounds, with $> 90\%$ of selected events expected to be W+jets, and hence mismodelling seen there can be attributed to the W+jets background.

2. The scaling factors for W+jets reweighting were determined bin by bin as a function of both the number of jets and the transverse momentum of the reconstructed W boson, p_{T}^{W}. This W+jets 2D reweighting function was defined inclusively for both the W+HF and W+light components, assuming the same mismodelling, and fitted to data after subtracting the other (subleading) backgrounds' expected contributions.

3. This derived reweighting was then applied to the W+jets MC samples in the preselection region.

4. The preselection region has a $t\bar{t}$+Wt purity of over 80%. Given the similar nature of $t\bar{t}$ and single-top Wt production, a single $t\bar{t}$+Wt reweighting function was used. This was determined bin by bin in the preselection region, as a 2D function of the leading-jet p_{T} and the leptonic p_{T}^{W}, after subtracting the expected contributions of other backgrounds, as in the case of W+jets reweighting.

5. Finally, the $t\bar{t}$+Wt reweighting function was applied to those MC samples in the preselection region.

The weights applied do not deviate markedly from 1 for the majority of 2D bins. For W+jets reweighting, the scaling factors are between 0.7 and 2.1, while for $t\bar{t}$+Wt reweighting, they are between 0.15 and 1. To show the effect of the combined reweighting, figures 3 and 4 display the $t\bar{t}$ control region m_{VLQ} and leading-jet p_{T} distributions, respectively, before and after reweighting.

Tables 4–5 report the event yields, with all statistical and systematic uncertainties included, in the W+jets and $t\bar{t}$ control regions, and in the signal region before the fit. "Other" includes diboson and other final states containing a top quark. For a 1.4–2.4 TeV vector-like Y quark, with a coupling $\kappa = 0.5$, the signal contamination in the high-p_{T}^{W}, W+jets and $t\bar{t}$ CRs ranges from 0.1% to 3% and from 2.5% to 19%, respectively.

8 Systematic uncertainties

Several sources of systematic uncertainty in this analysis can affect the normalisation of the signal and background and/or their corresponding m_{VLQ} distributions used for the statistical

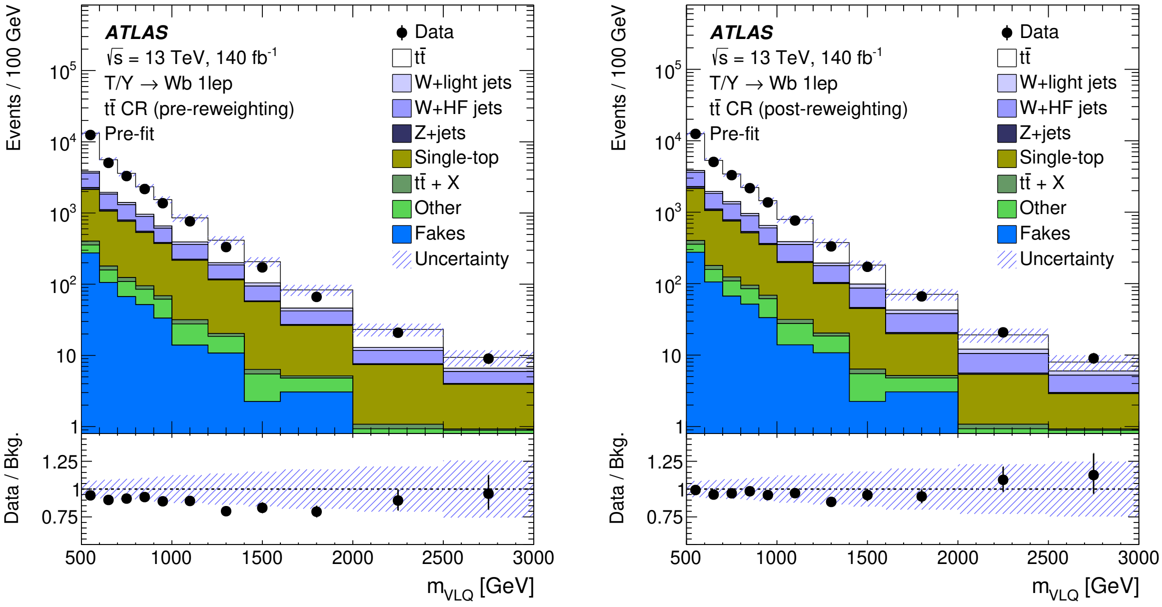

(a) (b)

Figure 3. m_{VLQ} distribution in the $t\bar{t}$ CR (a) before and (b) after reweighting. Shaded bands include statistical and systematic uncertainties, but not those related to the reweighting procedure. The last bin includes overflow.

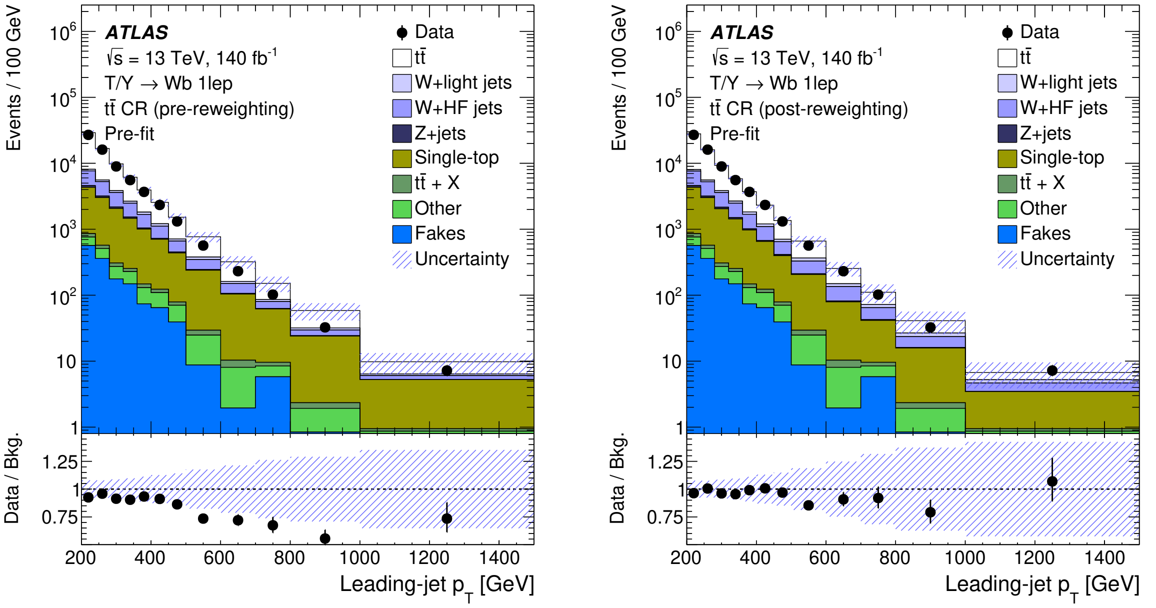

(a) (b)

Figure 4. Leading-jet p_{T} distribution in the $t\bar{t}$ CR (a) before and (b) after reweighting. Shaded bands include statistical and systematic uncertainties, but not those related to the reweighting procedure. The last bin includes overflow.

	W+jets low-p_{T}^{W}	W+jets mid-p_{T}^{W}	W+jets high-p_{T}^{W}
$t\bar{t}$	7110 ± 890	1930 ± 310	210 ± 100
W+light jets	12 200 ± 1500	4140 ± 620	1070 ± 270
W+HF jets	12 510 ± 850	3020 ± 380	610 ± 140
Z+jets	854 ± 80	129 ± 55	22.2 ± 4.5
Single top	2000 ± 790	700 ± 340	140 ± 130
$t\bar{t}V$	33.2 ± 4.3	16.7 ± 2.8	5.1 ± 1.0
$t\bar{t}H$	7.10 ± 0.94	2.04 ± 0.33	0.42 ± 0.11
Other	954 ± 74	400 ± 51	130 ± 22
Fakes (e)	510 ± 250	30 ± 15	29 ± 14
Fakes (μ)	940 ± 470	91 ± 45	12.2 ± 6.1
Y (1.4 TeV, $\kappa = 0.5$)	228 ± 10	210.2 ± 8.8	65.7 ± 2.8
Y (1.9 TeV, $\kappa = 0.5$)	97.8 ± 4.4	31.8 ± 1.5	9.50 ± 0.36
Y (2.4 TeV, $\kappa = 0.5$)	31.8 ± 1.5	6.89 ± 0.29	2.073 ± 0.082
Total background	37 100 ± 2500	10 460 ± 990	2230 ± 380
Data	38 191	11 046	2425

Table 4. W+jets control region yields after reweighting the W+jets and top backgrounds. Expected Y signals, for coupling $\kappa = 0.5$ and three masses, are also listed.

	$t\bar{t}$ CR low-p_{T}^{W}	$t\bar{t}$ CR mid-p_{T}^{W}	$t\bar{t}$ CR high-p_{T}^{W}
$t\bar{t}$	16 500 ± 1000	1040 ± 150	119 ± 57
W+light jets	530 ± 160	131 ± 44	35 ± 14
W+HF jets	3140 ± 370	559 ± 87	113 ± 31
Z+jets	264 ± 42	20.7 ± 4.5	2.4 ± 1.2
Single top	3800 ± 1200	642 ± 430	150 ± 150
$t\bar{t}V$	66.5 ± 7.4	11.9 ± 2.2	2.93 ± 0.73
$t\bar{t}H$	29.7 ± 3.2	3.22 ± 0.48	0.52 ± 0.11
Other	224 ± 28	59 ± 17	13.0 ± 5.8
Fakes (e)	220 ± 110	5.3 ± 2.7	2.4 ± 1.2
Fakes (μ)	370 ± 180	20 ± 10	2.1 ± 1.1
Y (1.4 TeV, $\kappa = 0.5$)	25.7 ± 1.2	71.0 ± 3.4	82.2 ± 4.8
Y (1.9 TeV, $\kappa = 0.5$)	3.35 ± 0.20	11.68 ± 0.65	33.7 ± 1.8
Y (2.4 TeV, $\kappa = 0.5$)	0.703 ± 0.051	2.12 ± 0.11	11.49 ± 0.69
Total background	25 200 ± 1800	2500 ± 500	440 ± 170
Data	24 582	2348	363

Table 5. $t\bar{t}$ control region yields after reweighting the W+jets and top backgrounds. Expected Y signals, for coupling $\kappa = 0.5$ and three masses, are also listed.

study. These include the modelling of the detector response, object-reconstruction algorithms, uncertainties in the theoretical modelling of the signals and backgrounds, and uncertainties arising from the limited size of the simulated event samples.

These effects were estimated using various methods described in this section, and were included in the statistical analysis via nuisance parameters. The largest systematic uncertainties in the SM background estimates arise from the jet-energy scale calibration, the flavour-tagging efficiencies (b, c and light), and the background modelling.

8.1 Experimental uncertainties

The estimated uncertainty in the integrated luminosity of the combined 2015–2018 dataset is 0.83%, obtained via a methodology similar to that detailed in ref. [42].

The efficiency and mistag rates of the flavour-tagging algorithm were measured using data control samples. Correction factors were then calculated to align the tagging rates in the simulation with the efficiencies observed in the data control samples [98–100]. These correction factors were determined only for b- and c-jets with $p_{\mathrm{T}} < 300$ GeV and light-flavour jets with $p_{\mathrm{T}} < 750$ GeV.

The uncertainties associated with the measurements used to derive these correction factors were factorised into groups of statistically independent sources, including six independent sources affecting b-jets and four independent sources affecting c-jets. Each of these uncertainties has a different dependence on the jet p_{T}. Seventeen sources of uncertainty affecting light-flavour jets are also considered, and these depend on jet p_{T} and η. An additional relative uncertainty, fully correlated among these three jet flavours, is applied for extrapolation of these corrections to jets beyond the p_{T}-reach of the data-calibration samples. An uncertainty related to the application of c-jet scale factors to τ-jets was considered, but was found to have a negligible impact in this analysis [103].

Additional detector-related systematic uncertainties arise from the reconstruction and measurement of jets [91], leptons [44, 45, 87, 88] and $E_{\mathrm{T}}^{\mathrm{miss}}$ [101]:

- Uncertainties associated with jets arise primarily from the jet-energy scale, jet-energy resolution, and the efficiency of the JVT requirement. The largest contribution is from the jet-energy scale: the dependence of this on jet p_{T} and η, jet flavour, and pile-up is encoded in 21 uncorrelated components that are treated independently in the statistical analysis [91].

- Uncertainties associated with leptons arise from the trigger, reconstruction, identification, and isolation efficiencies, as well as the lepton-momentum scale and resolution. These were studied using $Z \to \ell^+\ell^-$ and $J/\psi \to \ell^+\ell^-$ decays in data.

- The systematic uncertainty in the $E_{\mathrm{T}}^{\mathrm{miss}}$ reconstruction is dominated by the uncertainties in the energy calibration and resolution of reconstructed jets and leptons. They are propagated to the $E_{\mathrm{T}}^{\mathrm{miss}}$ via their inclusion among the uncertainties associated with those objects [101]. Subleading contributions are also included via the p_{T} scale and resolution uncertainties of reconstructed tracks that are associated with the hard-scatter vertex but not matched to any reconstructed objects.

The flavour-tagging systematic uncertainties are the leading source of experimental uncertainty: added in quadrature, they account for an 8.7% uncertainty in the expected background yield in the SR. Other significant detector-specific uncertainties arise from jet-energy scale uncertainties (a 6.4% effect on the expected background yield) and jet-energy resolution uncertainties (a 2.7% effect on the expected background yield). The total systematic uncertainty associated with $E_{\mathrm{T}}^{\mathrm{miss}}$ reconstruction is about 0.3% of the expected SR background yield.

For the data-driven multijet background, which contributes very little to the SR and CRs, a 50% normalisation uncertainty is applied in order to fully cover discrepancies between the observed data and the SM expectation in control regions enhanced in multijet background.

8.2 Theoretical modelling uncertainties

A number of systematic uncertainties arise in the theoretical modelling of the signal and background processes detailed in section 3, and these were estimated using various strategies. All samples include theoretical-uncertainty estimates from variations of the matrix-element factorisation and renormalisation scales (μ_{f} and μ_{r}), and from standard PDF-set variations that capture the statistical and modelling uncertainties in the PDF fits.

Signal-modelling systematic uncertainties. The systematic uncertainties in the modelling of the high-mass Y/T-quark signal sample which correspond to the choice of PDF set were evaluated following the PDF4LHC15 prescription [104]. No further systematic uncertainties in the signal modelling, and no uncertainties in the NLO signal-production cross-section, are considered. In addition, a uniform systematic uncertainty of about 2.5% is applied to cover small differences in the reconstructed VLQ mass between signal samples passed through the full simulation of the detector and signal samples produced with the faster simulation.

Background-modelling systematic uncertainties. For the $t\bar{t}$ process, NLO+LO QCD effects on the top-quark kinematics are considered a source of systematic uncertainty. Three effects were combined into one nuisance parameterisation to account for systematic uncertainties in initial-state radiation (ISR): the POWHEG h_{damp} parameter was varied from the nominal $1.5m_t$ to $3m_t$; the scales μ_{f} and μ_{r} were raised and lowered by factors of two; and the Var3c set of parameter variations were applied in the parton shower's A14 tune [78]. In addition, the QCD final-state radiation (FSR) uncertainty was estimated by varying the strong coupling constant α_{s} in the PYTHIA parton shower.

For single top-quark production, the "diagram subtraction" scheme [81] was considered as an alternative to the nominal "diagram removal" scheme for treating overlap between $t\bar{t}$ and Wt final states, with the full difference between the two methods applied as a shape and normalisation uncertainty [105]. The effect of a possible overestimation of ISR was evaluated by comparing the nominal sample with one obtained by doubling the renormalisation and factorisation scales and choosing the "Var3cDown" weight of the A14 tune [106]. The effect of a possible underestimation of ISR was evaluated by comparing the nominal sample with one produced with h_{damp} increased to $3m_t$, the renormalisation and factorisation scales halved, and using the "Var3cUp" weight of the A14 tune. The size of the uncertainty in the modelling of FSR was estimated by doubling or halving the renormalisation scale for emissions from the parton shower.

The normalisations of the $t\bar{t}$ and W+jets backgrounds are treated as free parameters in the fit and hence no *a priori* uncertainty is assigned to them. The normalisation of the single-top background is assigned an uncertainty of 6.8% [107]. For the W+jets and Z+jets processes modelled using SHERPA, systematic uncertainties from the choice of generator were estimated via comparison with the MADGRAPH5_AMC@NLO alternative samples. The modelling of the Z+jets and diboson background processes includes a 5% effect from their normalisation to the theoretical NNLO or NLO cross-section, respectively [108–110]. Since both of these backgrounds are very small, this effect is applied as an uncertainty in the sum of the predicted Z+jets and diboson backgrounds.

All normalisation uncertainties in the different background processes are treated as uncorrelated. For background estimates based on simulations, the largest theoretical modelling uncertainties are due to the choice of parton shower and hadronisation model (2%–4%), the choice of generator (about 1%–3% in the expected background yield), and varying the parameters controlling the initial- and final-state radiation (about 0.1% in the expected background yield), where the theoretical modelling uncertainties from $t\bar{t}$ contribute the most.

The uncertainty from the data-driven reweighting of the W+jets and $t\bar{t}$ simulations, described in section 7, was estimated as 100% of the difference between those samples with and without the reweighting factors applied. The reweighting and other modelling uncertainties are not treated as being correlated between W+light and W+HF, so the fit has the freedom to further correct W+light and W+HF differently if needed. These uncertainties were separated into independent sources of systematic uncertainty in the three p_{T}^{W} subregions for the statistical fit.

9 Results

9.1 Statistical interpretation

Testing for the presence of a VLQ signal is performed through binned profile-likelihood fits of the models to the data, incorporating the previously estimated systematic uncertainties via nuisance parameters. The inputs to the fit are the binned distributions of reconstructed VLQ candidate mass m_{VLQ} in the SR and the two CRs, each subdivided into low, middle, and high W-boson p_{T}. An independent parameter fit was performed for each signal hypothesis — a combination of VLQ flavour, multiplet, mass and coupling.

The binned likelihood function $\mathcal{L}(\mu, \theta)$ is constructed as a product of Poisson probability terms over all m_{VLQ} bins in the SR and CRs. For each model point, this function depends on the signal-strength parameter μ, which multiplies the nominal theoretical prediction of the signal-production cross-section, and the set of nuisance parameters θ, which encode the effects of systematic uncertainties in the signal and background expectations. The systematic uncertainties are implemented as unit Gaussian constraints on the nuisance parameters, which interpolate model variations of the m_{VLQ} spectrum away from the nominal estimates, as well as unconstrained scale factors for the nominal $t\bar{t}$ and W+jets background normalisations. Uncertainties in each bin of the m_{VLQ} distributions due to the finite size of the simulation samples are included using dedicated fit parameters and are propagated to the signal-strength parameter μ.

The nuisance parameters θ allow variations of the expectations for signal and background according to the corresponding systematic uncertainties, and their fitted values $\hat{\theta}$ correspond to the deviations from the nominal expectations which globally provide the best fit to the data. This procedure reduces the impact of systematic uncertainties on the search sensitivity by taking advantage of the well-populated background-dominated CRs included in the likelihood fit to provide data-driven constraints from phase-space regions close to the SR, and allowing the CRs to improve the description of the data by using non-BSM aspects of the statistical model.

For models where interference plays a role, $\sqrt{\mu}$ replaces μ as the signal-strength parameter varied in the fit. This applies to the signal S, interference I, and background B as

$$\mu \cdot S + \sqrt{\mu} \cdot I + B\,,$$

where the interference term I is obtained as described in section 3.1. Due to the size of the interference effect, a uniform uncertainty of 2.5% is assigned to the interference term.

The test statistic q_μ is defined as the profile log-likelihood ratio, $q_\mu = -2\ln[\mathcal{L}(\mu, \hat{\hat{\theta}}_\mu)/\mathcal{L}(\hat{\mu}, \hat{\theta})]$, where $\hat{\mu}$ and $\hat{\theta}$ are the values of the parameters that maximise the likelihood function (with the constraint $0 \leq \hat{\mu} \leq \mu$), and $\hat{\hat{\theta}}_\mu$ are the values of the nuisance parameters that maximise the likelihood function conditional on a fixed value of μ. For models including interference, the nominal-μ test statistic $q_{1,0} = -2\ln[\mathcal{L}(1, \hat{\hat{\theta}}_1)/\mathcal{L}(0, \hat{\hat{\theta}}_0)]$ (with doubly conditional θ optimisation), is used instead to stabilise the profiling [111].

In the absence of any significant deviation from the background expectation, q_μ and q_0 are used in the asymptotic approximation of the $\mathrm{CL_s}$ method [112–114] to set an upper limit on the signal-production cross-section times branching ratio. For a given signal scenario, values of the production cross-section (parameterised by μ) which yield $\mathrm{CL_s} < 0.05$ are excluded at 95% confidence level (CL). In interference-sensitive model interpretations using the $q_{1,0}$ test statistic, the limit bands are calculated using the modified method described in ref. [111].

9.2 Background-only fit

First, a fit to the data is performed for the background-only hypothesis, i.e. it depends only on θ, with $\mu = 0$. Figure 5 presents the m_{VLQ} distributions after the simultaneous fit of the SR, W+jets CR, and $t\bar{t}$ CR, each split into the low-, middle- and high-p_{T}^{W} subregions used in the fit. The fitted values of the overall normalisation factors for W+light, W+HF and $t\bar{t}$ contributions are found to be 0.87 ± 0.17, 1.09 ± 0.24, and 1.08 ± 0.15, respectively. It is possible to extract separate factors for W+light and W+HF due to the p_{T}^{W}-based splitting in both the W+jets and $t\bar{t}$ CRs. The background model and the data are in good agreement, also in the validation regions. The tables 6–8 show the yields after the fit, including their statistical and systematic uncertainties. Note that the uncertainty on the total background after the fit is smaller than the quadratic sum of the components, because of correlations in the post-fit uncertainties.

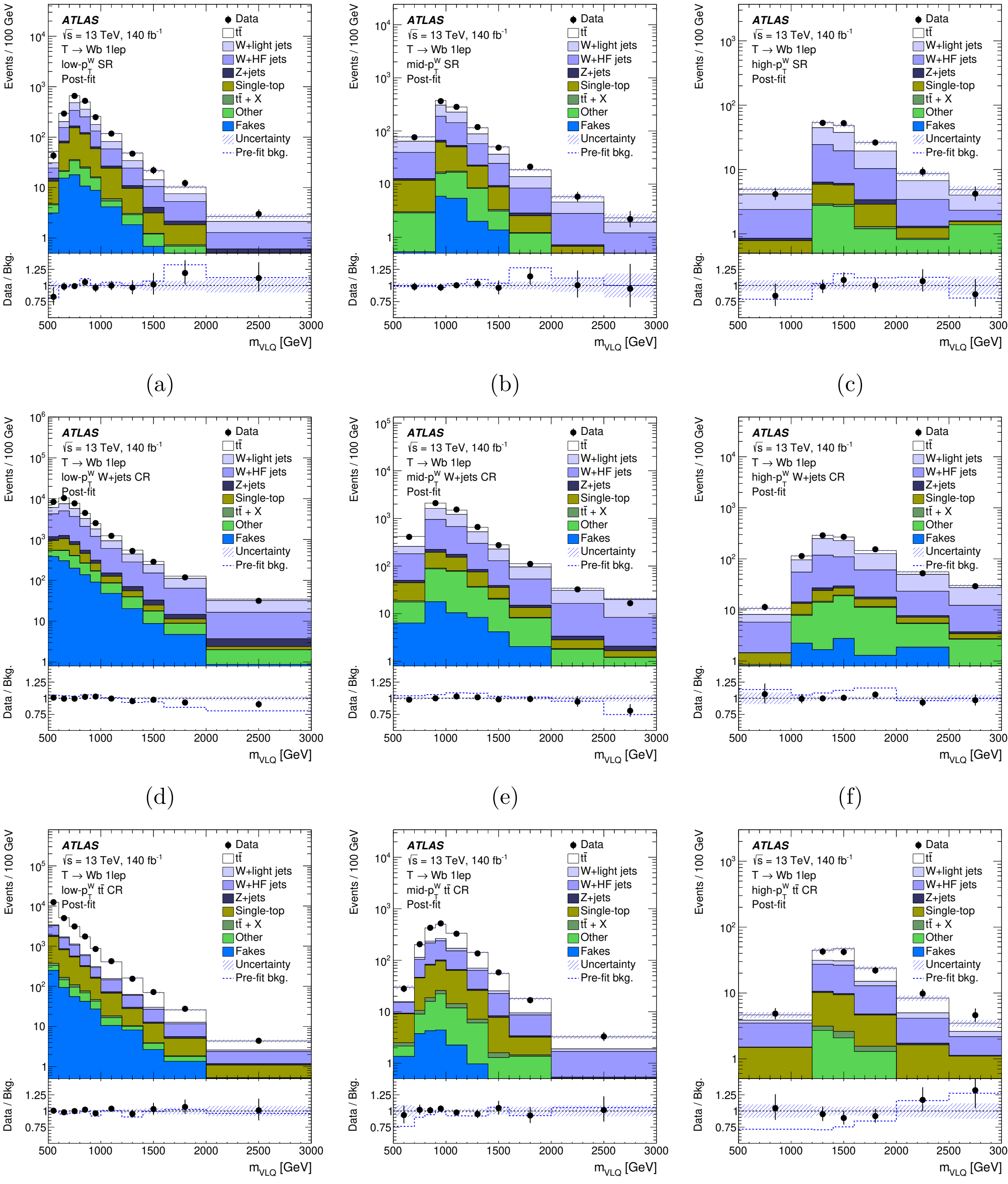

(a) (b) (c)

(d) (e) (f)

(g) (h) (i)

Figure 5. Distributions of the VLQ-candidate mass, m_{VLQ}, in the (a–c) SRs, (d–f) W+jets CRs and (g–i) $t\bar{t}$ CRs after the fit to the background-only hypothesis. The columns correspond from left to right to the low-, middle-, and high-p_{T}^{W} bins in each region. “Other” includes remaining backgrounds from top quarks or that contain two W/Z bosons. The last bin includes overflow. The lower panels show the ratios of data to the fitted total prediction. The error bars represent the statistical uncertainty of the data. The band represents the total systematic uncertainty after the maximum-likelihood fit. The dashed line represents the data-to-background ratio before the fit. The worst agreement is in the low-p_{T}^{W} subregion of the W+jets CR, where the χ^2 probabilities before and after the fit are 0.018 and 0.57, respectively.

	W+jets low-p_{T}^{W}	W+jets mid-p_{T}^{W}	W+jets high-p_{T}^{W}
$t\bar{t}$	9800 ± 1400	2420 ± 320	330 ± 120
W+light jets	9700 ± 1800	3600 ± 700	1100 ± 200
W+HF jets	13 900 ± 3000	3700 ± 930	740 ± 230
Z+jets	866 ± 67	163 ± 42	24.2 ± 3.1
Single top	1630 ± 490	560 ± 260	76 ± 42
$t\bar{t}V$	36.6 ± 4.2	19.2 ± 2.5	6.17 ± 0.93
$t\bar{t}H$	7.87 ± 0.93	2.36 ± 0.30	0.55 ± 0.10
Other	957 ± 66	429 ± 38	140 ± 15
Fakes (e)	320 ± 160	18.5 ± 9.2	17.9 ± 8.8
Fakes (μ)	970 ± 450	94 ± 43	12.7 ± 5.8
Total background	38 210 ± 210	11 020 ± 110	2410 ± 50
Data	38 191	11 046	2425

Table 6. W+jets control region yields after the background-only fit.

	$t\bar{t}$ CR low-p_{T}^{W}	$t\bar{t}$ CR mid-p_{T}^{W}	$t\bar{t}$ CR high-p_{T}^{W}
$t\bar{t}$	16 890 ± 840	1120 ± 140	122 ± 36
W+light jets	410 ± 120	117 ± 33	34.7 ± 9.8
W+HF jets	3240 ± 710	640 ± 160	130 ± 40
Z+jets	274 ± 35	22.0 ± 3.2	3.24 ± 0.91
Single top	2940 ± 740	340 ± 130	56 ± 35
$t\bar{t}V$	67.2 ± 7.1	13.4 ± 1.8	3.56 ± 0.62
$t\bar{t}H$	30.0 ± 3.1	3.59 ± 0.43	0.599 ± 0.087
Other	234 ± 22	72 ± 13	17.7 ± 4.8
Fakes (e)	137 ± 68	3.3 ± 1.6	1.54 ± 0.76
Fakes (μ)	380 ± 170	21.0 ± 9.6	2.2 ± 1.0
Total background	24 600 ± 180	2354 ± 48	371 ± 18
Data	24 582	2348	363

Table 7. $t\bar{t}$ control region yields after the background-only fit.

	SR low-p_{T}^{W}		SR mid-p_{T}^{W}		SR high-p_{T}^{W}	
$t\bar{t}$	650	$\pm\,120$	345	$\pm\,71$	87	$\pm\,36$
W+light jets	443	$\pm\,88$	499	$\pm\,98$	150	$\pm\,30$
W+HF jets	570	$\pm\,130$	550	$\pm\,130$	116	$\pm\,36$
Z+jets	47.3	$\pm\,6.5$	20.6	$\pm\,2.9$	4.70	$\pm\,0.97$
Single top	371	$\pm\,97$	189	$\pm\,53$	23	$\pm\,19$
$t\bar{t}V$	5.2	$\pm\,1.3$	3.76	$\pm\,0.94$	1.20	$\pm\,0.25$
$t\bar{t}H$	1.62	$\pm\,0.23$	0.768	$\pm\,0.096$	0.240	$\pm\,0.055$
Other	51.1	$\pm\,7.7$	63.1	$\pm\,8.8$	24.7	$\pm\,3.6$
Fakes (e)	27	$\pm\,13$	16.5	$\pm\,8.1$	2.0	$\pm\,1.0$
Fakes (μ)	46	$\pm\,21$	11.7	$\pm\,5.4$	2.5	$\pm\,1.1$
Total background	2212	$\pm\,49$	1696	$\pm\,40$	412	$\pm\,19$
Data	2217		1694		412	

Table 8. Signal region yields after the background-only fit.

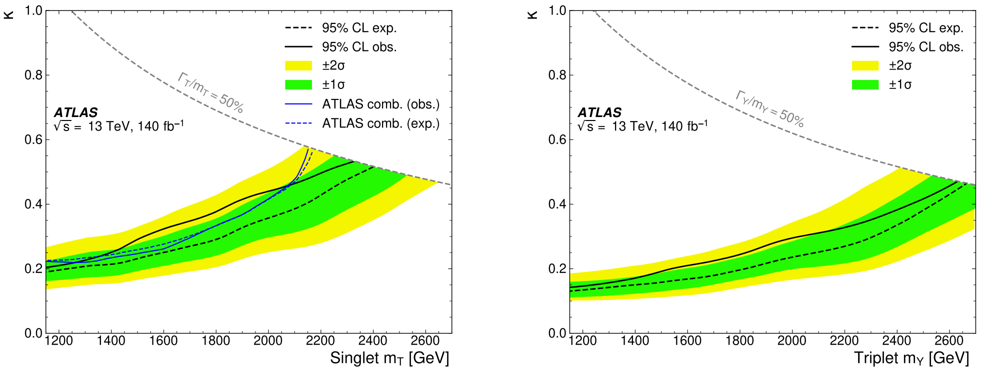

(a)

(b)

Figure 6. Expected (background-only) and observed 95% CL upper limits on the VLQ coupling κ as functions of the VLQ mass m_Q, for T-singlet (a) and Y-triplet (b) vector-like quarks. The green and yellow bands indicate the systematic uncertainties which are profiled in the fit for the observed upper limits. For the T-singlet model, the result of the latest ATLAS combination of searches for single vector-like top-quarks [115] is overlaid; this includes the decay modes $T \to Ht$ and $T \to Zt$. These interpretations are limited to parameter combinations for which the model corrections are valid, by restricting the VLQ relative width to $\Gamma_Q/m_Q < 0.5$, as indicated by the grey dashed line.

9.3 Limits on VLQ production

When fitting the signal models to the data, the largest observed local signal significance is 1.5σ, corresponding to a local p-value of 0.064, at a mass of 1500 GeV. In addition, since the background-only fit shows compatibility with the data, profile-likelihood fits are performed with upper-limit test statistics [114], to obtain the expected and observed 95% CL exclusion constraints on the T/Y VLQ models. The models considered all have a single active VLQ species through a combination of multiplet structure and chiral couplings. VLQ interference with the SM affects the m_{VLQ} distribution in two models (the T-singlet, and left-handed Y in a (T, B, Y) triplet); for these, interference effects (σ_{I}) are accounted for, as described in section 9.1, although in the case of the Y these are negligible.

Scans over m_Q versus κ are presented for the T-singlet and Y-triplet in figure 6. As in ref. [65], these interpretations are limited to regions of model space in which $\Gamma_Q/m_Q < 0.5$, to ensure the validity of the correction factors for the finite-width approximation and non-resonant contributions, as noted in section 3. Upper limits at 95% CL are set on the single-Q production cross-section times $Q \to Wb$ branching ratio as a function of the VLQ mass for a coupling value of $\kappa = 0.5$, and range from 40 fb to 9 fb between m_{VLQ} values of 1.2 TeV and 2.5 TeV. The effect of the different theory cross-sections in the two VLQ models is visible: in the Y-triplet model, with a higher theory cross-section, a given cross-section limit is reached with a lower κ multiplier, resulting in stronger κ limits. The T-singlet 95% CL upper limit on κ ranges from 0.22 at the lowest masses to 0.52 at $m_Q \approx 2300$ GeV; at this point the high relative width of the VLQ reaches the edge of validity for the NLO and finite-width corrections. Due to its higher theory cross-section, more stringent limits are set for the Y-triplet, ranging from $\kappa < 0.14$ at the lowest mass to $\kappa < 0.46$ at $m_Q = 2600$ GeV. The largest contributions to the uncertainty come from systematic effects in the $t\bar{t}$ and single-top MC generators and the $t\bar{t}$ and W+jets reweighting procedure, affecting the high-p_{T}^{W} regions especially.

10 Conclusion

A search for the production of a single vector-like quark Q decaying into Wb, where Q can be either a T or Y quark, has been performed with the ATLAS experiment at the CERN LHC. The data used in this search correspond to an integrated luminosity of $140\,\mathrm{fb}^{-1}$ of pp collisions with a centre-of-mass energy $\sqrt{s} = 13$ TeV recorded between 2015 and 2018, and supersedes the previous ATLAS search for this process performed with $36.1\,\mathrm{fb}^{-1}$ of data taken in 2015 and 2016.

Events with exactly one isolated electron or muon, a high-p_{T} b-tagged jet, missing transverse momentum, and at least one forward jet were selected. A Q candidate was then reconstructed and its mass used as the discriminating variable in a maximum-likelihood fit in bins of p_{T}^{W}. The observed data distributions are compatible with the expected Standard Model background and no significant excess is observed.

The results were interpreted for $Q = T$ in a T-singlet model and $Q = Y$ in a (T, B, Y) triplet, taking into account the effects of signal-model interference with the Standard Model background. Upper limits at 95% CL were set on the single-Q production cross-section times $Q \to Wb$ branching ratio as a function of the VLQ mass for a coupling value of $\kappa = 0.5$, and limits were set on κ, assuming the theory production cross-sections for the VLQ models.

These results complement those of a similar ATLAS search in the fully hadronic final state, while reinforcing and extending the mass coverage of ATLAS' single-VLQ upper limits. The observed limits are slightly weaker than the expectation, making the present search less constraining than the current ATLAS single $T \to Ht$ and $T \to Zt$ search combination, instead of setting stronger limits across the considered mass range as expected. However, they will provide important contributions to future combinations of searches sensitive to BSM physics.

Acknowledgments

We thank CERN for the very successful operation of the LHC and its injectors, as well as the support staff at CERN and at our institutions worldwide without whom ATLAS could not be operated efficiently.

The crucial computing support from all WLCG partners is acknowledged gratefully, in particular from CERN, the ATLAS Tier-1 facilities at TRIUMF/SFU (Canada), NDGF (Denmark, Norway, Sweden), CC-IN2P3 (France), KIT/GridKA (Germany), INFN-CNAF (Italy), NL-T1 (Netherlands), PIC (Spain), RAL (U.K.) and BNL (U.S.A.), the Tier-2 facilities worldwide and large non-WLCG resource providers. Major contributors of computing resources are listed in ref. [116].

We gratefully acknowledge the support of ANPCyT, Argentina; YerPhI, Armenia; ARC, Australia; BMWFW and FWF, Austria; ANAS, Azerbaijan; CNPq and FAPESP, Brazil; NSERC, NRC and CFI, Canada; CERN; ANID, Chile; CAS, MOST and NSFC, China; Minciencias, Colombia; MEYS CR, Czech Republic; DNRF and DNSRC, Denmark; IN2P3-CNRS and CEA-DRF/IRFU, France; SRNSFG, Georgia; BMFTR, HGF and MPG, Germany; GSRI, Greece; RGC and Hong Kong SAR, China; ICHEP and Academy of Sciences and Humanities, Israel; INFN, Italy; MEXT and JSPS, Japan; CNRST, Morocco; NWO, Netherlands; RCN, Norway; MNiSW, Poland; FCT, Portugal; MNE/IFA, Romania; MSTDI, Serbia; MSSR, Slovakia; ARIS and MVZI, Slovenia; DSI/NRF, South Africa; MICIU/AEI, Spain; SRC and Wallenberg Foundation, Sweden; SERI, SNSF and Cantons of Bern and Geneva, Switzerland; NSTC, Taipei; TENMAK, Türkiye; STFC/UKRI, United Kingdom; DOE and NSF, United States of America.

Individual groups and members have received support from BCKDF, CANARIE, CRC and DRAC, Canada; CERN-CZ, FORTE and PRIMUS, Czech Republic; COST, ERC, ERDF, Horizon 2020, ICSC-NextGenerationEU and Marie Skłodowska-Curie Actions, European Union; Investissements d'Avenir Labex, Investissements d'Avenir Idex and ANR, France; DFG and AvH Foundation, Germany; Herakleitos, Thales and Aristeia programmes co-financed by EU-ESF and the Greek NSRF, Greece; BSF-NSF and MINERVA, Israel; NCN and NAWA, Poland; La Caixa Banking Foundation, CERCA Programme Generalitat de Catalunya and PROMETEO and GenT Programmes Generalitat Valenciana, Spain; Göran Gustafssons Stiftelse, Sweden; The Royal Society and Leverhulme Trust, United Kingdom.

In addition, individual members wish to acknowledge support from Armenia: Yerevan Physics Institute (FAPERJ); CERN: European Organization for Nuclear Research (CERN DOCT); Chile: Agencia Nacional de Investigación y Desarrollo (FONDECYT 1230812, FONDECYT 1240864, Fondecyt 3240661, Fondecyt Regular 1240721); China: Chinese Ministry of Science and Technology (MOST-2023YFA1605700, MOST-2023YFA1609300), National Natural Science Foundation of China (NSFC — 12175119, NSFC 12275265); Czech Republic: Czech Science Foundation (GACR — 24-11373S), Ministry of Education Youth and Sports (ERC-CZ-LL2327, FORTE CZ.02.01.01/00/22_008/0004632), PRIMUS Research Programme (PRIMUS/21/SCI/017); EU: H2020 European Research Council (ERC — 101002463); European Union: European Research Council (BARD No. 101116429, ERC — 948254, ERC 101089007), European Regional Development Fund (SMASH COFUND 101081355, SLO ERDF), Horizon 2020 Framework Programme (MUCCA — CHIST-ERA-19-XAI-00), European Union, Future Artificial Intelligence Research (FAIR-NextGenerationEU PE00000013), Horizon 2020 (EuroHPC — EHPC-DEV-2024D11-051), Italian Center for High Performance Computing, Big Data and Quantum Computing (ICSC, NextGenerationEU); France: Agence Nationale de la Recherche (ANR-21-CE31-0022, ANR-22-EDIR-0002, ANR-24-CE31-0504-01); Germany: Baden-Württemberg Stiftung (BW Stiftung-Postdoc Eliteprogramme), Deutsche Forschungsgemeinschaft (DFG — 469666862, DFG — CR 312/5-2); China: Research Grants Council (GRF); Italy: Istituto Nazionale di Fisica Nucleare (ICSC, NextGenerationEU), Ministero dell'Università e della Ricerca (NextGenEU 153D23001490006 M4C2.1.1, NextGenEU I53D23000820006 M4C2.1.1, NextGenEU I53D23001490006 M4C2.1.1); Japan: Japan Society for the Promotion of Science (JSPS KAKENHI JP22H01227, JSPS KAKENHI JP22H04944, JSPS KAKENHI JP22KK0227, JSPS KAKENHI JP23KK0245, JSPS KAKENHI JP24K23939); Norway: Research Council of Norway (RCN-314472); Poland: Ministry of Science and Higher Education (IDUB AGH, POB8, D4 no 9722), Polish National Science Centre (NCN 2021/42/E/ST2/00350, NCN OPUS 2023/51/B/ST2/02507, NCN OPUS nr 2022/47/B/ST2/03059, NCN UMO-2019/34/E/ST2/00393, UMO-2022/47/O/ST2/00148, UMO-2023/49/B/ST2/04085, UMO-2023/51/B/ST2/00920, UMO-2024/53/N/ST2/00869); Portugal: Foundation for Science and Technology (FCT); Spain: Generalitat Valenciana (Artemisa, FEDER, IDIFEDER/2018/048), Ministry of Science and Innovation (MCIN & NextGenEU PCI2022-135018-2, MICIN & FEDER PID2021-125273NB, RYC2019-028510-I, RYC2020-030254-I, RYC2021-031273-I, RYC2022-038164-I); Sweden: Carl Trygger Foundation (Carl Trygger Foundation CTS 22:2312), Swedish Research Council (Swedish Research Council 2023-04654, VR 2021-03651, VR 2022-03845, VR 2022-04683, VR 2023-03403, VR 2024-05451), Knut and Alice Wallenberg Foundation (KAW 2018.0458, KAW 2022.0358, KAW 2023.0366); Switzerland: Swiss National Science Foundation (SNSF — PCEFP2_194658); United Kingdom: Leverhulme Trust (Leverhulme Trust RPG-2020-004), Royal Society (NIF-R1-231091); United States of America: U.S. Department of Energy (ECA DE-AC02-76SF00515), Neubauer Family Foundation.

Data Availability Statement. The public release of data supporting the findings of this article will follow the CERN Open Data Policy [117]. The values of relevant plots and tables associated with this article are stored in HEPData: `https://www.hepdata.net/record/161563`.

Code Availability Statement. The ATLAS Collaboration's Athena software, including the configuration of the event generators, is open source (`http://gitlab.cern.ch/atlas/athena`).

References

[1] J.A. Aguilar-Saavedra, R. Benbrik, S. Heinemeyer and M. Pérez-Victoria, *Handbook of vectorlike quarks: mixing and single production*, *Phys. Rev. D* **88** (2013) 094010 [arXiv:1306.0572] [INSPIRE].

[2] ATLAS collaboration, *Observation of a new particle in the search for the Standard Model Higgs boson with the ATLAS detector at the LHC*, *Phys. Lett. B* **716** (2012) 1 [arXiv:1207.7214] [INSPIRE].

[3] CMS collaboration, *Observation of a new boson at a mass of 125 GeV with the CMS experiment at the LHC*, *Phys. Lett. B* **716** (2012) 30 [arXiv:1207.7235] [INSPIRE].

[4] O. Eberhardt et al., *Impact of a Higgs boson at a mass of 126 GeV on the standard model with three and four fermion generations*, *Phys. Rev. Lett.* **109** (2012) 241802 [arXiv:1209.1101] [INSPIRE].

[5] L. Randall and R. Sundrum, *A large mass hierarchy from a small extra dimension*, *Phys. Rev. Lett.* **83** (1999) 3370 [hep-ph/9905221] [INSPIRE].

[6] D.B. Kaplan, H. Georgi and S. Dimopoulos, *Composite Higgs scalars*, *Phys. Lett. B* **136** (1984) 187 [INSPIRE].

[7] N. Vignaroli, *Discovering the composite Higgs through the decay of a heavy fermion*, *JHEP* **07** (2012) 158 [`arXiv:1204.0468`] [INSPIRE].

[8] M. Schmaltz and D. Tucker-Smith, *Little Higgs review*, *Ann. Rev. Nucl. Part. Sci.* **55** (2005) 229 [`hep-ph/0502182`] [INSPIRE].

[9] S.P. Martin, *Extra vector-like matter and the lightest Higgs scalar boson mass in low-energy supersymmetry*, *Phys. Rev. D* **81** (2010) 035004 [`arXiv:0910.2732`] [INSPIRE].

[10] M.-L. Xiao and J.-H. Yu, *Stabilizing electroweak vacuum in a vectorlike fermion model*, *Phys. Rev. D* **90** (2014) 014007 [*Addendum ibid.* **90** (2014) 019901] [`arXiv:1404.0681`] [INSPIRE].

[11] F. del Aguila and M.J. Bowick, *The possibility of new fermions with $\Delta I = 0$ mass*, *Nucl. Phys. B* **224** (1983) 107 [INSPIRE].

[12] G. Cacciapaglia et al., *Heavy vector-like top partners at the LHC and flavour constraints*, *JHEP* **03** (2012) 070 [`arXiv:1108.6329`] [INSPIRE].

[13] K.S. Babu and J. Julio, *Radiative neutrino mass generation through vector-like quarks*, *Phys. Rev. D* **85** (2012) 073005 [`arXiv:1112.5452`] [INSPIRE].

[14] R. Franceschini and R.N. Mohapatra, *Radiatively induced type II seesaw models and vectorlike 5/3 charge quarks*, *Phys. Rev. D* **89** (2014) 055013 [`arXiv:1306.6108`] [INSPIRE].

[15] A. Batra et al., *Axion framework with color-mediated Dirac neutrino masses*, *Phys. Lett. B* **868** (2025) 139629 [`arXiv:2501.13156`] [INSPIRE].

[16] ATLAS collaboration, *Search for single-production of vector-like quarks decaying into Wb in the fully hadronic final state in pp collisions at $\sqrt{s} = 13$ TeV with the ATLAS detector*, *JHEP* **02** (2025) 075 [`arXiv:2409.20273`] [INSPIRE].

[17] ATLAS collaboration, *Search for pair-produced vectorlike quarks coupling to light quarks in the lepton plus jets final state using 13 TeV pp collisions with the ATLAS detector*, *Phys. Rev. D* **110** (2024) 052009 [`arXiv:2405.19862`] [INSPIRE].

[18] A. De Simone, O. Matsedonskyi, R. Rattazzi and A. Wulzer, *A first top partner Hunter's guide*, *JHEP* **04** (2013) 004 [`arXiv:1211.5663`] [INSPIRE].

[19] O. Matsedonskyi, G. Panico and A. Wulzer, *On the interpretation of top partners searches*, *JHEP* **12** (2014) 097 [`arXiv:1409.0100`] [INSPIRE].

[20] ATLAS collaboration, *Search for pair and single production of new heavy quarks that decay to a Z boson and a third-generation quark in pp collisions at $\sqrt{s} = 8$ TeV with the ATLAS detector*, *JHEP* **11** (2014) 104 [`arXiv:1409.5500`] [INSPIRE].

[21] ATLAS collaboration, *Search for single production of vector-like quarks decaying into Wb in pp collisions at $\sqrt{s} = 8$ TeV with the ATLAS detector*, *Eur. Phys. J. C* **76** (2016) 442 [`arXiv:1602.05606`] [INSPIRE].

[22] ATLAS collaboration, *Search for pair- and single-production of vector-like quarks in final states with at least one Z boson decaying into a pair of electrons or muons in pp collision data collected with the ATLAS detector at $\sqrt{s} = 13$ TeV*, *Phys. Rev. D* **98** (2018) 112010 [`arXiv:1806.10555`] [INSPIRE].

[23] ATLAS collaboration, *Search for single production of vector-like quarks decaying into Wb in pp collisions at $\sqrt{s} = 13$ TeV with the ATLAS detector*, *JHEP* **05** (2019) 164 [`arXiv:1812.07343`] [INSPIRE].

[24] CMS collaboration, *Search for single production of a heavy vector-like T quark decaying to a Higgs boson and a top quark with a lepton and jets in the final state*, *Phys. Lett. B* **771** (2017) 80 [`arXiv:1612.00999`] [INSPIRE].

[25] CMS collaboration, *Search for electroweak production of a vector-like quark decaying to a top quark and a Higgs boson using boosted topologies in fully hadronic final states*, *JHEP* **04** (2017) 136 [`arXiv:1612.05336`] [INSPIRE].

[26] CMS collaboration, *Search for single production of a vector-like T quark decaying to a Z boson and a top quark in proton-proton collisions at $\sqrt{s} = 13$ TeV*, *Phys. Lett. B* **781** (2018) 574 [`arXiv:1708.01062`] [INSPIRE].

[27] M. Buchkremer, G. Cacciapaglia, A. Deandrea and L. Panizzi, *Model independent framework for searches of top partners*, *Nucl. Phys. B* **876** (2013) 376 [`arXiv:1305.4172`] [INSPIRE].

[28] ATLAS collaboration, *Search for production of vector-like quark pairs and of four top quarks in the lepton-plus-jets final state in pp collisions at $\sqrt{s} = 8$ TeV with the ATLAS detector*, *JHEP* **08** (2015) 105 [`arXiv:1505.04306`] [INSPIRE].

[29] ATLAS collaboration, *Search for pair production of vector-like top quarks in events with one lepton, jets, and missing transverse momentum in $\sqrt{s} = 13$ TeV pp collisions with the ATLAS detector*, *JHEP* **08** (2017) 052 [`arXiv:1705.10751`] [INSPIRE].

[30] CMS collaboration, *Search for vector-like T quarks decaying to top quarks and Higgs bosons in the all-hadronic channel using jet substructure*, *JHEP* **06** (2015) 080 [`arXiv:1503.01952`] [INSPIRE].

[31] CMS collaboration, *Inclusive search for a vector-like T quark with charge $\frac{2}{3}$ in pp collisions at $\sqrt{s} = 8$ TeV*, *Phys. Lett. B* **729** (2014) 149 [`arXiv:1311.7667`] [INSPIRE].

[32] CMS collaboration, *Search for pair production of vector-like quarks in the $bW\bar{b}W$ channel from proton-proton collisions at $\sqrt{s} = 13$ TeV*, *Phys. Lett. B* **779** (2018) 82 [`arXiv:1710.01539`] [INSPIRE].

[33] ATLAS collaboration, *Analysis of events with b-jets and a pair of leptons of the same charge in pp collisions at $\sqrt{s} = 8$ TeV with the ATLAS detector*, *JHEP* **10** (2015) 150 [`arXiv:1504.04605`] [INSPIRE].

[34] ATLAS collaboration, *Search for pair production of up-type vector-like quarks and for four-top-quark events in final states with multiple b-jets with the ATLAS detector*, *JHEP* **07** (2018) 089 [`arXiv:1803.09678`] [INSPIRE].

[35] CMS collaboration, *Search for pair production of vector-like T and B quarks in single-lepton final states using boosted jet substructure in proton-proton collisions at $\sqrt{s} = 13$ TeV*, *JHEP* **11** (2017) 085 [`arXiv:1706.03408`] [INSPIRE].

[36] CMS collaboration, *Search for single production of vector-like quarks decaying to a Z boson and a top or a bottom quark in proton-proton collisions at $\sqrt{s} = 13$ TeV*, *JHEP* **05** (2017) 029 [`arXiv:1701.07409`] [INSPIRE].

[37] ATLAS collaboration, *Search for pair production of heavy vector-like quarks decaying to high-p_T W bosons and b quarks in the lepton-plus-jets final state in pp collisions at $\sqrt{s} = 13$ TeV with the ATLAS detector*, *JHEP* **10** (2017) 141 [`arXiv:1707.03347`] [INSPIRE].

[38] CMS collaboration, *Search for vector-like T and B quark pairs in final states with leptons at $\sqrt{s} = 13$ TeV*, *JHEP* **08** (2018) 177 [`arXiv:1805.04758`] [INSPIRE].

[39] CMS collaboration, *Search for single production of vector-like quarks decaying into a b quark and a W boson in proton-proton collisions at $\sqrt{s} = 13$ TeV*, Phys. Lett. B **772** (2017) 634 [arXiv:1701.08328] [INSPIRE].

[40] ATLAS collaboration, *Combination of the searches for pair-produced vector-like partners of the third-generation quarks at $\sqrt{s} = 13$ TeV with the ATLAS detector*, Phys. Rev. Lett. **121** (2018) 211801 [arXiv:1808.02343] [INSPIRE].

[41] A. Buckley et al., *New sensitivity of current LHC measurements to vector-like quarks*, SciPost Phys. **9** (2020) 069 [arXiv:2006.07172] [INSPIRE].

[42] ATLAS collaboration, *Luminosity determination in pp collisions at $\sqrt{s} = 13$ TeV using the ATLAS detector at the LHC*, Eur. Phys. J. C **83** (2023) 982 [arXiv:2212.09379] [INSPIRE].

[43] G. Avoni et al., *The new LUCID-2 detector for luminosity measurement and monitoring in ATLAS*, 2018 *JINST* **13** P07017 [INSPIRE].

[44] ATLAS collaboration, *Performance of electron and photon triggers in ATLAS during LHC run 2*, Eur. Phys. J. C **80** (2020) 47 [arXiv:1909.00761] [INSPIRE].

[45] ATLAS collaboration, *Performance of the ATLAS muon triggers in run 2*, 2020 *JINST* **15** P09015 [arXiv:2004.13447] [INSPIRE].

[46] ATLAS collaboration, *ATLAS data quality operations and performance for 2015–2018 data-taking*, 2020 *JINST* **15** P04003 [arXiv:1911.04632] [INSPIRE].

[47] ATLAS collaboration, *The ATLAS experiment at the CERN Large Hadron Collider*, 2008 *JINST* **3** S08003 [INSPIRE].

[48] L. Evans and P. Bryant, *LHC machine*, 2008 *JINST* **3** S08001 [INSPIRE].

[49] ATLAS collaboration, *ATLAS Insertable B-Layer technical design report*, CERN-LHCC-2010-013, CERN, Geneva, Switzerland (2010) [INSPIRE].

[50] ATLAS IBL collaboration, *Production and integration of the ATLAS Insertable B-Layer*, 2018 *JINST* **13** T05008 [arXiv:1803.00844] [INSPIRE].

[51] ATLAS collaboration, *Performance of the ATLAS trigger system in 2015*, Eur. Phys. J. C **77** (2017) 317 [arXiv:1611.09661] [INSPIRE].

[52] ATLAS collaboration, *Software and computing for run 3 of the ATLAS experiment at the LHC*, Eur. Phys. J. C **85** (2025) 234 [arXiv:2404.06335] [INSPIRE].

[53] ATLAS collaboration, *The ATLAS simulation infrastructure*, Eur. Phys. J. C **70** (2010) 823 [arXiv:1005.4568] [INSPIRE].

[54] GEANT4 collaboration, *GEANT4 — a simulation toolkit*, Nucl. Instrum. Meth. A **506** (2003) 250 [INSPIRE].

[55] T. Sjöstrand, S. Mrenna and P.Z. Skands, *A brief introduction to PYTHIA 8.1*, Comput. Phys. Commun. **178** (2008) 852 [arXiv:0710.3820] [INSPIRE].

[56] T. Gleisberg et al., *Event generation with SHERPA 1.1*, JHEP **02** (2009) 007 [arXiv:0811.4622] [INSPIRE].

[57] D.J. Lange, *The EvtGen particle decay simulation package*, Nucl. Instrum. Meth. A **462** (2001) 152 [INSPIRE].

[58] G. Cacciapaglia et al., *Next-to-leading-order predictions for single vector-like quark production at the LHC*, Phys. Lett. B **793** (2019) 206 [arXiv:1811.05055] [INSPIRE].

[59] J. Alwall et al., *The automated computation of tree-level and next-to-leading order differential cross sections, and their matching to parton shower simulations*, *JHEP* **07** (2014) 079 [`arXiv:1405.0301`] [INSPIRE].

[60] R.D. Ball et al., *Parton distributions with LHC data*, *Nucl. Phys. B* **867** (2013) 244 [`arXiv:1207.1303`] [INSPIRE].

[61] T. Sjöstrand et al., *An introduction to PYTHIA 8.2*, *Comput. Phys. Commun.* **191** (2015) 159 [`arXiv:1410.3012`] [INSPIRE].

[62] ATLAS collaboration, *ATLAS Pythia 8 tunes to 7 TeV data*, ATL-PHYS-PUB-2014-021, CERN, Geneva, Switzerland (2014) [INSPIRE].

[63] A. Roy, N. Nikiforou, N. Castro and T. Andeen, *Novel interpretation strategy for searches of singly produced vectorlike quarks at the LHC*, *Phys. Rev. D* **101** (2020) 115027 [`arXiv:2003.00640`] [INSPIRE].

[64] A. Roy and T. Andeen, *Non-resonant diagrams for single production of top and bottom partners*, *Phys. Lett. B* **833** (2022) 137330 [`arXiv:2202.02640`] [INSPIRE].

[65] A. Deandrea et al., *Single production of vector-like quarks: the effects of large width, interference and NLO corrections*, *JHEP* **08** (2021) 107 [*Erratum ibid.* **11** (2022) 028] [`arXiv:2105.08745`] [INSPIRE].

[66] P. Nason, *A new method for combining NLO QCD with shower Monte Carlo algorithms*, *JHEP* **11** (2004) 040 [`hep-ph/0409146`] [INSPIRE].

[67] S. Frixione, P. Nason and C. Oleari, *Matching NLO QCD computations with parton shower simulations: the POWHEG method*, *JHEP* **11** (2007) 070 [`arXiv:0709.2092`] [INSPIRE].

[68] S. Alioli, P. Nason, C. Oleari and E. Re, *A general framework for implementing NLO calculations in shower Monte Carlo programs: the POWHEG BOX*, *JHEP* **06** (2010) 043 [`arXiv:1002.2581`] [INSPIRE].

[69] NNPDF collaboration, *Parton distributions for the LHC run II*, *JHEP* **04** (2015) 040 [`arXiv:1410.8849`] [INSPIRE].

[70] M. Cacciari et al., *Top-pair production at hadron colliders with next-to-next-to-leading logarithmic soft-gluon resummation*, *Phys. Lett. B* **710** (2012) 612 [`arXiv:1111.5869`] [INSPIRE].

[71] M. Beneke, P. Falgari, S. Klein and C. Schwinn, *Hadronic top-quark pair production with NNLL threshold resummation*, *Nucl. Phys. B* **855** (2012) 695 [`arXiv:1109.1536`] [INSPIRE].

[72] P. Bärnreuther, M. Czakon and A. Mitov, *Percent level precision physics at the Tevatron: first genuine NNLO QCD corrections to $q\bar{q} \to t\bar{t} + X$*, *Phys. Rev. Lett.* **109** (2012) 132001 [`arXiv:1204.5201`] [INSPIRE].

[73] M. Czakon and A. Mitov, *NNLO corrections to top-pair production at hadron colliders: the all-fermionic scattering channels*, *JHEP* **12** (2012) 054 [`arXiv:1207.0236`] [INSPIRE].

[74] M. Czakon and A. Mitov, *NNLO corrections to top pair production at hadron colliders: the quark-gluon reaction*, *JHEP* **01** (2013) 080 [`arXiv:1210.6832`] [INSPIRE].

[75] M. Czakon, P. Fiedler and A. Mitov, *Total top-quark pair-production cross section at hadron colliders through $O(\alpha_S^4)$*, *Phys. Rev. Lett.* **110** (2013) 252004 [`arXiv:1303.6254`] [INSPIRE].

[76] M. Czakon and A. Mitov, *Top++: a program for the calculation of the top-pair cross-section at hadron colliders*, *Comput. Phys. Commun.* **185** (2014) 2930 [`arXiv:1112.5675`] [INSPIRE].

[77] J.H. Kühn, A. Scharf and P. Uwer, *Weak interactions in top-quark pair production at hadron colliders: an update*, Phys. Rev. D **91** (2015) 014020 [`arXiv:1305.5773`] [INSPIRE].

[78] ATLAS collaboration, *Studies on top-quark Monte Carlo modelling with Sherpa and MG5_aMC@NLO*, ATL-PHYS-PUB-2017-007, CERN, Geneva, Switzerland (2017) [INSPIRE].

[79] M. Bähr et al., *Herwig++ physics and manual*, Eur. Phys. J. C **58** (2008) 639 [`arXiv:0803.0883`] [INSPIRE].

[80] S. Frixione, E. Laenen, P. Motylinski and B.R. Webber, *Single-top production in MC@NLO*, JHEP **03** (2006) 092 [`hep-ph/0512250`] [INSPIRE].

[81] S. Frixione et al., *Single-top hadroproduction in association with a W boson*, JHEP **07** (2008) 029 [`arXiv:0805.3067`] [INSPIRE].

[82] S. Höche, F. Krauss, S. Schumann and F. Siegert, *QCD matrix elements and truncated showers*, JHEP **05** (2009) 053 [`arXiv:0903.1219`] [INSPIRE].

[83] T. Gleisberg and S. Höche, *Comix, a new matrix element generator*, JHEP **12** (2008) 039 [`arXiv:0808.3674`] [INSPIRE].

[84] F. Cascioli, P. Maierhöfer and S. Pozzorini, *Scattering amplitudes with OpenLoops*, Phys. Rev. Lett. **108** (2012) 111601 [`arXiv:1111.5206`] [INSPIRE].

[85] S. Schumann and F. Krauss, *A parton shower algorithm based on Catani-Seymour dipole factorisation*, JHEP **03** (2008) 038 [`arXiv:0709.1027`] [INSPIRE].

[86] S. Höche, F. Krauss, M. Schönherr and F. Siegert, *QCD matrix elements + parton showers: the NLO case*, JHEP **04** (2013) 027 [`arXiv:1207.5030`] [INSPIRE].

[87] ATLAS collaboration, *Electron and photon performance measurements with the ATLAS detector using the 2015–2017 LHC proton-proton collision data*, 2019 JINST **14** P12006 [`arXiv:1908.00005`] [INSPIRE].

[88] ATLAS collaboration, *Muon reconstruction and identification efficiency in ATLAS using the full Run 2 pp collision data set at* $\sqrt{s} = 13$ TeV, Eur. Phys. J. C **81** (2021) 578 [`arXiv:2012.00578`] [INSPIRE].

[89] M. Cacciari, G.P. Salam and G. Soyez, *The anti-*k_t *jet clustering algorithm*, JHEP **04** (2008) 063 [`arXiv:0802.1189`] [INSPIRE].

[90] M. Cacciari, G.P. Salam and G. Soyez, *FastJet user manual*, Eur. Phys. J. C **72** (2012) 1896 [`arXiv:1111.6097`] [INSPIRE].

[91] ATLAS collaboration, *Jet energy scale and resolution measured in proton–proton collisions at* $\sqrt{s} = 13$ *TeV with the ATLAS detector*, Eur. Phys. J. C **81** (2021) 689 [`arXiv:2007.02645`] [INSPIRE].

[92] ATLAS collaboration, *Jet reconstruction and performance using particle flow with the ATLAS detector*, Eur. Phys. J. C **77** (2017) 466 [`arXiv:1703.10485`] [INSPIRE].

[93] ATLAS collaboration, *Selection of jets produced in 13TeV proton-proton collisions with the ATLAS detector*, ATLAS-CONF-2015-029, CERN, Geneva, Switzerland (2015) [INSPIRE].

[94] ATLAS collaboration, *Performance of pile-up mitigation techniques for jets in pp collisions at* $\sqrt{s} = 8$ *TeV using the ATLAS detector*, Eur. Phys. J. C **76** (2016) 581 [`arXiv:1510.03823`] [INSPIRE].

[95] ATLAS collaboration, *Forward jet vertex tagging using the particle flow algorithm*, ATL-PHYS-PUB-2019-026, CERN, Geneva, Switzerland (2019) [INSPIRE].

[96] ATLAS collaboration, *ATLAS flavour-tagging algorithms for the LHC run 2 pp collision dataset*, *Eur. Phys. J. C* **83** (2023) 681 [`arXiv:2211.16345`] [INSPIRE].

[97] ATLAS collaboration, *Identification of jets containing b-hadrons with recurrent neural networks at the ATLAS experiment*, ATL-PHYS-PUB-2017-003, CERN, Geneva, Switzerland (2017) [INSPIRE].

[98] ATLAS collaboration, *ATLAS b-jet identification performance and efficiency measurement with $t\bar{t}$ events in pp collisions at $\sqrt{s} = 13$ TeV*, *Eur. Phys. J. C* **79** (2019) 970 [`arXiv:1907.05120`] [INSPIRE].

[99] ATLAS collaboration, *Measurement of the c-jet mistagging efficiency in $t\bar{t}$ events using pp collision data at $\sqrt{s} = 13$ TeV collected with the ATLAS detector*, *Eur. Phys. J. C* **82** (2022) 95 [`arXiv:2109.10627`] [INSPIRE].

[100] ATLAS collaboration, *Calibration of the light-flavour jet mistagging efficiency of the b-tagging algorithms with Z+jets events using 139 fb^{-1} of ATLAS proton–proton collision data at $\sqrt{s} = 13$ TeV*, *Eur. Phys. J. C* **83** (2023) 728 [`arXiv:2301.06319`] [INSPIRE].

[101] ATLAS collaboration, *The performance of missing transverse momentum reconstruction and its significance with the ATLAS detector using 140 fb^{-1} of $\sqrt{s} = 13$ TeV pp collisions*, *Eur. Phys. J. C* **85** (2025) 606 [`arXiv:2402.05858`] [INSPIRE].

[102] M. Czakon et al., *Top-pair production at the LHC through NNLO QCD and NLO EW*, *JHEP* **10** (2017) 186 [`arXiv:1705.04105`] [INSPIRE].

[103] ATLAS collaboration, *Measurements of b-jet tagging efficiency with the ATLAS detector using $t\bar{t}$ events at $\sqrt{s} = 13$ TeV*, *JHEP* **08** (2018) 089 [`arXiv:1805.01845`] [INSPIRE].

[104] J. Butterworth et al., *PDF4LHC recommendations for LHC run II*, *J. Phys. G* **43** (2016) 023001 [`arXiv:1510.03865`] [INSPIRE].

[105] C.D. White, S. Frixione, E. Laenen and F. Maltoni, *Isolating Wt production at the LHC*, *JHEP* **11** (2009) 074 [`arXiv:0908.0631`] [INSPIRE].

[106] ATLAS collaboration, *Study of top-quark pair modelling and uncertainties using ATLAS measurements at $\sqrt{s} = 13$ TeV*, ATL-PHYS-PUB-2020-023, CERN, Geneva, Switzerland (2020) [INSPIRE].

[107] N. Kidonakis, *Two-loop soft anomalous dimensions for single top quark associated production with a W^- or H^-*, *Phys. Rev. D* **82** (2010) 054018 [`arXiv:1005.4451`] [INSPIRE].

[108] K. Melnikov and F. Petriello, *Electroweak gauge boson production at hadron colliders through $O(\alpha_s^2)$*, *Phys. Rev. D* **74** (2006) 114017 [`hep-ph/0609070`] [INSPIRE].

[109] J.M. Campbell and R.K. Ellis, *An update on vector boson pair production at hadron colliders*, *Phys. Rev. D* **60** (1999) 113006 [`hep-ph/9905386`] [INSPIRE].

[110] C. Anastasiou, L.J. Dixon, K. Melnikov and F. Petriello, *High precision QCD at hadron colliders: electroweak gauge boson rapidity distributions at NNLO*, *Phys. Rev. D* **69** (2004) 094008 [`hep-ph/0312266`] [INSPIRE].

[111] ATLAS collaboration, *Search for heavy neutral Higgs bosons decaying into a top quark pair in 140 fb^{-1} of proton-proton collision data at $\sqrt{s} = 13$ TeV with the ATLAS detector*, *JHEP* **08** (2024) 013 [`arXiv:2404.18986`] [INSPIRE].

[112] T. Junk, *Confidence level computation for combining searches with small statistics*, *Nucl. Instrum. Meth. A* **434** (1999) 435 [`hep-ex/9902006`] [INSPIRE].

[113] A.L. Read, *Presentation of search results: the CL_s technique*, *J. Phys. G* **28** (2002) 2693 [INSPIRE].

[114] G. Cowan, K. Cranmer, E. Gross and O. Vitells, *Asymptotic formulae for likelihood-based tests of new physics*, *Eur. Phys. J. C* **71** (2011) 1554 [*Erratum ibid.* **73** (2013) 2501] [`arXiv:1007.1727`] [INSPIRE].

[115] ATLAS collaboration, *Combination of searches for singly produced vectorlike top quarks in pp collisions at $\sqrt{s} = 13$ TeV with the ATLAS detector*, *Phys. Rev. D* **111** (2025) 012012 [`arXiv:2408.08789`] [INSPIRE].

[116] ATLAS collaboration, *ATLAS computing acknowledgements*, ATL-SOFT-PUB-2025-001, CERN, Geneva, Switzerland (2025) [INSPIRE].

[117] CERN, *CERN open data policy for the LHC experiments*, CERN-OPEN-2020-013, CERN, Geneva, Switzerland (2020).

The ATLAS collaboration

G. Aad[104], E. Aakvaag[17], B. Abbott[123], S. Abdelhameed[119a], K. Abeling[55], N.J. Abicht[49], S.H. Abidi[30], M. Aboelela[45], A. Aboulhorma[36e], H. Abramowicz[157], Y. Abulaiti[120], B.S. Acharya[69a,69b,n], A. Ackermann[63a], C. Adam Bourdarios[4], L. Adamczyk[87a], S.V. Addepalli[149], M.J. Addison[103], J. Adelman[118], A. Adiguzel[22c], T. Adye[137], A.A. Affolder[139], Y. Afik[40], M.N. Agaras[13], A. Aggarwal[102], C. Agheorghiesei[28c], F. Ahmadov[39,ae], S. Ahuja[97], X. Ai[143b], G. Aielli[76a,76b], A. Aikot[169], M. Ait Tamlihat[36e], B. Aitbenchikh[36a], M. Akbiyik[102], T.P.A. Åkesson[100], A.V. Akimov[151], D. Akiyama[174], N.N. Akolkar[25], S. Aktas[22a], G.L. Alberghi[24b], J. Albert[171], P. Albicocco[53], G.L. Albouy[60], S. Alderweireldt[52], Z.L. Alegria[124], M. Aleksa[37], I.N. Aleksandrov[39], C. Alexa[28b], T. Alexopoulos[10], F. Alfonsi[24b], M. Algren[56], M. Alhroob[173], B. Ali[135], H.M.J. Ali[93,x], S. Ali[32], S.W. Alibocus[94], M. Aliev[34c], G. Alimonti[71a], W. Alkakhi[55], C. Allaire[66], B.M.M. Allbrooke[152], J.S. Allen[103], J.F. Allen[52], P.P. Allport[21], A. Aloisio[72a,72b], F. Alonso[92], C. Alpigiani[142], Z.M.K. Alsolami[93], A. Alvarez Fernandez[102], M. Alves Cardoso[56], M.G. Alviggi[72a,72b], M. Aly[103], Y. Amaral Coutinho[83b], A. Ambler[106], C. Amelung[37], M. Amerl[103], C.G. Ames[111], T. Amezza[130], D. Amidei[108], B. Amini[54], K. Amirie[161], A. Amirkhanov[39], S.P. Amor Dos Santos[133a], K.R. Amos[169], D. Amperiadou[158], S. An[84], C. Anastopoulos[145], T. Andeen[11], J.K. Anders[94], A.C. Anderson[59], A. Andreazza[71a,71b], S. Angelidakis[9], A. Angerami[42], A.V. Anisenkov[39], A. Annovi[74a], C. Antel[56], E. Antipov[151], M. Antonelli[53], F. Anulli[75a], M. Aoki[84], T. Aoki[159], M.A. Aparo[152], L. Aperio Bella[48], M. Apicella[31], C. Appelt[157], A. Apyan[27], S.J. Arbiol Val[88], C. Arcangeletti[53], A.T.H. Arce[51], J-F. Arguin[110], S. Argyropoulos[158], J.-H. Arling[48], O. Arnaez[4], H. Arnold[151], G. Artoni[75a,75b], H. Asada[113], K. Asai[121], S. Asai[159], S. Asatryan[179], N.A. Asbah[37], R.A. Ashby Pickering[173], A.M. Aslam[97], K. Assamagan[30], R. Astalos[29a], K.S.V. Astrand[100], S. Atashi[165], R.J. Atkin[34a], H. Atmani[36f], P.A. Atmasiddha[131], K. Augsten[135], A.D. Auriol[41], V.A. Austrup[103], G. Avolio[37], K. Axiotis[56], G. Azuelos[110,ai], D. Babal[29b], H. Bachacou[138], K. Bachas[158,r], A. Bachiu[35], E. Bachmann[50], M.J. Backes[63a], A. Badea[40], T.M. Baer[108], P. Bagnaia[75a,75b], M. Bahmani[19], D. Bahner[54], K. Bai[126], J.T. Baines[137], L. Baines[96], O.K. Baker[178], E. Bakos[16], D. Bakshi Gupta[8], L.E. Balabram Filho[83b], V. Balakrishnan[123], R. Balasubramanian[4], E.M. Baldin[38], P. Balek[87a], E. Ballabene[24b,24a], F. Balli[138], L.M. Baltes[63a], W.K. Balunas[33], J. Balz[102], I. Bamwidhi[119b], E. Banas[88], M. Bandieramonte[132], A. Bandyopadhyay[25], S. Bansal[25], L. Barak[157], M. Barakat[48], E.L. Barberio[107], D. Barberis[18b], M. Barbero[104], M.Z. Barel[117], T. Barillari[112], M-S. Barisits[37], T. Barklow[149], P. Baron[136], D.A. Baron Moreno[103], A. Baroncelli[62], A.J. Barr[129], J.D. Barr[98], F. Barreiro[101], J. Barreiro Guimarães da Costa[14], M.G. Barros Teixeira[133a], S. Barsov[38], F. Bartels[63a], R. Bartoldus[149], A.E. Barton[93], P. Bartos[29a], A. Basan[102], M. Baselga[49], S. Bashiri[88], A. Bassalat[66,b], M.J. Basso[162a], S. Bataju[45], R. Bate[170], R.L. Bates[59], S. Batlamous[101], M. Battaglia[139], D. Battulga[19], M. Bauce[75a,75b], M. Bauer[79], P. Bauer[25], L.T. Bayer[48], L.T. Bazzano Hurrell[31], J.B. Beacham[112], T. Beau[130], J.Y. Beaucamp[92], P.H. Beauchemin[164], P. Bechtle[25], H.P. Beck[20,q], K. Becker[173], A.J. Beddall[82], V.A. Bednyakov[39], C.P. Bee[151],

L.J. Beemster[16], M. Begalli[83d], M. Begel[30], J.K. Behr[48], J.F. Beirer[37], F. Beisiegel[25],
M. Belfkir[119b], G. Bella[157], L. Bellagamba[24b], A. Bellerive[35], C.D. Bellgraph[68],
P. Bellos[21], K. Beloborodov[38], D. Benchekroun[36a], F. Bendebba[36a], Y. Benhammou[157],
K.C. Benkendorfer[61], L. Beresford[48], M. Beretta[53], E. Bergeaas Kuutmann[167], N. Berger[4],
B. Bergmann[135], J. Beringer[18a], G. Bernardi[5], C. Bernius[149], F.U. Bernlochner[25],
F. Bernon[37], A. Berrocal Guardia[13], T. Berry[97], P. Berta[136], A. Berthold[50], A. Berti[133a],
R. Bertrand[104], S. Bethke[112], A. Betti[75a,75b], A.J. Bevan[96], L. Bezio[56], N.K. Bhalla[54],
S. Bharthuar[112], S. Bhatta[151], P. Bhattarai[149], Z.M. Bhatti[120], K.D. Bhide[54],
V.S. Bhopatkar[124], R.M. Bianchi[132], G. Bianco[24b,24a], O. Biebel[111], M. Biglietti[77a],
C.S. Billingsley[45], Y. Bimgdi[36f], M. Bindi[55], A. Bingham[177], A. Bingul[22b], C. Bini[75a,75b],
G.A. Bird[33], M. Birman[175], M. Biros[136], S. Biryukov[152], T. Bisanz[49], E. Bisceglie[24b,24a],
J.P. Biswal[137], D. Biswas[147], I. Bloch[48], A. Blue[59], U. Blumenschein[96],
J. Blumenthal[102], V.S. Bobrovnikov[39], M. Boehler[54], B. Boehm[172], D. Bogavac[13],
A.G. Bogdanchikov[38], L.S. Boggia[130], V. Boisvert[97], P. Bokan[37], T. Bold[87a],
M. Bomben[5], M. Bona[96], M. Boonekamp[138], A.G. Borbély[59], I.S. Bordulev[38],
G. Borissov[93], D. Bortoletto[129], D. Boscherini[24b], M. Bosman[13], K. Bouaouda[36a],
N. Bouchhar[169], L. Boudet[4], J. Boudreau[132], E.V. Bouhova-Thacker[93], D. Boumediene[41],
R. Bouquet[57b,57a], A. Boveia[122], J. Boyd[37], D. Boye[30], I.R. Boyko[39], L. Bozianu[56],
J. Bracinik[21], N. Brahimi[4], G. Brandt[177], O. Brandt[33], B. Brau[105], J.E. Brau[126],
R. Brener[175], L. Brenner[117], R. Brenner[167], S. Bressler[175], G. Brianti[78a,78b],
D. Britton[59], D. Britzger[112], I. Brock[25], R. Brock[109], G. Brooijmans[42], A.J. Brooks[68],
E.M. Brooks[162b], E. Brost[30], L.M. Brown[171,162a], L.E. Bruce[61], T.L. Bruckler[129],
P.A. Bruckman de Renstrom[88], B. Brüers[48], A. Bruni[24b], G. Bruni[24b], D. Brunner[47a,47b],
M. Bruschi[24b], N. Bruscino[75a,75b], T. Buanes[17], Q. Buat[142], D. Buchin[112],
A.G. Buckley[59], O. Bulekov[82], B.A. Bullard[149], S. Burdin[94], C.D. Burgard[49],
A.M. Burger[91], B. Burghgrave[8], O. Burlayenko[54], J. Burleson[168], J.C. Burzynski[148],
E.L. Busch[42], V. Büscher[102], P.J. Bussey[59], J.M. Butler[26], C.M. Buttar[59],
J.M. Butterworth[98], W. Buttinger[137], C.J. Buxo Vazquez[109], A.R. Buzykaev[39],
S. Cabrera Urbán[169], L. Cadamuro[66], D. Caforio[58], H. Cai[132], Y. Cai[24b,114c,24a],
Y. Cai[114a], V.M.M. Cairo[37], O. Cakir[3a], N. Calace[37], P. Calafiura[18a], G. Calderini[130],
P. Calfayan[35], G. Callea[59], L.P. Caloba[83b], D. Calvet[41], S. Calvet[41], R. Camacho Toro[130],
S. Camarda[37], D. Camarero Munoz[27], P. Camarri[76a,76b], C. Camincher[171],
M. Campanelli[98], A. Camplani[43], V. Canale[72a,72b], A.C. Canbay[3a], E. Canonero[97],
J. Cantero[169], Y. Cao[168], F. Capocasa[27], M. Capua[44b,44a], A. Carbone[71a,71b],
R. Cardarelli[76a], J.C.J. Cardenas[8], M.P. Cardiff[27], G. Carducci[44b,44a], T. Carli[37],
G. Carlino[72a], J.I. Carlotto[13], B.T. Carlson[132,s], E.M. Carlson[171], J. Carmignani[94],
L. Carminati[71a,71b], A. Carnelli[4], M. Carnesale[37], S. Caron[116], E. Carquin[140f],
I.B. Carr[107], S. Carrá[73a,73b], G. Carratta[24b,24a], A.M. Carroll[126], M.P. Casado[13,i],
M. Caspar[48], F.L. Castillo[4], L. Castillo Garcia[13], V. Castillo Gimenez[169],
N.F. Castro[133a,133e], A. Catinaccio[37], J.R. Catmore[128], T. Cavaliere[4], V. Cavaliere[30],
L.J. Caviedes Betancourt[23b], Y.C. Cekmecelioglu[48], E. Celebi[82], S. Cella[37], V. Cepaitis[56],
K. Cerny[125], A.S. Cerqueira[83a], A. Cerri[74a,74b,al], L. Cerrito[76a,76b], F. Cerutti[18a],
B. Cervato[71a,71b], A. Cervelli[24b], G. Cesarini[53], S.A. Cetin[82], P.M. Chabrillat[130],

S. Chakraborty[173], J. Chan[18a], W.Y. Chan[159], J.D. Chapman[33], E. Chapon[138],
B. Chargeishvili[155b], D.G. Charlton[21], C. Chauhan[136], Y. Che[114a], S. Chekanov[6],
S.V. Chekulaev[162a], G.A. Chelkov[39,a], B. Chen[157], B. Chen[171], H. Chen[114a], H. Chen[30],
J. Chen[144a], J. Chen[148], M. Chen[129], S. Chen[89], S.J. Chen[114a], X. Chen[144a],
X. Chen[15,ah], Z. Chen[62], C.L. Cheng[176], H.C. Cheng[64a], S. Cheong[149], A. Cheplakov[39],
E. Cherepanova[117], R. Cherkaoui El Moursli[36e], E. Cheu[7], K. Cheung[65], L. Chevalier[138],
V. Chiarella[53], G. Chiarelli[74a], G. Chiodini[70a], A.S. Chisholm[21], A. Chitan[28b],
M. Chitishvili[169], M.V. Chizhov[39,t], K. Choi[11], Y. Chou[142], E.Y.S. Chow[116],
K.L. Chu[175], M.C. Chu[64a], X. Chu[14,114c], Z. Chubinidze[53], J. Chudoba[134],
J.J. Chwastowski[88], D. Cieri[112], K.M. Ciesla[87a], V. Cindro[95], A. Ciocio[18a],
F. Cirotto[72a,72b], Z.H. Citron[175], M. Citterio[71a], D.A. Ciubotaru[28b], A. Clark[56],
P.J. Clark[52], N. Clarke Hall[98], C. Clarry[161], S.E. Clawson[48], C. Clement[47a,47b],
Y. Coadou[104], M. Cobal[69a,69c], A. Coccaro[57b], R.F. Coelho Barrue[133a],
R. Coelho Lopes De Sa[105], S. Coelli[71a], L.S. Colangeli[161], B. Cole[42], P. Collado Soto[101],
J. Collot[60], R. Coluccia[70a,70b], P. Conde Muiño[133a,133g], M.P. Connell[34c], S.H. Connell[34c],
E.I. Conroy[129], M. Contreras Cossio[11], F. Conventi[72a,aj], H.G. Cooke[21],
A.M. Cooper-Sarkar[129], L. Corazzina[75a,75b], F.A. Corchia[24b,24a], A. Cordeiro Oudot Choi[142],
L.D. Corpe[41], M. Corradi[75a,75b], F. Corriveau[106,ac], A. Cortes-Gonzalez[159], M.J. Costa[169],
F. Costanza[4], D. Costanzo[145], B.M. Cote[122], J. Couthures[4], G. Cowan[97], K. Cranmer[176],
L. Cremer[49], D. Cremonini[24b,24a], S. Crépé-Renaudin[60], F. Crescioli[130], T. Cresta[73a,73b],
M. Cristinziani[147], M. Cristoforetti[78a,78b], V. Croft[117], J.E. Crosby[124], G. Crosetti[44b,44a],
A. Cueto[101], H. Cui[98], Z. Cui[7], W.R. Cunningham[59], F. Curcio[169], J.R. Curran[52],
M.J. Da Cunha Sargedas De Sousa[57b,57a], J.V. Da Fonseca Pinto[83b], C. Da Via[103],
W. Dabrowski[87a], T. Dado[37], S. Dahbi[154], T. Dai[108], D. Dal Santo[20], C. Dallapiccola[105],
M. Dam[43], G. D'amen[30], V. D'Amico[111], J. Damp[102], J.R. Dandoy[35], D. Dannheim[37],
G. D'anniballe[74a,74b], M. Danninger[148], V. Dao[151], G. Darbo[57b], S.J. Das[30],
F. Dattola[48], S. D'Auria[71a,71b], A. D'Avanzo[72a,72b], T. Davidek[136], J. Davidson[173],
I. Dawson[96], K. De[8], C. De Almeida Rossi[161], R. De Asmundis[72a], N. De Biase[48],
S. De Castro[24b,24a], N. De Groot[116], P. de Jong[117], H. De la Torre[118], A. De Maria[114a],
A. De Salvo[75a], U. De Sanctis[76a,76b], F. De Santis[70a,70b], A. De Santo[152],
J.B. De Vivie De Regie[60], J. Debevc[95], D.V. Dedovich[39], J. Degens[94], A.M. Deiana[45],
J. Del Peso[101], L. Delagrange[130], F. Deliot[138], C.M. Delitzsch[49], M. Della Pietra[72a,72b],
D. Della Volpe[56], A. Dell'Acqua[37], L. Dell'Asta[71a,71b], M. Delmastro[4], C.C. Delogu[102],
P.A. Delsart[60], S. Demers[178], M. Demichev[39], S.P. Denisov[38], H. Denizli[22a,m],
L. D'Eramo[41], D. Derendarz[88], F. Derue[130], P. Dervan[94,*], K. Desch[25],
F.A. Di Bello[57b,57a], A. Di Ciaccio[76a,76b], L. Di Ciaccio[4], A. Di Domenico[75a,75b],
C. Di Donato[72a,72b], A. Di Girolamo[37], G. Di Gregorio[37], A. Di Luca[78a,78b],
B. Di Micco[77a,77b], R. Di Nardo[77a,77b], K.F. Di Petrillo[40], M. Diamantopoulou[35],
F.A. Dias[117], M.A. Diaz[140a,140b], A.R. Didenko[39], M. Didenko[169], S.D. Diefenbacher[18a],
E.B. Diehl[108], S. Díez Cornell[48], C. Diez Pardos[147], C. Dimitriadi[150], A. Dimitrievska[21],
A. Dimri[151], J. Dingfelder[25], T. Dingley[129], I-M. Dinu[28b], S.J. Dittmeier[63b], F. Dittus[37],
M. Divisek[136], B. Dixit[94], F. Djama[104], T. Djobava[155b], C. Doglioni[103,100],
A. Dohnalova[29a], Z. Dolezal[136], K. Domijan[87a], K.M. Dona[40], M. Donadelli[83d],

B. Dong[109], J. Donini[41], A. D'Onofrio[72a,72b], M. D'Onofrio[94], J. Dopke[137], A. Doria[72a],
N. Dos Santos Fernandes[133a], P. Dougan[103], M.T. Dova[92], A.T. Doyle[59], M.A. Draguet[129],
M.P. Drescher[55], E. Dreyer[175], I. Drivas-koulouris[10], M. Drnevich[120], M. Drozdova[56],
D. Du[62], T.A. du Pree[117], Z. Duan[114a], F. Dubinin[39], M. Dubovsky[29a], E. Duchovni[175],
G. Duckeck[111], P.K. Duckett[98], O.A. Ducu[28b], D. Duda[52], A. Dudarev[37], E.R. Duden[27],
M. D'uffizi[103], L. Duflot[66], M. Dührssen[37], I. Duminica[28g], A.E. Dumitriu[28b],
M. Dunford[63a], S. Dungs[49], K. Dunne[47a,47b], A. Duperrin[104], H. Duran Yildiz[3a],
M. Düren[58], A. Durglishvili[155b], D. Duvnjak[35], B.L. Dwyer[118], G.I. Dyckes[18a],
M. Dyndal[87a], B.S. Dziedzic[37], Z.O. Earnshaw[152], G.H. Eberwein[129], B. Eckerova[29a],
S. Eggebrecht[55], E. Egidio Purcino De Souza[83e], G. Eigen[17], K. Einsweiler[18a],
T. Ekelof[167], P.A. Ekman[100], S. El Farkh[36b], Y. El Ghazali[62], H. El Jarrari[37],
A. El Moussaouy[36a], V. Ellajosyula[167], M. Ellert[167], F. Ellinghaus[177], N. Ellis[37],
J. Elmsheuser[30], M. Elsawy[119a], M. Elsing[37], D. Emeliyanov[137], Y. Enari[84], I. Ene[18a],
S. Epari[110], D. Ernani Martins Neto[88], F. Ernst[37], M. Errenst[177], M. Escalier[66],
C. Escobar[169], E. Etzion[157], G. Evans[133a,133b], H. Evans[68], L.S. Evans[97], A. Ezhilov[38],
S. Ezzarqtouni[36a], F. Fabbri[24b,24a], L. Fabbri[24b,24a], G. Facini[98], V. Fadeyev[139],
R.M. Fakhrutdinov[38], D. Fakoudis[102], S. Falciano[75a], L.F. Falda Ulhoa Coelho[133a],
F. Fallavollita[112], G. Falsetti[44b,44a], J. Faltova[136], C. Fan[168], K.Y. Fan[64b], Y. Fan[14],
Y. Fang[14,114c], M. Fanti[71a,71b], M. Faraj[69a,69b], Z. Farazpay[99], A. Farbin[8], A. Farilla[77a],
T. Farooque[109], J.N. Farr[178], S.M. Farrington[137,52], F. Fassi[36e], D. Fassouliotis[9],
L. Fayard[66], P. Federic[136], P. Federicova[134], O.L. Fedin[38,a], M. Feickert[176],
L. Feligioni[104], D.E. Fellers[18a], C. Feng[143a], Z. Feng[117], M.J. Fenton[165], L. Ferencz[48],
B. Fernandez Barbadillo[93], P. Fernandez Martinez[67], M.J.V. Fernoux[104], J. Ferrando[93],
A. Ferrari[167], P. Ferrari[117,116], R. Ferrari[73a], D. Ferrere[56], C. Ferretti[108], M.P. Fewell[1],
D. Fiacco[75a,75b], F. Fiedler[102], P. Fiedler[135], S. Filimonov[39], M.S. Filip[28b,u],
A. Filipčič[95], E.K. Filmer[162a], F. Filthaut[116], M.C.N. Fiolhais[133a,133c,c], L. Fiorini[169],
W.C. Fisher[109], T. Fitschen[103], P.M. Fitzhugh[138], I. Fleck[147], P. Fleischmann[108],
T. Flick[177], M. Flores[34d,ag], L.R. Flores Castillo[64a], L. Flores Sanz De Acedo[37],
F.M. Follega[78a,78b], N. Fomin[33], J.H. Foo[161], A. Formica[138], A.C. Forti[103], E. Fortin[37],
A.W. Fortman[18a], L. Foster[18a], L. Fountas[9,j], D. Fournier[66], H. Fox[93],
P. Francavilla[74a,74b], S. Francescato[61], S. Franchellucci[56], M. Franchini[24b,24a],
S. Franchino[63a], D. Francis[37], L. Franco[116], V. Franco Lima[37], L. Franconi[48],
M. Franklin[61], G. Frattari[27], Y.Y. Frid[157], J. Friend[59], N. Fritzsche[37], A. Froch[56],
D. Froidevaux[37], J.A. Frost[129], Y. Fu[109], S. Fuenzalida Garrido[140f], M. Fujimoto[104],
K.Y. Fung[64a], E. Furtado De Simas Filho[83e], M. Furukawa[159], J. Fuster[169], A. Gaa[55],
A. Gabrielli[24b,24a], A. Gabrielli[161], P. Gadow[37], G. Gagliardi[57b,57a], L.G. Gagnon[18a],
S. Gaid[85b], S. Galantzan[157], J. Gallagher[1], E.J. Gallas[129], A.L. Gallen[167],
B.J. Gallop[137], K.K. Gan[122], S. Ganguly[159], Y. Gao[52], A. Garabaglu[142],
F.M. Garay Walls[140a,140b], C. García[169], A. Garcia Alonso[117], A.G. Garcia Caffaro[178],
J.E. García Navarro[169], M. Garcia-Sciveres[18a], G.L. Gardner[131], R.W. Gardner[40],
N. Garelli[164], R.B. Garg[149], J.M. Gargan[52], C.A. Garner[161], C.M. Garvey[34a],
V.K. Gassmann[164], G. Gaudio[73a], V. Gautam[13], P. Gauzzi[75a,75b], J. Gavranovic[95],
I.L. Gavrilenko[133a], A. Gavrilyuk[38], C. Gay[170], G. Gaycken[126], E.N. Gazis[10], A. Gekow[122],

C. Gemme[57b], M.H. Genest[60], A.D. Gentry[115], S. George[97], T. Geralis[46], A.A. Gerwin[123], P. Gessinger-Befurt[37], M.E. Geyik[177], M. Ghani[173], K. Ghorbanian[96], A. Ghosal[147], A. Ghosh[165], A. Ghosh[7], B. Giacobbe[24b], S. Giagu[75a,75b], T. Giani[117], A. Giannini[62], S.M. Gibson[97], M. Gignac[139], D.T. Gil[87b], A.K. Gilbert[87a], B.J. Gilbert[42], D. Gillberg[35], G. Gilles[117], D.M. Gingrich[2,ai], M.P. Giordani[69a,69c], P.F. Giraud[138], G. Giugliarelli[69a,69c], D. Giugni[71a], F. Giuli[76a,76b], I. Gkialas[9,j], L.K. Gladilin[38], C. Glasman[101], M. Glazewska[20], R.M. Gleason[165], G. Glemža[48], M. Glisic[126], I. Gnesi[44b], Y. Go[30], M. Goblirsch-Kolb[37], B. Gocke[49], D. Godin[110], B. Gokturk[22a], S. Goldfarb[107], T. Golling[56], M.G.D. Gololo[34c], D. Golubkov[38], J.P. Gombas[109], A. Gomes[133a,133b], G. Gomes Da Silva[147], A.J. Gomez Delegido[169], R. Gonçalo[133a], L. Gonella[21], A. Gongadze[155c], F. Gonnella[21], J.L. Gonski[149], R.Y. González Andana[52], S. González de la Hoz[169], M.V. Gonzalez Rodrigues[48], R. Gonzalez Suarez[167], S. Gonzalez-Sevilla[56], L. Goossens[37], B. Gorini[37], E. Gorini[70a,70b], A. Gorišek[95], T.C. Gosart[131], A.T. Goshaw[51], M.I. Gostkin[39], S. Goswami[124], C.A. Gottardo[37], S.A. Gotz[111], M. Gouighri[36b], A.G. Goussiou[142], N. Govender[34c], R.P. Grabarczyk[129], I. Grabowska-Bold[87a], K. Graham[35], E. Gramstad[128], S. Grancagnolo[70a,70b], C.M. Grant[1], P.M. Gravila[28f], F.G. Gravili[70a,70b], H.M. Gray[18a], M. Greco[112], M.J. Green[1], C. Grefe[25], A.S. Grefsrud[17], I.M. Gregor[48], K.T. Greif[165], P. Grenier[149], S.G. Grewe[112], A.A. Grillo[139], K. Grimm[32], S. Grinstein[13,y], J.-F. Grivaz[66], E. Gross[175], J. Grosse-Knetter[55], L. Guan[108], G. Guerrieri[37], R. Guevara[128], R. Gugel[102], J.A.M. Guhit[108], A. Guida[19], E. Guilloton[173], S. Guindon[37], F. Guo[14,114c], J. Guo[144a], L. Guo[48], L. Guo[114b,w], Y. Guo[108], A. Gupta[49], R. Gupta[132], S. Gupta[27], S. Gurbuz[25], S.S. Gurdasani[48], G. Gustavino[75a,75b], P. Gutierrez[123], L.F. Gutierrez Zagazeta[131], M. Gutsche[50], C. Gutschow[98], C. Gwenlan[129], C.B. Gwilliam[94], E.S. Haaland[128], A. Haas[120], M. Habedank[59], C. Haber[18a], H.K. Hadavand[8], A. Haddad[41], A. Hadef[50], A.I. Hagan[93], J.J. Hahn[147], E.H. Haines[98], M. Haleem[172], J. Haley[124], G.D. Hallewell[104], L. Halser[20], K. Hamano[171], M. Hamer[25], S.E.D. Hammoud[66], E.J. Hampshire[97], J. Han[143a], L. Han[114a], L. Han[62], S. Han[18a], K. Hanagaki[84], M. Hance[139], D.A. Hangal[42], H. Hanif[148], M.D. Hank[131], J.B. Hansen[43], P.H. Hansen[43], D. Harada[56], T. Harenberg[177], S. Harkusha[179], M.L. Harris[105], Y.T. Harris[25], J. Harrison[13], N.M. Harrison[122], P.F. Harrison[173], M.L.E. Hart[98], N.M. Hartman[112], N.M. Hartmann[111], R.Z. Hasan[97,137], Y. Hasegawa[146], F. Haslbeck[129], S. Hassan[17], R. Hauser[109], M. Haviernik[136], C.M. Hawkes[21], R.J. Hawkings[37], Y. Hayashi[159], D. Hayden[109], C. Hayes[108], R.L. Hayes[117], C.P. Hays[129], J.M. Hays[96], H.S. Hayward[94], M. He[14,114c], Y. He[48], Y. He[98], N.B. Heatley[96], V. Hedberg[100], C. Heidegger[54], K.K. Heidegger[54], J. Heilman[35], S. Heim[48], T. Heim[18a], J.G. Heinlein[131], J.J. Heinrich[126], L. Heinrich[112], J. Hejbal[134], M. Helbig[50], A. Held[176], S. Hellesund[17], C.M. Helling[170], S. Hellman[47a,47b], A.M. Henriques Correia[37], H. Herde[100], Y. Hernández Jiménez[151], L.M. Herrmann[25], T. Herrmann[50], G. Herten[54], R. Hertenberger[111], L. Hervas[37], M.E. Hesping[102], N.P. Hessey[162a], J. Hessler[112], M. Hidaoui[36b], N. Hidic[136], E. Hill[161], T.S. Hillersoy[17], S.J. Hillier[21], J.R. Hinds[109], F. Hinterkeuser[25], M. Hirose[127], S. Hirose[163], D. Hirschbuehl[177], T.G. Hitchings[103], B. Hiti[95], J. Hobbs[151], R. Hobincu[28e], N. Hod[175], A.M. Hodges[168], M.C. Hodgkinson[145], B.H. Hodkinson[129], A. Hoecker[37], D.D. Hofer[108], J. Hofer[169], M. Holzbock[37], L.B.A.H. Hommels[33], V. Homsak[129], B.P. Honan[103], J.J. Hong[68], T.M. Hong[132], B.H. Hooberman[168], W.H. Hopkins[6], M.C. Hoppesch[168], Y. Horii[113], M.E. Horstmann[112], S. Hou[154], M.R. Housenga[168], A.S. Howard[95], J. Howarth[59], J. Hoya[6], M. Hrabovsky[125], T. Hryn'ova[4], P.J. Hsu[65], S.-C. Hsu[142], T. Hsu[66], M. Hu[18a], Q. Hu[62], S. Huang[33], X. Huang[14,114c], Y. Huang[136], Y. Huang[114b], Y. Huang[102], Y. Huang[14], Z. Huang[66], Z. Hubacek[135], M. Huebner[25], F. Huegging[25], T.B. Huffman[129], M. Hufnagel Maranha De Faria[83a], C.A. Hugli[48], M. Huhtinen[37], S.K. Huiberts[17], R. Hulsken[106], C.E. Hultquist[18a], N. Huseynov[12,g], J. Huston[109], J. Huth[61], R. Hyneman[7], G. Iacobucci[56], G. Iakovidis[30], L. Iconomidou-Fayard[66], J.P. Iddon[37], P. Iengo[72a,72b], R. Iguchi[159], Y. Iiyama[159], T. Iizawa[159], Y. Ikegami[84], D. Iliadis[158], N. Ilic[161], H. Imam[36a], G. Inacio Goncalves[83d], S.A. Infante Cabanas[140c], T. Ingebretsen Carlson[47a,47b], J.M. Inglis[96], G. Introzzi[73a,73b], M. Iodice[77a], V. Ippolito[75a,75b], R.K. Irwin[94], M. Ishino[159], W. Islam[176], C. Issever[19], S. Istin[22a,an], K. Itabashi[84], H. Ito[174], R. Iuppa[78a,78b], A. Ivina[175], V. Izzo[72a], P. Jacka[134], P. Jackson[1], P. Jain[48], K. Jakobs[54], T. Jakoubek[175], J. Jamieson[59], W. Jang[159], S. Jankovych[136], M. Javurkova[105], P. Jawahar[103], L. Jeanty[126], J. Jejelava[155a,af], P. Jenni[54,f], C.E. Jessiman[35], C. Jia[143a], H. Jia[170], J. Jia[151], X. Jia[14,114c], Z. Jia[114a], C. Jiang[52], Q. Jiang[64b], S. Jiggins[48], M. Jimenez Ortega[169], J. Jimenez Pena[13], S. Jin[114a], A. Jinaru[28b], O. Jinnouchi[141], P. Johansson[145], K.A. Johns[7], J.W. Johnson[139], F.A. Jolly[48], D.M. Jones[152], E. Jones[48], K.S. Jones[8], P. Jones[33], R.W.L. Jones[93], T.J. Jones[94], H.L. Joos[55,37], R. Joshi[122], J. Jovicevic[16], X. Ju[18a], J.J. Junggeburth[37], T. Junkermann[63a], A. Juste Rozas[13,y], M.K. Juzek[88], S. Kabana[140e], A. Kaczmarska[88], M. Kado[112], H. Kagan[122], M. Kagan[149], A. Kahn[131], C. Kahra[102], T. Kaji[159], E. Kajomovitz[156], N. Kakati[175], N. Kakoty[13], I. Kalaitzidou[54], S. Kandel[8], N.J. Kang[139], D. Kar[34g], K. Karava[129], E. Karentzos[25], O. Karkout[117], S.N. Karpov[39], Z.M. Karpova[39], V. Kartvelishvili[93], A.N. Karyukhin[38], E. Kasimi[158], J. Katzy[48], S. Kaur[35], K. Kawade[146], M.P. Kawale[123], C. Kawamoto[89], T. Kawamoto[62], E.F. Kay[37], F.I. Kaya[164], S. Kazakos[109], V.F. Kazanin[38], J.M. Keaveney[34a], R. Keeler[171], G.V. Kehris[61], J.S. Keller[35], J.J. Kempster[152], O. Kepka[134], J. Kerr[162b], B.P. Kerridge[137], B.P. Kerševan[95], L. Keszeghova[29a], R.A. Khan[132], A. Khanov[124], A.G. Kharlamov[38], T. Kharlamova[38], E.E. Khoda[142], M. Kholodenko[133a], T.J. Khoo[19], G. Khoriauli[172], Y. Khoulaki[36a], J. Khubua[155b,*], Y.A.R. Khwaira[130], B. Kibirige[34g], D. Kim[6], D.W. Kim[47a,47b], Y.K. Kim[40], N. Kimura[98], M.K. Kingston[55], A. Kirchhoff[55], C. Kirfel[25], F. Kirfel[25], J. Kirk[137], A.E. Kiryunin[112], S. Kita[163], O. Kivernyk[25], M. Klassen[164], C. Klein[35], L. Klein[172], M.H. Klein[45], S.B. Klein[56], U. Klein[94], A. Klimentov[30], T. Klioutchnikova[37], P. Kluit[117], S. Kluth[112], E. Kneringer[79], T.M. Knight[161], A. Knue[49], M. Kobel[50], D. Kobylianskii[175], S.F. Koch[129], M. Kocian[149], P. Kodyš[136], D.M. Koeck[126], T. Koffas[35], O. Kolay[50], I. Koletsou[4], T. Komarek[88], K. Köneke[55], A.X.Y. Kong[1], T. Kono[121], N. Konstantinidis[98], P. Kontaxakis[56], B. Konya[100], R. Kopeliansky[42], S. Koperny[87a], K. Korcyl[88], K. Kordas[158,d], A. Korn[98], S. Korn[55], I. Korolkov[13], N. Korotkova[38], B. Kortman[117], O. Kortner[112], S. Kortner[112], W.H. Kostecka[118], M. Kostov[29a], V.V. Kostyukhin[147], A. Kotsokechagia[37], A. Kotwal[51],

A. Koulouris[37], A. Kourkoumeli-Charalampidi[73a,73b], C. Kourkoumelis[9], E. Kourlitis[112], O. Kovanda[126], R. Kowalewski[171], W. Kozanecki[126], A.S. Kozhin[38], V.A. Kramarenko[38], G. Kramberger[95], P. Kramer[25], M.W. Krasny[130], A. Krasznahorkay[105], A.C. Kraus[118], J.W. Kraus[177], J.A. Kremer[48], N.B. Krengel[147], T. Kresse[50], L. Kretschmann[177], J. Kretzschmar[94], K. Kreul[19], P. Krieger[161], K. Krizka[21], K. Kroeninger[49], H. Kroha[112], J. Kroll[134], J. Kroll[131], K.S. Krowpman[109], U. Kruchonak[39], H. Krüger[25], N. Krumnack[81], M.C. Kruse[51], O. Kuchinskaia[39], S. Kuday[3a], S. Kuehn[37], R. Kuesters[54], T. Kuhl[48], V. Kukhtin[39], Y. Kulchitsky[39], S. Kuleshov[140d,140b], J. Kull[1], M. Kumar[34g], N. Kumari[48], P. Kumari[162b], A. Kupco[134], T. Kupfer[49], A. Kupich[38], O. Kuprash[54], H. Kurashige[86], L.L. Kurchaninov[162a], O. Kurdysh[4], Y.A. Kurochkin[38], A. Kurova[38], M. Kuze[141], A.K. Kvam[105], J. Kvita[125], N.G. Kyriacou[108], C. Lacasta[169], F. Lacava[75a,75b], H. Lacker[19], D. Lacour[130], N.N. Lad[98], E. Ladygin[39], A. Lafarge[41], B. Laforge[130], T. Lagouri[178], F.Z. Lahbabi[36a], S. Lai[55], J.E. Lambert[171], S. Lammers[68], W. Lampl[7], C. Lampoudis[158,d], G. Lamprinoudis[102], A.N. Lancaster[118], E. Lançon[30], U. Landgraf[54], M.P.J. Landon[96], V.S. Lang[54], O.K.B. Langrekken[128], A.J. Lankford[165], F. Lanni[37], K. Lantzsch[25], A. Lanza[73a], M. Lanzac Berrocal[169], J.F. Laporte[138], T. Lari[71a], D. Larsen[17], L. Larson[11], F. Lasagni Manghi[24b], M. Lassnig[37], S.D. Lawlor[145], R. Lazaridou[173], M. Lazzaroni[71a,71b], H.D.M. Le[109], E.M. Le Boulicaut[178], L.T. Le Pottier[18a], B. Leban[24b,24a], F. Ledroit-Guillon[60], T.F. Lee[162b], L.L. Leeuw[34c], M. Lefebvre[171], C. Leggett[18a], G. Lehmann Miotto[37], M. Leigh[56], W.A. Leight[105], W. Leinonen[116], A. Leisos[158,v], M.A.L. Leite[83c], C.E. Leitgeb[19], R. Leitner[136], K.J.C. Leney[45], T. Lenz[25], S. Leone[74a], C. Leonidopoulos[52], A. Leopold[150], J.H. Lepage Bourbonnais[35], R. Les[109], C.G. Lester[33], M. Levchenko[38], J. Levêque[4], L.J. Levinson[175], G. Levrini[24b,24a], M.P. Lewicki[88], C. Lewis[142], D.J. Lewis[4], L. Lewitt[145], A. Li[30], B. Li[143a], C. Li[108], C-Q. Li[112], H. Li[143a], H. Li[103], H. Li[15], H. Li[62], H. Li[143a], J. Li[144a], K. Li[14], L. Li[144a], R. Li[178], S. Li[14,114c], S. Li[144b,144a], T. Li[5], X. Li[106], Z. Li[159], Z. Li[14,114c], Z. Li[62], S. Liang[14,114c], Z. Liang[14], M. Liberatore[138], B. Liberti[76a], K. Lie[64c], J. Lieber Marin[83e], H. Lien[68], H. Lin[108], S.F. Lin[151], L. Linden[111], R.E. Lindley[7], J.H. Lindon[37], J. Ling[61], E. Lipeles[131], A. Lipniacka[17], A. Lister[170], J.D. Little[68], B. Liu[14], B.X. Liu[114b], D. Liu[144b,144a], D. Liu[139], E.H.L. Liu[21], J.K.K. Liu[120], K. Liu[144b], K. Liu[144b,144a], M. Liu[62], M.Y. Liu[62], P. Liu[14], Q. Liu[144b,142,144a], X. Liu[62], X. Liu[143a], Y. Liu[114b,114c], Y.L. Liu[143a], Y.W. Liu[62], Z. Liu[66,l], S.L. Lloyd[96], E.M. Lobodzinska[48], P. Loch[7], E. Lodhi[161], T. Lohse[19], K. Lohwasser[145], E. Loiacono[48], J.D. Lomas[21], J.D. Long[42], I. Longarini[165], R. Longo[168], A. Lopez Solis[13], N.A. Lopez-canelas[7], N. Lorenzo Martinez[4], A.M. Lory[111], M. Losada[119a], G. Löschcke Centeno[152], X. Lou[47a,47b], X. Lou[14,114c], A. Lounis[66], P.A. Love[93], M. Lu[66], S. Lu[131], Y.J. Lu[154], H.J. Lubatti[142], C. Luci[75a,75b], F.L. Lucio Alves[114a], F. Luehring[68], B.S. Lunday[131], O. Lundberg[150], J. Lunde[37], N.A. Luongo[6], M.S. Lutz[37], A.B. Lux[26], D. Lynn[30], R. Lysak[134], V. Lysenko[135], E. Lytken[100], V. Lyubushkin[39], T. Lyubushkina[39], M.M. Lyukova[151], H. Ma[30], K. Ma[62], L.L. Ma[143a], W. Ma[62], Y. Ma[124], J.C. MacDonald[102], P.C. Machado De Abreu Farias[83e], R. Madar[41], T. Madula[98], J. Maeda[86], T. Maeno[30], P.T. Mafa[34c,k], H. Maguire[145], V. Maiboroda[66], A. Maio[133a,133b,133d], K. Maj[87a],

O. Majersky[48], S. Majewski[126], R. Makhmanazarov[38], N. Makovec[66], V. Maksimovic[16], B. Malaescu[130], J. Malamant[128], Pa. Malecki[88], V.P. Maleev[38], F. Malek[60,p], M. Mali[95], D. Malito[97], U. Mallik[80,*], A. Maloizel[5], S. Maltezos[10], A. Malvezzi Lopes[83d], S. Malyukov[39], J. Mamuzic[13], G. Mancini[53], M.N. Mancini[27], G. Manco[73a,73b], J.P. Mandalia[96], S.S. Mandarry[152], I. Mandić[95], L. Manhaes de Andrade Filho[83a], I.M. Maniatis[175], J. Manjarres Ramos[91], D.C. Mankad[175], A. Mann[111], T. Manoussos[37], M.N. Mantinan[40], S. Manzoni[37], L. Mao[144a], X. Mapekula[34c], A. Marantis[158], R.R. Marcelo Gregorio[96], G. Marchiori[5], M. Marcisovsky[134], C. Marcon[71a], E. Maricic[16], M. Marinescu[48], S. Marium[48], M. Marjanovic[123], A. Markhoos[54], M. Markovitch[66], M.K. Maroun[105], G.T. Marsden[103], E.J. Marshall[93], Z. Marshall[18a], S. Marti-Garcia[169], J. Martin[98], T.A. Martin[137], V.J. Martin[52], B. Martin dit Latour[17], L. Martinelli[75a,75b], M. Martinez[13,y], P. Martinez Agullo[169], V.I. Martinez Outschoorn[105], P. Martinez Suarez[13], S. Martin-Haugh[137], G. Martinovicova[136], V.S. Martoiu[28b], A.C. Martyniuk[98], A. Marzin[37], D. Mascione[78a,78b], L. Masetti[102], J. Masik[103], A.L. Maslennikov[39], S.L. Mason[42], P. Massarotti[72a,72b], P. Mastrandrea[74a,74b], A. Mastroberardino[44b,44a], T. Masubuchi[127], T.T. Mathew[126], J. Matousek[136], D.M. Mattern[49], J. Maurer[28b], T. Maurin[59], A.J. Maury[66], B. Maček[95], C. Mavungu Tsava[104], D.A. Maximov[38], A.E. May[103], E. Mayer[41], R. Mazini[34g], I. Maznas[118], S.M. Mazza[139], E. Mazzeo[37], J.P. Mc Gowan[171], S.P. Mc Kee[108], C.A. Mc Lean[6], C.C. McCracken[170], E.F. McDonald[107], A.E. McDougall[117], L.F. Mcelhinney[93], J.A. Mcfayden[152], R.P. McGovern[131], R.P. Mckenzie[34g], T.C. Mclachlan[48], D.J. Mclaughlin[98], S.J. McMahon[137], C.M. Mcpartland[94], R.A. McPherson[171,ac], S. Mehlhase[111], A. Mehta[94], D. Melini[169], B.R. Mellado Garcia[34g], A.H. Melo[55], F. Meloni[48], A.M. Mendes Jacques Da Costa[103], L. Meng[93], S. Menke[112], M. Mentink[37], E. Meoni[44b,44a], G. Mercado[118], S. Merianos[158], C. Merlassino[69a,69c], C. Meroni[71a,71b], J. Metcalfe[6], A.S. Mete[6], E. Meuser[102], C. Meyer[68], J-P. Meyer[138], Y. Miao[114a], R.P. Middleton[137], M. Mihovilovic[66], L. Mijović[52], G. Mikenberg[175], M. Mikestikova[134], M. Mikuž[95], H. Mildner[102], A. Milic[37], D.W. Miller[40], E.H. Miller[149], L.S. Miller[35], A. Milov[175], D.A. Milstead[47a,47b], T. Min[114a], A.A. Minaenko[38], I.A. Minashvili[155b], A.I. Mincer[120], B. Mindur[87a], M. Mineev[39], Y. Mino[89], L.M. Mir[13], M. Miralles Lopez[59], M. Mironova[18a], M. Missio[116], A. Mitra[173], V.A. Mitsou[169], Y. Mitsumori[113], O. Miu[161], P.S. Miyagawa[96], T. Mkrtchyan[63a], M. Mlinarevic[98], T. Mlinarevic[98], M. Mlynarikova[37], S. Mobius[20], M.H. Mohamed Farook[115], S. Mohapatra[42], M.F. Mohd Soberi[52], S. Mohiuddin[124], G. Mokgatitswane[34g], L. Moleri[175], U. Molinatti[129], L.G. Mollier[20], B. Mondal[134], S. Mondal[135], K. Mönig[48], E. Monnier[104], L. Monsonis Romero[169], J. Montejo Berlingen[13], A. Montella[47a,47b], M. Montella[122], F. Montereali[77a,77b], F. Monticelli[92], S. Monzani[69a,69c], A. Morancho Tarda[43], N. Morange[66], A.L. Moreira De Carvalho[48], M. Moreno Llácer[169], C. Moreno Martinez[56], J.M. Moreno Perez[23b], P. Morettini[57b], S. Morgenstern[37], M. Morii[61], M. Morinaga[159], M. Moritsu[90], F. Morodei[75a,75b], P. Moschovakos[37], B. Moser[54], M. Mosidze[155b], T. Moskalets[45], P. Moskvitina[116], J. Moss[32], P. Moszkowicz[87a], A. Moussa[36d], Y. Moyal[175], H. Moyano Gomez[13], E.J.W. Moyse[105], O. Mtintsilana[34g], S. Muanza[104], M. Mucha[25], J. Mueller[132], R. Müller[37], G.A. Mullier[167], A.J. Mullin[33], J.J. Mullin[51], A.C. Mullins[45], A.E. Mulski[61], D.P. Mungo[161], D. Munoz Perez[169], F.J. Munoz Sanchez[103], W.J. Murray[173,137], M. Muškinja[95], C. Mwewa[48], A.G. Myagkov[38,a], A.J. Myers[8], G. Myers[108], M. Myska[135], B.P. Nachman[18a], K. Nagai[129], K. Nagano[84], R. Nagasaka[159], J.L. Nagle[30,ak], E. Nagy[104], A.M. Nairz[37], Y. Nakahama[84], K. Nakamura[84], K. Nakkalil[5], A. Nandi[63b], H. Nanjo[127], E.A. Narayanan[45], Y. Narukawa[159], I. Naryshkin[38], L. Nasella[71a,71b], S. Nasri[119b], C. Nass[25], G. Navarro[23a], J. Navarro-Gonzalez[169], A. Nayaz[19], P.Y. Nechaeva[38], S. Nechaeva[24b,24a], F. Nechansky[134], L. Nedic[129], T.J. Neep[21], A. Negri[73a,73b], M. Negrini[24b], C. Nellist[117], C. Nelson[106], K. Nelson[108], S. Nemecek[134], M. Nessi[37,h], M.S. Neubauer[168], J. Newell[94], P.R. Newman[21], Y.W.Y. Ng[168], B. Ngair[119a], H.D.N. Nguyen[110], J.D. Nichols[123], R.B. Nickerson[129], R. Nicolaidou[138], J. Nielsen[139], M. Niemeyer[55], J. Niermann[37], N. Nikiforou[37], V. Nikolaenko[38,a], I. Nikolic-Audit[130], P. Nilsson[30], I. Ninca[48], G. Ninio[157], A. Nisati[75a], N. Nishu[2], R. Nisius[112], N. Nitika[69a,69c], J-E. Nitschke[50], E.K. Nkadimeng[34b], T. Nobe[159], T. Nommensen[153], M.B. Norfolk[145], B.J. Norman[35], M. Noury[36a], J. Novak[95], T. Novak[95], R. Novotny[135], L. Nozka[125], K. Ntekas[165], N.M.J. Nunes De Moura Junior[83b], J. Ocariz[130], A. Ochi[86], I. Ochoa[133a], S. Oerdek[48,z], J.T. Offermann[40], A. Ogrodnik[136], A. Oh[103], C.C. Ohm[150], H. Oide[84], M.L. Ojeda[37], Y. Okumura[159], L.F. Oleiro Seabra[133a], I. Oleksiyuk[56], G. Oliveira Correa[13], D. Oliveira Damazio[30], J.L. Oliver[165], Ö.O. Öncel[54], A.P. O'Neill[20], A. Onofre[133a,133e,e], P.U.E. Onyisi[11], M.J. Oreglia[40], D. Orestano[77a,77b], R. Orlandini[77a,77b], R.S. Orr[161], L.M. Osojnak[131], Y. Osumi[113], G. Otero y Garzon[31], H. Otono[90], G.J. Ottino[18a], M. Ouchrif[36d], F. Ould-Saada[128], T. Ovsiannikova[142], M. Owen[59], R.E. Owen[137], V.E. Ozcan[22a], F. Ozturk[88], N. Ozturk[8], S. Ozturk[82], H.A. Pacey[129], K. Pachal[162a], A. Pacheco Pages[13], C. Padilla Aranda[13], G. Padovano[75a,75b], S. Pagan Griso[18a], G. Palacino[68], A. Palazzo[70a,70b], J. Pampel[25], J. Pan[178], T. Pan[64a], D.K. Panchal[11], C.E. Pandini[60], J.G. Panduro Vazquez[137], H.D. Pandya[1], H. Pang[138], P. Pani[48], G. Panizzo[69a,69c], L. Panwar[130], L. Paolozzi[56], S. Parajuli[168], A. Paramonov[6], C. Paraskevopoulos[53], D. Paredes Hernandez[64b], A. Pareti[73a,73b], K.R. Park[42], T.H. Park[112], F. Parodi[57b,57a], J.A. Parsons[42], U. Parzefall[54], B. Pascual Dias[41], L. Pascual Dominguez[101], E. Pasqualucci[75a], S. Passaggio[57b], F. Pastore[97], P. Patel[88], U.M. Patel[51], J.R. Pater[103], T. Pauly[37], F. Pauwels[136], C.I. Pazos[164], M. Pedersen[128], R. Pedro[133a], S.V. Peleganchuk[38], O. Penc[37], E.A. Pender[52], S. Peng[15], G.D. Penn[178], K.E. Penski[111], M. Penzin[38], B.S. Peralva[83d], A.P. Pereira Peixoto[142], L. Pereira Sanchez[149], D.V. Perepelitsa[30,ak], G. Perera[105], E. Perez Codina[37], M. Perganti[10], H. Pernegger[37], S. Perrella[75a,75b], O. Perrin[41], K. Peters[48], R.F.Y. Peters[103], B.A. Petersen[37], T.C. Petersen[43], E. Petit[104], V. Petousis[135], A.R. Petri[71a,71b], C. Petridou[158,d], T. Petru[136], A. Petrukhin[147], M. Pettee[18a], A. Petukhov[82], K. Petukhova[37], R. Pezoa[140f], L. Pezzotti[24b,24a], G. Pezzullo[178], L. Pfaffenbichler[37], A.J. Pfleger[37], T.M. Pham[176], T. Pham[107], P.W. Phillips[137], G. Piacquadio[151], E. Pianori[18a], F. Piazza[126], R. Piegaia[31], D. Pietreanu[28b], A.D. Pilkington[103], M. Pinamonti[69a,69c], J.L. Pinfold[2], B.C. Pinheiro Pereira[133a], J. Pinol Bel[13], A.E. Pinto Pinoargote[130], L. Pintucci[69a,69c], K.M. Piper[152], A. Pirttikoski[56], D.A. Pizzi[35], L. Pizzimento[64b], A. Plebani[33],

JHEP12(2025)012

M.-A. Pleier[30], V. Pleskot[136], E. Plotnikova[39], G. Poddar[96], R. Poettgen[100], L. Poggioli[130], S. Polacek[136], G. Polesello[73a], A. Poley[148], A. Polini[24b], C.S. Pollard[173], Z.B. Pollock[122], E. Pompa Pacchi[123], N.I. Pond[98], D. Ponomarenko[68], L. Pontecorvo[37], S. Popa[28a], G.A. Popeneciu[28d], A. Poreba[37], D.M. Portillo Quintero[162a], S. Pospisil[135], M.A. Postill[145], P. Postolache[28c], K. Potamianos[173], P.A. Potepa[87a], I.N. Potrap[39], C.J. Potter[33], H. Potti[153], J. Poveda[169], M.E. Pozo Astigarraga[37], R. Pozzi[37], A. Prades Ibanez[76a,76b], J. Pretel[171], D. Price[103], M. Primavera[70a], L. Primomo[69a,69c], M.A. Principe Martin[101], R. Privara[125], T. Procter[87b], M.L. Proffitt[142], N. Proklova[131], K. Prokofiev[64c], G. Proto[112], J. Proudfoot[6], M. Przybycien[87a], W.W. Przygoda[87b], A. Psallidas[46], J.E. Puddefoot[145], D. Pudzha[53], D. Pyatiizbyantseva[116], J. Qian[108], R. Qian[109], D. Qichen[103], Y. Qin[13], T. Qiu[52], A. Quadt[55], M. Queitsch-Maitland[103], G. Quetant[56], R.P. Quinn[170], G. Rabanal Bolanos[61], D. Rafanoharana[112], F. Raffaeli[76a,76b], F. Ragusa[71a,71b], J.L. Rainbolt[40], J.A. Raine[56], S. Rajagopalan[30], E. Ramakoti[39], L. Rambelli[57b,57a], I.A. Ramirez-Berend[35], K. Ran[48,114c], D.S. Rankin[131], N.P. Rapheeha[34g], H. Rasheed[28b], D.F. Rassloff[63a], A. Rastogi[18a], S. Rave[102], S. Ravera[57b,57a], B. Ravina[37], I. Ravinovich[175], M. Raymond[37], A.L. Read[128], N.P. Readioff[145], D.M. Rebuzzi[73a,73b], A.S. Reed[112], K. Reeves[27], J.A. Reidelsturz[177], D. Reikher[126], A. Rej[49], C. Rembser[37], H. Ren[62], M. Renda[28b], F. Renner[48], A.G. Rennie[59], A.L. Rescia[48], S. Resconi[71a], M. Ressegotti[57b,57a], S. Rettie[37], W.F. Rettie[35], E. Reynolds[18a], O.L. Rezanova[39], P. Reznicek[136], H. Riani[36d], N. Ribaric[51], E. Ricci[78a,78b], R. Richter[112], S. Richter[47a,47b], E. Richter-Was[87b], M. Ridel[130], S. Ridouani[36d], P. Rieck[120], P. Riedler[37], E.M. Riefel[47a,47b], J.O. Rieger[117], M. Rijssenbeek[151], M. Rimoldi[37], L. Rinaldi[24b,24a], P. Rincke[167,55], G. Ripellino[167], I. Riu[13], J.C. Rivera Vergara[171], F. Rizatdinova[124], E. Rizvi[96], B.R. Roberts[18a], S.S. Roberts[139], D. Robinson[33], M. Robles Manzano[102], A. Robson[59], A. Rocchi[76a,76b], C. Roda[74a,74b], S. Rodriguez Bosca[37], Y. Rodriguez Garcia[23a], A.M. Rodríguez Vera[118], S. Roe[37], J.T. Roemer[37], O. Røhne[128], R.A. Rojas[37], C.P.A. Roland[130], A. Romaniouk[79], E. Romano[73a,73b], M. Romano[24b], A.C. Romero Hernandez[168], N. Rompotis[94], L. Roos[130], S. Rosati[75a], B.J. Rosser[40], E. Rossi[129], E. Rossi[72a,72b], L.P. Rossi[61], L. Rossini[54], R. Rosten[122], M. Rotaru[28b], B. Rottler[54], D. Rousseau[66], D. Rousso[48], S. Roy-Garand[161], A. Rozanov[104], Z.M.A. Rozario[59], Y. Rozen[156], A. Rubio Jimenez[169], V.H. Ruelas Rivera[19], T.A. Ruggeri[1], A. Ruggiero[129], A. Ruiz-Martinez[169], A. Rummler[37], Z. Rurikova[54], N.A. Rusakovich[39], H.L. Russell[171], G. Russo[75a,75b], J.P. Rutherfoord[7], S. Rutherford Colmenares[33], M. Rybar[136], P. Rybczynski[87a], A. Ryzhov[45], J.A. Sabater Iglesias[56], H.F-W. Sadrozinski[139], F. Safai Tehrani[75a], S. Saha[1], M. Sahinsoy[82], B. Sahoo[175], A. Saibel[169], B.T. Saifuddin[123], M. Saimpert[138], G.T. Saito[83c], M. Saito[159], T. Saito[159], A. Sala[71a,71b], A. Salnikov[149], J. Salt[169], A. Salvador Salas[157], F. Salvatore[152], A. Salzburger[37], D. Sammel[54], E. Sampson[93], D. Sampsonidis[158,d], D. Sampsonidou[126], J. Sánchez[169], V. Sanchez Sebastian[169], H. Sandaker[128], C.O. Sander[48], J.A. Sandesara[176], M. Sandhoff[177], C. Sandoval[23b], L. Sanfilippo[63a], D.P.C. Sankey[137], T. Sano[89], A. Sansoni[53], L. Santi[37], C. Santoni[41], H. Santos[133a,133b], A. Santra[175], E. Sanzani[24b,24a], K.A. Saoucha[85b], J.G. Saraiva[133a,133d], J. Sardain[7], O. Sasaki[84], K. Sato[163], C. Sauer[37], E. Sauvan[4], P. Savard[161,ai],

R. Sawada[159], C. Sawyer[137], L. Sawyer[99], C. Sbarra[24b], A. Sbrizzi[24b,24a], T. Scanlon[98], J. Schaarschmidt[142], U. Schäfer[102], A.C. Schaffer[66,45], D. Schaile[111], R.D. Schamberger[151], C. Scharf[19], M.M. Schefer[20], V.A. Schegelsky[38], D. Scheirich[136], F. Schenck[19], M. Schernau[140e], C. Scheulen[56], C. Schiavi[57b,57a], M. Schioppa[44b,44a], B. Schlag[149], S. Schlenker[37], J. Schmeing[177], E. Schmidt[112], M.A. Schmidt[177], K. Schmieden[102], C. Schmitt[102], N. Schmitt[102], S. Schmitt[48], L. Schoeffel[138], A. Schoening[63b], P.G. Scholer[35], E. Schopf[147], M. Schott[25], S. Schramm[56], T. Schroer[56], H-C. Schultz-Coulon[63a], M. Schumacher[54], B.A. Schumm[139], Ph. Schune[138], H.R. Schwartz[139], A. Schwartzman[149], T.A. Schwarz[108], Ph. Schwemling[138], R. Schwienhorst[109], F.G. Sciacca[20], A. Sciandra[30], G. Sciolla[27], F. Scuri[74a], C.D. Sebastiani[37], K. Sedlaczek[118], S.C. Seidel[115], A. Seiden[139], B.D. Seidlitz[42], C. Seitz[48], J.M. Seixas[83b], G. Sekhniaidze[72a], L. Selem[60], N. Semprini-Cesari[24b,24a], A. Semushin[179], D. Sengupta[56], V. Senthilkumar[169], L. Serin[66], M. Sessa[72a,72b], H. Severini[123], F. Sforza[57b,57a], A. Sfyrla[56], Q. Sha[14], E. Shabalina[55], H. Shaddix[118], A.H. Shah[33], R. Shaheen[150], J.D. Shahinian[131], M. Shamim[37], L.Y. Shan[14], M. Shapiro[18a], A. Sharma[37], A.S. Sharma[170], P. Sharma[30], P.B. Shatalov[38], K. Shaw[152], S.M. Shaw[103], Q. Shen[14], D.J. Sheppard[148], P. Sherwood[98], L. Shi[98], X. Shi[14], S. Shimizu[84], C.O. Shimmin[178], I.P.J. Shipsey[129,*], S. Shirabe[90], M. Shiyakova[39,aa], M.J. Shochet[40], D.R. Shope[128], B. Shrestha[123], S. Shrestha[122,am], I. Shreyber[39], M.J. Shroff[171], P. Sicho[134], A.M. Sickles[168], E. Sideras Haddad[34g,166], A.C. Sidley[117], A. Sidoti[24b], F. Siegert[50], Dj. Sijacki[16], F. Sili[92], J.M. Silva[52], I. Silva Ferreira[83b], M.V. Silva Oliveira[30], S.B. Silverstein[47a], S. Simion[66], R. Simoniello[37], E.L. Simpson[103], H. Simpson[152], L.R. Simpson[6], S. Simsek[82], S. Sindhu[55], P. Sinervo[161], S.N. Singh[27], S. Singh[30], S. Sinha[48], S. Sinha[103], M. Sioli[24b,24a], K. Sioulas[9], I. Siral[37], E. Sitnikova[48], J. Sjölin[47a,47b], A. Skaf[55], E. Skorda[21], P. Skubic[123], M. Slawinska[88], I. Slazyk[17], I. Sliusar[128], V. Smakhtin[175], B.H. Smart[137], S.Yu. Smirnov[140b], Y. Smirnov[82], L.N. Smirnova[38,a], O. Smirnova[100], A.C. Smith[42], D.R. Smith[165], J.L. Smith[103], M.B. Smith[35], R. Smith[149], H. Smitmanns[102], M. Smizanska[93], K. Smolek[135], P. Smolyanskiy[135], A.A. Snesarev[39], H.L. Snoek[117], S. Snyder[30], R. Sobie[171,ac], A. Soffer[157], C.A. Solans Sanchez[37], E.Yu. Soldatov[39], U. Soldevila[169], A.A. Solodkov[34g], S. Solomon[27], A. Soloshenko[39], K. Solovieva[54], O.V. Solovyanov[41], P. Sommer[50], A. Sonay[13], A. Sopczak[135], A.L. Sopio[52], F. Sopkova[29b], J.D. Sorenson[115], I.R. Sotarriva Alvarez[141], V. Sothilingam[63a], O.J. Soto Sandoval[140c,140b], S. Sottocornola[68], R. Soualah[85a], Z. Soumaimi[36e], D. South[48], N. Soybelman[175], S. Spagnolo[70a,70b], M. Spalla[112], D. Sperlich[54], B. Spisso[72a,72b], D.P. Spiteri[59], L. Splendori[104], M. Spousta[136], E.J. Staats[35], R. Stamen[63a], E. Stanecka[88], W. Stanek-Maslouska[48], M.V. Stange[50], B. Stanislaus[18a], M.M. Stanitzki[48], B. Stapf[48], E.A. Starchenko[38], G.H. Stark[139], J. Stark[91], P. Staroba[134], P. Starovoitov[85b], R. Staszewski[88], G. Stavropoulos[46], A. Stefl[37], P. Steinberg[30], B. Stelzer[148,162a], H.J. Stelzer[132], O. Stelzer[162a], H. Stenzel[58], T.J. Stevenson[152], G.A. Stewart[37], J.R. Stewart[124], M.C. Stockton[37], G. Stoicea[28b], M. Stolarski[133a], S. Stonjek[112], A. Straessner[50], J. Strandberg[150], S. Strandberg[47a,47b], M. Stratmann[177], M. Strauss[123], T. Strebler[104], P. Strizenec[29b], R. Ströhmer[172], D.M. Strom[126], R. Stroynowski[45], A. Strubig[47a,47b],

S.A. Stucci[30], B. Stugu[17], J. Stupak[123], N.A. Styles[48], D. Su[149], S. Su[62], X. Su[62],
D. Suchy[29a], K. Sugizaki[131], V.V. Sulin[38], M.J. Sullivan[94], D.M.S. Sultan[129],
L. Sultanaliyeva[38], S. Sultansoy[3b], S. Sun[176], W. Sun[14], O. Sunneborn Gudnadottir[167],
N. Sur[100], M.R. Sutton[152], H. Suzuki[163], M. Svatos[134], P.N. Swallow[33],
M. Swiatlowski[162a], T. Swirski[172], I. Sykora[29a], M. Sykora[136], T. Sykora[136], D. Ta[102],
K. Tackmann[48,z], A. Taffard[165], R. Tafirout[162a], Y. Takubo[84], M. Talby[104],
A.A. Talyshev[38], K.C. Tam[64b], N.M. Tamir[157], A. Tanaka[159], J. Tanaka[159],
R. Tanaka[66], M. Tanasini[151], Z. Tao[170], S. Tapia Araya[140f], S. Tapprogge[102],
A. Tarek Abouelfadl Mohamed[109], S. Tarem[156], K. Tariq[14], G. Tarna[28b], G.F. Tartarelli[71a],
M.J. Tartarin[91], P. Tas[136], M. Tasevsky[134], E. Tassi[44b,44a], A.C. Tate[168], G. Tateno[159],
Y. Tayalati[36e,ab], G.N. Taylor[107], W. Taylor[162b], A.S. Tegetmeier[91], P. Teixeira-Dias[97],
J.J. Teoh[161], K. Terashi[159], J. Terron[101], S. Terzo[13], M. Testa[53], R.J. Teuscher[161,ac],
A. Thaler[79], O. Theiner[56], T. Theveneaux-Pelzer[104], D.W. Thomas[97], J.P. Thomas[21],
E.A. Thompson[18a], P.D. Thompson[21], E. Thomson[131], R.E. Thornberry[45], C. Tian[62],
Y. Tian[56], V. Tikhomirov[82], Yu.A. Tikhonov[39], S. Timoshenko[38], D. Timoshyn[136],
E.X.L. Ting[1], P. Tipton[178], A. Tishelman-Charny[30], K. Todome[141], S. Todorova-Nova[136],
S. Todt[50], L. Toffolin[69a,69c], M. Togawa[84], J. Tojo[90], S. Tokár[29a], O. Toldaiev[68],
G. Tolkachev[104], M. Tomoto[84,113], L. Tompkins[149,o], E. Torrence[126], H. Torres[91],
E. Torró Pastor[169], M. Toscani[31], C. Tosciri[40], M. Tost[11], D.R. Tovey[145], T. Trefzger[172],
P.M. Tricarico[13], A. Tricoli[30], I.M. Trigger[162a], S. Trincaz-Duvoid[130], D.A. Trischuk[27],
A. Tropina[39], L. Truong[34c], M. Trzebinski[88], A. Trzupek[88], F. Tsai[151], M. Tsai[108],
A. Tsiamis[158], P.V. Tsiareshka[39], S. Tsigaridas[162a], A. Tsirigotis[158,v], V. Tsiskaridze[161],
E.G. Tskhadadze[155a], M. Tsopoulou[158], Y. Tsujikawa[89], I.I. Tsukerman[38], V. Tsulaia[18a],
S. Tsuno[84], K. Tsuri[121], D. Tsybychev[151], Y. Tu[64b], A. Tudorache[28b], V. Tudorache[28b],
S. Turchikhin[57b,57a], I. Turk Cakir[3a], R. Turra[71a], T. Turtuvshin[39,ad], P.M. Tuts[42],
S. Tzamarias[158,d], E. Tzovara[102], Y. Uematsu[84], F. Ukegawa[163],
P.A. Ulloa Poblete[140c,140b], E.N. Umaka[30], G. Unal[37], A. Undrus[30], G. Unel[165],
J. Urban[29b], P. Urrejola[140a], G. Usai[8], R. Ushioda[160], M. Usman[110], F. Ustuner[52],
Z. Uysal[82], V. Vacek[135], B. Vachon[106], T. Vafeiadis[37], A. Vaitkus[98], C. Valderanis[111],
E. Valdes Santurio[47a,47b], M. Valente[37], S. Valentinetti[24b,24a], A. Valero[169],
E. Valiente Moreno[169], A. Vallier[91], J.A. Valls Ferrer[169], D.R. Van Arneman[117],
T.R. Van Daalen[142], A. Van Der Graaf[49], H.Z. Van Der Schyf[34g], P. Van Gemmeren[6],
M. Van Rijnbach[37], S. Van Stroud[98], I. Van Vulpen[117], P. Vana[136], M. Vanadia[76a,76b],
U.M. Vande Voorde[150], W. Vandelli[37], E.R. Vandewall[124], D. Vannicola[157], L. Vannoli[53],
R. Vari[75a], M. Varma[178], E.W. Varnes[7], C. Varni[18b], D. Varouchas[66], L. Varriale[169],
K.E. Varvell[153], M.E. Vasile[28b], L. Vaslin[84], M.D. Vassilev[149], A. Vasyukov[39],
L.M. Vaughan[124], R. Vavricka[136], T. Vazquez Schroeder[13], J. Veatch[32], V. Vecchio[103],
M.J. Veen[105], I. Veliscek[30], I. Velkovska[95], L.M. Veloce[161], F. Veloso[133a,133c],
S. Veneziano[75a], A. Ventura[70a,70b], S. Ventura Gonzalez[138], A. Verbytskyi[112],
M. Verducci[74a,74b], C. Vergis[96], M. Verissimo De Araujo[83b], W. Verkerke[117],
J.C. Vermeulen[117], C. Vernieri[149], M. Vessella[165], M.C. Vetterli[148,ai], A. Vgenopoulos[102],
N. Viaux Maira[140f], T. Vickey[145], O.E. Vickey Boeriu[145], G.H.A. Viehhauser[129],
L. Vigani[63b], M. Vigl[112], M. Villa[24b,24a], M. Villaplana Perez[169], E.M. Villhauer[40],

E. Vilucchi[53], M.G. Vincter[35], A. Visibile[117], C. Vittori[37], I. Vivarelli[24b,24a], E. Voevodina[112], F. Vogel[111], J.C. Voigt[50], P. Vokac[135], Yu. Volkotrub[87b], E. Von Toerne[25], B. Vormwald[37], K. Vorobev[51], M. Vos[169], K. Voss[147], M. Vozak[37], L. Vozdecky[123], N. Vranjes[16], M. Vranjes Milosavljevic[16], M. Vreeswijk[117], N.K. Vu[144b,144a], R. Vuillermet[37], O. Vujinovic[102], I. Vukotic[40], I.K. Vyas[35], J.F. Wack[33], S. Wada[163], C. Wagner[149], J.M. Wagner[18a], W. Wagner[177], S. Wahdan[177], H. Wahlberg[92], C.H. Waits[123], J. Walder[137], R. Walker[111], K. Walkingshaw Pass[59], W. Walkowiak[147], A. Wall[131], E.J. Wallin[100], T. Wamorkar[18a], A. Wang[62], A.Z. Wang[139], C. Wang[102], C. Wang[11], H. Wang[18a], J. Wang[64c], P. Wang[103], P. Wang[98], R. Wang[61], R. Wang[6], S.M. Wang[154], S. Wang[14], T. Wang[62], T. Wang[62], W.T. Wang[80], W. Wang[14], X. Wang[168], X. Wang[144a], X. Wang[48], Y. Wang[114a], Y. Wang[62], Z. Wang[108], Z. Wang[144b], Z. Wang[108], C. Wanotayaroj[84], A. Warburton[106], A.L. Warnerbring[147], N. Warrack[59], S. Waterhouse[97], A.T. Watson[21], H. Watson[52], M.F. Watson[21], E. Watton[59], G. Watts[142], B.M. Waugh[98], J.M. Webb[54], C. Weber[30], H.A. Weber[19], M.S. Weber[20], S.M. Weber[63a], C. Wei[62], Y. Wei[54], A.R. Weidberg[129], E.J. Weik[120], J. Weingarten[49], C. Weiser[54], C.J. Wells[48], T. Wenaus[30], B. Wendland[49], T. Wengler[37], N.S. Wenke[112], N. Wermes[25], M. Wessels[63a], A.M. Wharton[93], A.S. White[61], A. White[8], M.J. White[1], D. Whiteson[165], L. Wickremasinghe[127], W. Wiedenmann[176], M. Wielers[137], R. Wierda[150], C. Wiglesworth[43], H.G. Wilkens[37], J.J.H. Wilkinson[33], D.M. Williams[42], H.H. Williams[131], S. Williams[33], S. Willocq[105], B.J. Wilson[103], D.J. Wilson[103], P.J. Windischhofer[40], F.I. Winkel[31], F. Winklmeier[126], B.T. Winter[54], M. Wittgen[149], M. Wobisch[99], T. Wojtkowski[60], Z. Wolffs[117], J. Wollrath[37], M.W. Wolter[88], H. Wolters[133a,133c], M.C. Wong[139], E.L. Woodward[42], S.D. Worm[48], B.K. Wosiek[88], K.W. Woźniak[88], S. Wozniewski[55], K. Wraight[59], C. Wu[161], C. Wu[21], J. Wu[159], M. Wu[114b], M. Wu[116], S.L. Wu[176], S. Wu[14], X. Wu[62], Y. Wu[62], Z. Wu[4], J. Wuerzinger[112], T.R. Wyatt[103], B.M. Wynne[52], S. Xella[43], L. Xia[114a], M. Xia[15], M. Xie[62], A. Xiong[126], J. Xiong[18a], D. Xu[14], H. Xu[62], L. Xu[62], R. Xu[131], T. Xu[108], Y. Xu[142], Z. Xu[52], Z. Xu[114a], B. Yabsley[153], S. Yacoob[34a], Y. Yamaguchi[84], E. Yamashita[159], H. Yamauchi[163], T. Yamazaki[18a], Y. Yamazaki[86], S. Yan[59], Z. Yan[105], H.J. Yang[144a,144b], H.T. Yang[62], S. Yang[62], T. Yang[64c], X. Yang[37], X. Yang[14], Y. Yang[159], Y. Yang[62], W-M. Yao[18a], C.L. Yardley[152], J. Ye[14], S. Ye[30], X. Ye[62], Y. Yeh[98], I. Yeletskikh[39], B. Yeo[18b], M.R. Yexley[98], T.P. Yildirim[129], P. Yin[42], K. Yorita[174], C.J.S. Young[37], C. Young[149], N.D. Young[126], Y. Yu[62], J. Yuan[14,114c], M. Yuan[108], R. Yuan[144b,144a], L. Yue[98], M. Zaazoua[62], B. Zabinski[88], I. Zahir[36a], A. Zaio[57b,57a], Z.K. Zak[88], T. Zakareishvili[169], S. Zambito[56], J.A. Zamora Saa[140d], J. Zang[159], R. Zanzottera[71a,71b], O. Zaplatilek[135], C. Zeitnitz[177], H. Zeng[14], J.C. Zeng[168], D.T. Zenger Jr[27], O. Zenin[38], T. Ženiš[29a], S. Zenz[96], D. Zerwas[66], M. Zhai[14,114c], D.F. Zhang[145], G. Zhang[14], J. Zhang[143a], J. Zhang[6], K. Zhang[14,114c], L. Zhang[62], L. Zhang[114a], P. Zhang[14,114c], R. Zhang[114a], S. Zhang[91], T. Zhang[159], Y. Zhang[142], Y. Zhang[98], Y. Zhang[62], Y. Zhang[114a], Z. Zhang[143a], Z. Zhang[66], H. Zhao[142], T. Zhao[143a], Y. Zhao[35], Z. Zhao[62], Z. Zhao[62], A. Zhemchugov[39], J. Zheng[114a], K. Zheng[168], X. Zheng[62], Z. Zheng[149], D. Zhong[168], B. Zhou[108], H. Zhou[7], N. Zhou[144a], Y. Zhou[15], Y. Zhou[114a], Y. Zhou[7], C.G. Zhu[143a], J. Zhu[108],

X. Zhu[144b], Y. Zhu[144a], Y. Zhu[62], X. Zhuang[14], K. Zhukov[68], N.I. Zimine[39], J. Zinsser[63b], M. Ziolkowski[147], L. Živković[16], A. Zoccoli[24b,24a], K. Zoch[61], A. Zografos[37], T.G. Zorbas[145], O. Zormpa[46], L. Zwalinski[37]

[1] Department of Physics, University of Adelaide, Adelaide; Australia
[2] Department of Physics, University of Alberta, Edmonton AB; Canada
[3] (a) Department of Physics, Ankara University, Ankara;(b) Division of Physics, TOBB University of Economics and Technology, Ankara; Türkiye
[4] LAPP, Université Savoie Mont Blanc, CNRS/IN2P3, Annecy; France
[5] APC, Université Paris Cité, CNRS/IN2P3, Paris; France
[6] High Energy Physics Division, Argonne National Laboratory, Argonne IL; United States of America
[7] Department of Physics, University of Arizona, Tucson AZ; United States of America
[8] Department of Physics, University of Texas at Arlington, Arlington TX; United States of America
[9] Physics Department, National and Kapodistrian University of Athens, Athens; Greece
[10] Physics Department, National Technical University of Athens, Zografou; Greece
[11] Department of Physics, University of Texas at Austin, Austin TX; United States of America
[12] Institute of Physics, Azerbaijan Academy of Sciences, Baku; Azerbaijan
[13] Institut de Física d'Altes Energies (IFAE), Barcelona Institute of Science and Technology, Barcelona; Spain
[14] Institute of High Energy Physics, Chinese Academy of Sciences, Beijing; China
[15] Physics Department, Tsinghua University, Beijing; China
[16] Institute of Physics, University of Belgrade, Belgrade; Serbia
[17] Department for Physics and Technology, University of Bergen, Bergen; Norway
[18] (a) Physics Division, Lawrence Berkeley National Laboratory, Berkeley CA;(b) University of California, Berkeley CA; United States of America
[19] Institut für Physik, Humboldt Universität zu Berlin, Berlin; Germany
[20] Albert Einstein Center for Fundamental Physics and Laboratory for High Energy Physics, University of Bern, Bern; Switzerland
[21] School of Physics and Astronomy, University of Birmingham, Birmingham; United Kingdom
[22] (a) Department of Physics, Bogazici University, Istanbul;(b) Department of Physics Engineering, Gaziantep University, Gaziantep;(c) Department of Physics, Istanbul University, Istanbul; Türkiye
[23] (a) Facultad de Ciencias y Centro de Investigaciónes, Universidad Antonio Nariño, Bogotá;(b) Departamento de Física, Universidad Nacional de Colombia, Bogotá; Colombia
[24] (a) Dipartimento di Fisica e Astronomia A. Righi, Università di Bologna, Bologna;(b) INFN Sezione di Bologna; Italy
[25] Physikalisches Institut, Universität Bonn, Bonn; Germany
[26] Department of Physics, Boston University, Boston MA; United States of America
[27] Department of Physics, Brandeis University, Waltham MA; United States of America
[28] (a) Transilvania University of Brasov, Brasov;(b) Horia Hulubei National Institute of Physics and Nuclear Engineering, Bucharest;(c) Department of Physics, Alexandru Ioan Cuza University of Iasi, Iasi;(d) National Institute for Research and Development of Isotopic and Molecular Technologies, Physics Department, Cluj-Napoca;(e) National University of Science and Technology Politechnica, Bucharest;(f) West University in Timisoara, Timisoara;(g) Faculty of Physics, University of Bucharest, Bucharest; Romania
[29] (a) Faculty of Mathematics, Physics and Informatics, Comenius University, Bratislava;(b) Department of Subnuclear Physics, Institute of Experimental Physics of the Slovak Academy of Sciences, Kosice; Slovak Republic
[30] Physics Department, Brookhaven National Laboratory, Upton NY; United States of America
[31] Universidad de Buenos Aires, Facultad de Ciencias Exactas y Naturales, Departamento de Física, y CONICET, Instituto de Física de Buenos Aires (IFIBA), Buenos Aires; Argentina
[32] California State University, CA; United States of America
[33] Cavendish Laboratory, University of Cambridge, Cambridge; United Kingdom
[34] (a) Department of Physics, University of Cape Town, Cape Town;(b) iThemba Labs, Western Cape;(c) Department of Mechanical Engineering Science, University of Johannesburg,

Johannesburg;[(d)] *National Institute of Physics, University of the Philippines Diliman (Philippines);*[(e)] *University of South Africa, Department of Physics, Pretoria;*[(f)] *University of Zululand, KwaDlangezwa;*[(g)] *School of Physics, University of the Witwatersrand, Johannesburg; South Africa*

[35] *Department of Physics, Carleton University, Ottawa ON; Canada*

[36] [(a)] *Faculté des Sciences Ain Chock, Université Hassan II de Casablanca;*[(b)] *Faculté des Sciences, Université Ibn-Tofail, Kénitra;*[(c)] *Faculté des Sciences Semlalia, Université Cadi Ayyad, LPHEA-Marrakech;*[(d)] *LPMR, Faculté des Sciences, Université Mohamed Premier, Oujda;*[(e)] *Faculté des sciences, Université Mohammed V, Rabat;*[(f)] *Institute of Applied Physics, Mohammed VI Polytechnic University, Ben Guerir; Morocco*

[37] *CERN, Geneva; Switzerland*

[38] *Affiliated with an institute formerly covered by a cooperation agreement with CERN*

[39] *Affiliated with an international laboratory covered by a cooperation agreement with CERN*

[40] *Enrico Fermi Institute, University of Chicago, Chicago IL; United States of America*

[41] *LPC, Université Clermont Auvergne, CNRS/IN2P3, Clermont-Ferrand; France*

[42] *Nevis Laboratory, Columbia University, Irvington NY; United States of America*

[43] *Niels Bohr Institute, University of Copenhagen, Copenhagen; Denmark*

[44] [(a)] *Dipartimento di Fisica, Università della Calabria, Rende;*[(b)] *INFN Gruppo Collegato di Cosenza, Laboratori Nazionali di Frascati; Italy*

[45] *Physics Department, Southern Methodist University, Dallas TX; United States of America*

[46] *National Centre for Scientific Research "Demokritos", Agia Paraskevi; Greece*

[47] [(a)] *Department of Physics, Stockholm University;*[(b)] *Oskar Klein Centre, Stockholm; Sweden*

[48] *Deutsches Elektronen-Synchrotron DESY, Hamburg and Zeuthen; Germany*

[49] *Fakultät Physik, Technische Universität Dortmund, Dortmund; Germany*

[50] *Institut für Kern- und Teilchenphysik, Technische Universität Dresden, Dresden; Germany*

[51] *Department of Physics, Duke University, Durham NC; United States of America*

[52] *SUPA — School of Physics and Astronomy, University of Edinburgh, Edinburgh; United Kingdom*

[53] *INFN e Laboratori Nazionali di Frascati, Frascati; Italy*

[54] *Physikalisches Institut, Albert-Ludwigs-Universität Freiburg, Freiburg; Germany*

[55] *II. Physikalisches Institut, Georg-August-Universität Göttingen, Göttingen; Germany*

[56] *Département de Physique Nucléaire et Corpusculaire, Université de Genève, Genève; Switzerland*

[57] [(a)] *Dipartimento di Fisica, Università di Genova, Genova;*[(b)] *INFN Sezione di Genova; Italy*

[58] *II. Physikalisches Institut, Justus-Liebig-Universität Giessen, Giessen; Germany*

[59] *SUPA — School of Physics and Astronomy, University of Glasgow, Glasgow; United Kingdom*

[60] *LPSC, Université Grenoble Alpes, CNRS/IN2P3, Grenoble INP, Grenoble; France*

[61] *Laboratory for Particle Physics and Cosmology, Harvard University, Cambridge MA; United States of America*

[62] *Department of Modern Physics and State Key Laboratory of Particle Detection and Electronics, University of Science and Technology of China, Hefei; China*

[63] [(a)] *Kirchhoff-Institut für Physik, Ruprecht-Karls-Universität Heidelberg, Heidelberg;*[(b)] *Physikalisches Institut, Ruprecht-Karls-Universität Heidelberg, Heidelberg; Germany*

[64] [(a)] *Department of Physics, Chinese University of Hong Kong, Shatin, N.T., Hong Kong;*[(b)] *Department of Physics, University of Hong Kong, Hong Kong;*[(c)] *Department of Physics and Institute for Advanced Study, Hong Kong University of Science and Technology, Clear Water Bay, Kowloon, Hong Kong; China*

[65] *Department of Physics, National Tsing Hua University, Hsinchu; Taiwan*

[66] *IJCLab, Université Paris-Saclay, CNRS/IN2P3, 91405, Orsay; France*

[67] *Centro Nacional de Microelectrónica (IMB-CNM-CSIC), Barcelona; Spain*

[68] *Department of Physics, Indiana University, Bloomington IN; United States of America*

[69] [(a)] *INFN Gruppo Collegato di Udine, Sezione di Trieste, Udine;*[(b)] *ICTP, Trieste;*[(c)] *Dipartimento Politecnico di Ingegneria e Architettura, Università di Udine, Udine; Italy*

[70] [(a)] *INFN Sezione di Lecce;*[(b)] *Dipartimento di Matematica e Fisica, Università del Salento, Lecce; Italy*

[71] [(a)] *INFN Sezione di Milano;*[(b)] *Dipartimento di Fisica, Università di Milano, Milano; Italy*

[72] [(a)] *INFN Sezione di Napoli;*[(b)] *Dipartimento di Fisica, Università di Napoli, Napoli; Italy*

[73] [(a)] *INFN Sezione di Pavia;*[(b)] *Dipartimento di Fisica, Università di Pavia, Pavia; Italy*

[74] [(a)] *INFN Sezione di Pisa;*[(b)] *Dipartimento di Fisica E. Fermi, Università di Pisa, Pisa; Italy*

75 *(a) INFN Sezione di Roma; (b) Dipartimento di Fisica, Sapienza Università di Roma, Roma; Italy*
76 *(a) INFN Sezione di Roma Tor Vergata; (b) Dipartimento di Fisica, Università di Roma Tor Vergata, Roma; Italy*
77 *(a) INFN Sezione di Roma Tre; (b) Dipartimento di Matematica e Fisica, Università Roma Tre, Roma; Italy*
78 *(a) INFN-TIFPA; (b) Università degli Studi di Trento, Trento; Italy*
79 *Universität Innsbruck, Department of Astro and Particle Physics, Innsbruck; Austria*
80 *University of Iowa, Iowa City IA; United States of America*
81 *Department of Physics and Astronomy, Iowa State University, Ames IA; United States of America*
82 *Istinye University, Sariyer, Istanbul; Türkiye*
83 *(a) Departamento de Engenharia Elétrica, Universidade Federal de Juiz de Fora (UFJF), Juiz de Fora; (b) Universidade Federal do Rio De Janeiro COPPE/EE/IF, Rio de Janeiro; (c) Instituto de Física, Universidade de São Paulo, São Paulo; (d) Rio de Janeiro State University, Rio de Janeiro; (e) Federal University of Bahia, Bahia; Brazil*
84 *KEK, High Energy Accelerator Research Organization, Tsukuba; Japan*
85 *(a) Khalifa University of Science and Technology, Abu Dhabi; (b) University of Sharjah, Sharjah; United Arab Emirates*
86 *Graduate School of Science, Kobe University, Kobe; Japan*
87 *(a) AGH University of Krakow, Faculty of Physics and Applied Computer Science, Krakow; (b) Marian Smoluchowski Institute of Physics, Jagiellonian University, Krakow; Poland*
88 *Institute of Nuclear Physics Polish Academy of Sciences, Krakow; Poland*
89 *Faculty of Science, Kyoto University, Kyoto; Japan*
90 *Research Center for Advanced Particle Physics and Department of Physics, Kyushu University, Fukuoka; Japan*
91 *L2IT, Université de Toulouse, CNRS/IN2P3, UPS, Toulouse; France*
92 *Instituto de Física La Plata, Universidad Nacional de La Plata and CONICET, La Plata; Argentina*
93 *Physics Department, Lancaster University, Lancaster; United Kingdom*
94 *Oliver Lodge Laboratory, University of Liverpool, Liverpool; United Kingdom*
95 *Department of Experimental Particle Physics, Jožef Stefan Institute and Department of Physics, University of Ljubljana, Ljubljana; Slovenia*
96 *Department of Physics and Astronomy, Queen Mary University of London, London; United Kingdom*
97 *Department of Physics, Royal Holloway University of London, Egham; United Kingdom*
98 *Department of Physics and Astronomy, University College London, London; United Kingdom*
99 *Louisiana Tech University, Ruston LA; United States of America*
100 *Fysiska institutionen, Lunds universitet, Lund; Sweden*
101 *Departamento de Física Teorica C-15 and CIAFF, Universidad Autónoma de Madrid, Madrid; Spain*
102 *Institut für Physik, Universität Mainz, Mainz; Germany*
103 *School of Physics and Astronomy, University of Manchester, Manchester; United Kingdom*
104 *CPPM, Aix-Marseille Université, CNRS/IN2P3, Marseille; France*
105 *Department of Physics, University of Massachusetts, Amherst MA; United States of America*
106 *Department of Physics, McGill University, Montreal QC; Canada*
107 *School of Physics, University of Melbourne, Victoria; Australia*
108 *Department of Physics, University of Michigan, Ann Arbor MI; United States of America*
109 *Department of Physics and Astronomy, Michigan State University, East Lansing MI; United States of America*
110 *Group of Particle Physics, University of Montreal, Montreal QC; Canada*
111 *Fakultät für Physik, Ludwig-Maximilians-Universität München, München; Germany*
112 *Max-Planck-Institut für Physik (Werner-Heisenberg-Institut), München; Germany*
113 *Graduate School of Science and Kobayashi-Maskawa Institute, Nagoya University, Nagoya; Japan*
114 *(a) Department of Physics, Nanjing University, Nanjing; (b) School of Science, Shenzhen Campus of Sun Yat-sen University; (c) University of Chinese Academy of Science (UCAS), Beijing; China*
115 *Department of Physics and Astronomy, University of New Mexico, Albuquerque NM; United States of America*

[116] *Institute for Mathematics, Astrophysics and Particle Physics, Radboud University/Nikhef, Nijmegen; Netherlands*
[117] *Nikhef National Institute for Subatomic Physics and University of Amsterdam, Amsterdam; Netherlands*
[118] *Department of Physics, Northern Illinois University, DeKalb IL; United States of America*
[119] *(a) New York University Abu Dhabi, Abu Dhabi; (b) United Arab Emirates University, Al Ain; United Arab Emirates*
[120] *Department of Physics, New York University, New York NY; United States of America*
[121] *Ochanomizu University, Otsuka, Bunkyo-ku, Tokyo; Japan*
[122] *Ohio State University, Columbus OH; United States of America*
[123] *Homer L. Dodge Department of Physics and Astronomy, University of Oklahoma, Norman OK; United States of America*
[124] *Department of Physics, Oklahoma State University, Stillwater OK; United States of America*
[125] *Palacký University, Joint Laboratory of Optics, Olomouc; Czech Republic*
[126] *Institute for Fundamental Science, University of Oregon, Eugene, OR; United States of America*
[127] *Graduate School of Science, University of Osaka, Osaka; Japan*
[128] *Department of Physics, University of Oslo, Oslo; Norway*
[129] *Department of Physics, Oxford University, Oxford; United Kingdom*
[130] *LPNHE, Sorbonne Université, Université Paris Cité, CNRS/IN2P3, Paris; France*
[131] *Department of Physics, University of Pennsylvania, Philadelphia PA; United States of America*
[132] *Department of Physics and Astronomy, University of Pittsburgh, Pittsburgh PA; United States of America*
[133] *(a) Laboratório de Instrumentação e Física Experimental de Partículas — LIP, Lisboa; (b) Departamento de Física, Faculdade de Ciências, Universidade de Lisboa, Lisboa; (c) Departamento de Física, Universidade de Coimbra, Coimbra; (d) Centro de Física Nuclear da Universidade de Lisboa, Lisboa; (e) Departamento de Física, Escola de Ciências, Universidade do Minho, Braga; (f) Departamento de Física Teórica y del Cosmos, Universidad de Granada, Granada (Spain); (g) Departamento de Física, Instituto Superior Técnico, Universidade de Lisboa, Lisboa; Portugal*
[134] *Institute of Physics of the Czech Academy of Sciences, Prague; Czech Republic*
[135] *Czech Technical University in Prague, Prague; Czech Republic*
[136] *Charles University, Faculty of Mathematics and Physics, Prague; Czech Republic*
[137] *Particle Physics Department, Rutherford Appleton Laboratory, Didcot; United Kingdom*
[138] *IRFU, CEA, Université Paris-Saclay, Gif-sur-Yvette; France*
[139] *Santa Cruz Institute for Particle Physics, University of California Santa Cruz, Santa Cruz CA; United States of America*
[140] *(a) Departamento de Física, Pontificia Universidad Católica de Chile, Santiago; (b) Millennium Institute for Subatomic physics at high energy frontier (SAPHIR), Santiago; (c) Instituto de Investigación Multidisciplinario en Ciencia y Tecnología, y Departamento de Física, Universidad de La Serena; (d) Universidad Andres Bello, Department of Physics, Santiago; (e) Instituto de Alta Investigación, Universidad de Tarapacá, Arica; (f) Departamento de Física, Universidad Técnica Federico Santa María, Valparaíso; Chile*
[141] *Department of Physics, Institute of Science, Tokyo; Japan*
[142] *Department of Physics, University of Washington, Seattle WA; United States of America*
[143] *(a) Institute of Frontier and Interdisciplinary Science and Key Laboratory of Particle Physics and Particle Irradiation (MOE), Shandong University, Qingdao; (b) School of Physics, Zhengzhou University; China*
[144] *(a) State Key Laboratory of Dark Matter Physics, School of Physics and Astronomy, Shanghai Jiao Tong University, Key Laboratory for Particle Astrophysics and Cosmology (MOE), SKLPPC, Shanghai; (b) State Key Laboratory of Dark Matter Physics, Tsung-Dao Lee Institute, Shanghai Jiao Tong University, Shanghai; China*
[145] *Department of Physics and Astronomy, University of Sheffield, Sheffield; United Kingdom*
[146] *Department of Physics, Shinshu University, Nagano; Japan*
[147] *Department Physik, Universität Siegen, Siegen; Germany*
[148] *Department of Physics, Simon Fraser University, Burnaby BC; Canada*
[149] *SLAC National Accelerator Laboratory, Stanford CA; United States of America*
[150] *Department of Physics, Royal Institute of Technology, Stockholm; Sweden*

[151] Departments of Physics and Astronomy, Stony Brook University, Stony Brook NY; United States of America
[152] Department of Physics and Astronomy, University of Sussex, Brighton; United Kingdom
[153] School of Physics, University of Sydney, Sydney; Australia
[154] Institute of Physics, Academia Sinica, Taipei; Taiwan
[155] (a) E. Andronikashvili Institute of Physics, Iv. Javakhishvili Tbilisi State University, Tbilisi; (b) High Energy Physics Institute, Tbilisi State University, Tbilisi; (c) University of Georgia, Tbilisi; Georgia
[156] Department of Physics, Technion, Israel Institute of Technology, Haifa; Israel
[157] Raymond and Beverly Sackler School of Physics and Astronomy, Tel Aviv University, Tel Aviv; Israel
[158] Department of Physics, Aristotle University of Thessaloniki, Thessaloniki; Greece
[159] International Center for Elementary Particle Physics and Department of Physics, University of Tokyo, Tokyo; Japan
[160] Graduate School of Science and Technology, Tokyo Metropolitan University, Tokyo; Japan
[161] Department of Physics, University of Toronto, Toronto ON; Canada
[162] (a) TRIUMF, Vancouver BC; (b) Department of Physics and Astronomy, York University, Toronto ON; Canada
[163] Division of Physics and Tomonaga Center for the History of the Universe, Faculty of Pure and Applied Sciences, University of Tsukuba, Tsukuba; Japan
[164] Department of Physics and Astronomy, Tufts University, Medford MA; United States of America
[165] Department of Physics and Astronomy, University of California Irvine, Irvine CA; United States of America
[166] University of West Attica, Athens; Greece
[167] Department of Physics and Astronomy, University of Uppsala, Uppsala; Sweden
[168] Department of Physics, University of Illinois, Urbana IL; United States of America
[169] Instituto de Física Corpuscular (IFIC), Centro Mixto Universidad de Valencia — CSIC, Valencia; Spain
[170] Department of Physics, University of British Columbia, Vancouver BC; Canada
[171] Department of Physics and Astronomy, University of Victoria, Victoria BC; Canada
[172] Fakultät für Physik und Astronomie, Julius-Maximilians-Universität Würzburg, Würzburg; Germany
[173] Department of Physics, University of Warwick, Coventry; United Kingdom
[174] Waseda University, Tokyo; Japan
[175] Department of Particle Physics and Astrophysics, Weizmann Institute of Science, Rehovot; Israel
[176] Department of Physics, University of Wisconsin, Madison WI; United States of America
[177] Fakultät für Mathematik und Naturwissenschaften, Fachgruppe Physik, Bergische Universität Wuppertal, Wuppertal; Germany
[178] Department of Physics, Yale University, New Haven CT; United States of America
[179] Yerevan Physics Institute, Yerevan; Armenia

[a] Also at Affiliated with an institute formerly covered by a cooperation agreement with CERN
[b] Also at An-Najah National University, Nablus; Palestine
[c] Also at Borough of Manhattan Community College, City University of New York, New York NY; United States of America
[d] Also at Center for Interdisciplinary Research and Innovation (CIRI-AUTH), Thessaloniki; Greece
[e] Also at Centre of Physics of the Universities of Minho and Porto (CF-UM-UP); Portugal
[f] Also at CERN, Geneva; Switzerland
[g] Also at CMD-AC UNEC Research Center, Azerbaijan State University of Economics (UNEC); Azerbaijan
[h] Also at Département de Physique Nucléaire et Corpusculaire, Université de Genève, Genève; Switzerland
[i] Also at Departament de Fisica de la Universitat Autonoma de Barcelona, Barcelona; Spain
[j] Also at Department of Financial and Management Engineering, University of the Aegean, Chios; Greece
[k] Also at Department of Mathematical Sciences, University of South Africa, Johannesburg; South Africa
[l] Also at Department of Modern Physics and State Key Laboratory of Particle Detection and Electronics, University of Science and Technology of China, Hefei; China
[m] Also at Department of Physics, Bolu Abant Izzet Baysal University, Bolu; Türkiye
[n] Also at Department of Physics, King's College London, London; United Kingdom
[o] Also at Department of Physics, Stanford University, Stanford CA; United States of America

[p] *Also at Department of Physics, Stellenbosch University; South Africa*
[q] *Also at Department of Physics, University of Fribourg, Fribourg; Switzerland*
[r] *Also at Department of Physics, University of Thessaly; Greece*
[s] *Also at Department of Physics, Westmont College, Santa Barbara; United States of America*
[t] *Also at Faculty of Physics, Sofia University, 'St. Kliment Ohridski', Sofia; Bulgaria*
[u] *Also at Faculty of Physics, University of Bucharest; Romania*
[v] *Also at Hellenic Open University, Patras; Greece*
[w] *Also at Henan University; China*
[x] *Also at Imam Mohammad Ibn Saud Islamic University; Saudi Arabia*
[y] *Also at Institucio Catalana de Recerca i Estudis Avancats, ICREA, Barcelona; Spain*
[z] *Also at Institut für Experimentalphysik, Universität Hamburg, Hamburg; Germany*
[aa] *Also at Institute for Nuclear Research and Nuclear Energy (INRNE) of the Bulgarian Academy of Sciences, Sofia; Bulgaria*
[ab] *Also at Institute of Applied Physics, Mohammed VI Polytechnic University, Ben Guerir; Morocco*
[ac] *Also at Institute of Particle Physics (IPP); Canada*
[ad] *Also at Institute of Physics and Technology, Mongolian Academy of Sciences, Ulaanbaatar; Mongolia*
[ae] *Also at Institute of Physics, Azerbaijan Academy of Sciences, Baku; Azerbaijan*
[af] *Also at Institute of Theoretical Physics, Ilia State University, Tbilisi; Georgia*
[ag] *Also at National Institute of Physics, University of the Philippines Diliman (Philippines); Philippines*
[ah] *Also at The Collaborative Innovation Center of Quantum Matter (CICQM), Beijing; China*
[ai] *Also at TRIUMF, Vancouver BC; Canada*
[aj] *Also at Università di Napoli Parthenope, Napoli; Italy*
[ak] *Also at University of Colorado Boulder, Department of Physics, Colorado; United States of America*
[al] *Also at University of Sienna; Italy*
[am] *Also at Washington College, Chestertown, MD; United States of America*
[an] *Also at Yeditepe University, Physics Department, Istanbul; Türkiye*
[*] *Deceased*